

Universidad Autónoma de Madrid

Facultad de Ciencias

Departamento de Física Teórica

Métodos de gran N aplicados a holografía y equivalencia planar

Memoria de Tesis Doctoral realizada por

D. Carlos Hoyos Badajoz,

presentada ante el Departamento de Física Teórica
de la Universidad Autónoma de Madrid
para la obtención del Título de Doctor en Ciencias.

Tesis Doctoral dirigida por

Dr. D. José Luis Fernández Barbón,

Científico Titular del C.S.I.C.

Tutor de la Tesis en el Departamento

Dr. D. Enrique Álvarez Vázquez,

Catedrático de la Universidad Autónoma de Madrid

Madrid, Abril 2006.

Agradecimientos

En primer lugar quiero agradecer a José L.F. Barbón por todo lo que he aprendido con él, mucha física pero no solamente, por ser tan pedagógico y haber mostrado tanta paciencia conmigo y por todos los cafés a los que me ha invitado, que son unos cuantos.

Quiero agradecer al Departamento de Física Teórica de la UAM y al Instituto de Física Teórica su hospitalidad todos estos años, y en especial a Enrique Álvarez y a Belén Gavela por haberme estimulado a hacer el doctorado. También quiero mencionar a Isabel, que me ha ahorrado más de un disgusto burocrático.

Quiero también agradecer la hospitalidad de la División Teórica del CERN, en Suiza, y del Perimeter Institute, en Canadá, por las agradables e interesantes estancias que he tenido allí. Quiero agradecer especialmente la amabilidad de Rob Myers y David Mateos durante la estancia en Canadá.

Y a mis compañeros de la física, por las conversaciones tan interesantes que hemos tenido, de física, y de lo divino y lo humano. Por lo que nos hemos reído y por lo bien que nos lo hemos pasado. Y por los cafés, comidas, cervezas, copas y viajes que hemos compartido. Especialmente, aunque ni mucho menos únicamente, a Edu, Dani “el argentino”, Diego, Jorge “el astur”, Jorge Bellorín, JP, Juan (muy especialmente, por esos ratos piscineros y por todo lo demás), Sergio “el cordobés” (probablemente con quien más he hablado de física), Sergio “el de Sanse” y Pablo (con quien además compartí la experiencia ginebrina). Y por los buenos ratos que hemos pasado en el despacho, a Alicia, África, Guillermo, Irene y Luismi.

Muchas gracias a mis compis pilaric@s, a la panda tricantina, a los que sufrieron en los barracones y a los que montaron en la olla, por tantas cosas que la tesis ocuparía el doble si las escribiera.

Por último, a mis padres porque siempre me han apoyado en todo, de todas las formas posibles, y a mi hermana Marina, que me alegra la vida.

Durante la realización del trabajo presentado en esta tesis, he sido financiado en parte por el Ministerio de Educación y Ciencia a través de una beca FPU.

Introducción

La equivalencia entre teorías gauge y teorías de gravedad es una de las propuestas más fascinantes en el campo de la física teórica y matemática. En la formulación original, la teoría de cuerdas de tipo IIB en la geometría $AdS_5 \times S^5$ con N unidades de flujo de 5-forma de RR es equivalente a $\mathcal{N} = 4$ $SU(N)$ Super-Yang-Mills en cuatro dimensiones. En principio, la equivalencia es válida en el límite de gran N , $N \rightarrow \infty$. Cuando la curvatura es pequeña y se puede utilizar la aproximación de supergravedad, la teoría gauge está a acoplo fuerte. La extensión a geometrías y teorías de campos más generales y menos simétricas ha generado gran cantidad de ejemplos, algunos más interesantes desde el punto de vista físico, pero donde la validez de la correspondencia está menos clara.

Podemos distinguir tres temas principales en los trabajos sobre la correspondencia, aunque como cualquier clasificación, es arbitraria y en muchos casos los temas están intrínsecamente relacionados y no pueden separarse dentro de algunos trabajos. En el primer tipo de trabajos se busca la elaboración de un diccionario entre ambas partes de la correspondencia. En esta línea podemos incluir tests no triviales que incluyen el cálculo de cantidades dinámicas. Normalmente la teoría de Yang-Mills es bien conocida sólo cuando el acoplo gauge es pequeño, mientras que para la teoría gravitatoria dual ocurre lo contrario. Esta característica es lo que hace la correspondencia tan difícil de probar (o refutar), y a la vez tan útil. Aunque todos los tests hechos hasta ahora muestran que la dualidad es robusta, carecemos aún de un procedimiento sistemático para equiparar cantidades a ambos lados de la correspondencia cuando no hay algo como supersimetría para proteger los cálculos.

El segundo tipo de trabajos trata acerca de los problemas habituales de gravedad como una teoría cuántica, especialmente cuando se estudian agujeros negros. Si cierta geometría de una teoría gravitatoria es equivalente a una teoría gauge, entonces la unitariedad de la teoría gravitatoria debería estar asegurada (a no ser que tratemos con un caso patológico).

Aunque nuestro entendimiento acerca de los agujeros negros en espacios AdS parece haber avanzado, la situación para agujeros negros de Schwarzschild o para escenarios cosmológicos como el espacio de Sitter no está clarificada aún, y los progresos en este sentido parecen ser difíciles.

El tercer tema es acerca del régimen de acoplo fuerte de las teorías gauge. De acuerdo con la correspondencia, podemos utilizar supergravedad para hacer cálculos analíticos que si no estarían fuera de nuestra capacidad técnica, especialmente si las teorías no son supersimétricas. Esta línea de trabajo ha sido explorada exhaustivamente, con muchos éxitos. Sin embargo, aún no podemos realizar cálculos con teorías asintóticamente libres (como QCD), ya que son duales a geometrías muy curvadas, donde la aproximación de supergravedad no es válida y perdemos control sobre nuestros resultados.

La variedad de aspectos de la correspondencia se refleja de alguna forma en las dos primeras partes de este trabajo. En la primera parte investigamos la extensión del diccionario de AdS/CFT para incluir multitrazas, lo cual implica ir más allá del límite de gran N . El análisis se hace utilizando las propiedades de campo medio de la teoría gauge, y después es utilizado para estimar el efecto sobre el diagrama de fases de la teoría gravitatoria. En la segunda parte de la tesis estudiamos la anomalía holográfica de la simetría $U(1)_A$ axial de una teoría gauge no supersimétrica con quarks. Para ello construimos la geometría dual e investigamos cómo la anomalía está implementada en ella. En la clasificación que hemos presentado antes, la primera parte está entre el primer y el segundo tipo de trabajos, mientras que la segunda parte está más relacionada con el tercer tipo de trabajos, aunque algunos aspectos están relacionados con el primer tipo.

La tercera parte de la tesis no está relacionada directamente con la correspondencia, pero es un subproducto de ella. AdS/CFT proporciona una nueva visión sobre teorías gauges (y de gravedad), y como tal puede ayudarnos a descubrir nuevas relaciones entre ellas que previamente no hubiéramos sospechado. Este es el caso de equivalencia planar. Hay algunas teorías gauge que pueden obtenerse proyectando una teoría supersimétrica madre de una forma definida. Gracias a la correspondencia, se descubrió que la teoría madre y la proyectada (o hija) son equivalentes en el límite de gran N . En la tercera parte investigaremos esta relación introduciendo las teorías en volumen finito.

Conclusiones

Parte I: Deformaciones de multitraza

En esta parte mostramos que el tratamiento que se hace en AdS/CFT de las multitrazas como condiciones de contorno no lineales es equivalente a la aproximación de Hartree. Hemos aplicado los métodos de campo medio para estudiar las deformaciones de multitraza de las teorías gauge para grandes valores de N . Las deformaciones son equivalentes a deformaciones de una sola traza con un acoplo que depende del campo medio y que tiene que ser evaluado de forma auto-consistente, utilizando la aproximación de Hartree. Las propiedades globales de la ecuación auto-consistente de campo medio, en concreto la monotonidad, están relacionadas con la estabilidad local del campo medio. Estas propiedades, y un desarrollo formal de una expansión sistemática $1/N$ pueden ser discutidos utilizando campos auxiliares. Como las deformaciones de multitraza corresponden a teorías de cuerdas no locales, hemos encontrado nuevas clases de inestabilidades taquiónicas para estos modelos, inducidas por las deformaciones de multitraza.

Como aplicación concreta, hemos estudiado el efecto de las multitrazas sobre el diagrama de fases termodinámico de D4 branas 'calientes' en volumen finito. Hemos encontrado que las transiciones de fase a gran N se ven enormemente afectadas cuando el acoplo es de $O(1)$ en unidades adimensionales. Las deformaciones analíticas afectan a la región donde podemos describir el sistema mediante una teoría gravitatoria. Para deformaciones no analíticas, se vería afectada la región descrita utilizando la teoría gauge.

Trabajos futuros pueden orientarse a entender mejor la inestabilidad taquiónica del campo medio desde el punto de vista del dual gravitatorio, y la relación con ruptura de supersimetría, que en nuestra geometría esta rota incluso en el caso sin deformaciones. También sería interesante calcular las correcciones a ordenes mayores de la expansión $1/N$.

Parte II: La anomalía holográfica

Muchas de las propiedades no perturbativas de las teorías gauge a acoplo fuerte pueden ser reproducidas utilizando duales gravitatorios. En este trabajo hemos seleccionado un dual holográfico de una teoría gauge confinante, el límite cercano al horizonte de N_c D4 branas compactificadas en un círculo con condiciones de contorno que rompen supersimetría. La circulación del flujo dos-forma de RR en el círculo que está en la frontera da el ángulo de vacío θ de la teoría gauge. El modelo presenta una susceptibilidad topológica diferente de cero y una estructura con múltiples ramas, de acuerdo con la física quiral de gran N. Añadimos sabor al modelo introduciendo N_f D6 branas de prueba, que no afectan a la geometría mientras $N_f \ll N_c$, por lo que es equivalente a trabajar en una aproximación 'quenched'.

La forma de la D6 dentro de la geometría tiene un modo cero en el límite quiral de quarks sin masas. Esto significa que la D6 puede moverse a lo largo de cierta dirección de la geometría sin coste de energía. El modo cero puede identificarse con el bosón de Goldstone de gran N asociado a la simetría $U(1)$ axial, conocido como η' . Podemos deducir la relación de la anomalía cuando tenemos en cuenta el flujo de RR del que son fuente las D6 branas, $\theta \rightarrow \theta + 2\sqrt{N_f}\eta'/f_\pi$. Damos argumentos para mostrar que el mecanismo de Witten-Veneziano debe ser realizado en supergravedad como una relación directa entre amplitudes de cuerdas abiertas y de cuerdas cerradas. Mostramos que existen acoplos no derivativos para el η' y calculamos el primer término del potencial generado para el η' , encontrando un acuerdo perfecto con la fórmula de Witten-Veneziano.

La masa del η' debe ser generada por un diagrama cilíndrico con una inserción del η' en cada frontera, emulando el mecanismo de aniquilación de quarks de Isgur-de Rújula-Georgi-Glashow. Sin embargo, los acoplos no derivativos del η' a las glueballs le darían una masa taquiónica, por lo que debe haber un término positivo de contacto proveniente de la compleción del diagrama de intercambio de glueballs en teoría de cuerdas. El intercambio de glueballs es la imagen natural cuando consideramos un cilindro que es largo respecto a su circunferencia. En la esquina opuesta del espacio de moduli, la interpretación natural desde el punto de vista de cuerdas abiertas es un bucle de mesones con inserciones del η' , lo cual proporciona la compleción UV del intercambio de glueballs.

Sería interesante extender el análisis más allá de la aproximación de branas de prueba, en una geometría donde la reacción de las branas haya sido tenido en cuenta. Como la

dependencia puramente gluónica en el ángulo θ viene de la energía de flujos de RR, el mecanismo debe ser similar a una modificación de Green-Schwarz de los campos. Sería interesante encontrar un polinomio de anomalía en diez dimensiones que permitiera la sustitución $\theta \rightarrow \theta + 2\sqrt{N_f}\eta'/f_\pi$ en la dos forma de RR, después de reducirse sobre el volumen de las D6 branas.

No hemos discutido características no Abelianas del sabor. En el modelo D4/D6, hay $N_f^2 - 1$ pseudoescalares ligeros extra que vienen de rotaciones independientes de las D6 branas. La asociación natural sería con los piones de la teoría dual. Sin embargo, los quarks se acoplan con escalares en la representación adjunta que rompen explícitamente el grupo de sabor al grupo diagonal junto con el $U(1)_A$ axial. Por tanto, esperamos que haya correcciones que levanten la masa de los 'piones'. Resultados similares aparecen en modelos $D3/D7$, por ejemplo. A pesar de esto, la masa de los escalares es mucho mayor que la masa a gran N de los 'piones', por lo que se puede dar una descripción aproximada de los mismos en términos de un Lagrangiano quiral a bajas energías. En modelos $D4/D8$, no hay acoplos con escalares porque las simetrías globales de sabor se identifican con simetrías gauge residuales de las D8 branas en la frontera, en vez de proceder de propiedades geométricas de la forma de la brana en la geometría. Otra forma de abordar el problema del sabor en modelos confinantes utilizando otro tipo de geometrías, como Klebanov-Strassler o Maldacena-Nuñez, parecen encontrar problemas para incluir quarks sin masa.

Parte III: Equivalencia planar en el toro

El análisis de teorías de campos orbifold y orientifold en volumen finito $\mathbf{R} \times \mathbf{T}^3$ presenta algunos caveats para equivalencia planar. Con condiciones periódicas, las holonomías a lo largo de las direcciones compactas del toro juegan el papel de grados de libertad a baja energía. Para algunos valores no triviales de las holonomías, hay violaciones de equivalencia planar. Esto puede verse en que el potencial efectivo a un bucle no se hace cero a primer orden ($O(N^2)$). Este resultado por sí mismo no descarta equivalencia planar en el régimen de acoplo fuerte, que corresponde a una situación física bastante diferente. Por ejemplo, a acoplo fuerte esperamos la formación de un condensado fermiónico y la ruptura de simetría quiral. Sin embargo, el resultado sugiere que cuando configuraciones con valores medios apreciables para los campos empiezan a ser importantes, como uno esperaría a acoplo fuerte, por lo que no es obvio que la equivalencia se satisfaga. Violaciones de equivalencia

planar ocurren de hecho en regiones pequeñas del espacio de moduli, que se hacen de medida cero en el límite $N \rightarrow \infty$, pero aun así hay que ser cuidadoso antes de asegurar que la equivalencia planar se mantiene a nivel no perturbativo.

Cuando estudiamos teorías orbifold con condiciones de contorno rotadas, encontramos dificultades para identificar cantidades equivalentes en la teoría madre y en la hija. Los resultados, especialmente los cálculos semiclásicos, sugieren que la teoría orbifold contiene un subsector supersimétrico asociado al grupo gauge diagonal de la teoría hija, en vez de al grupo gauge de la teoría madre. Sería interesante comprobar si para el caso orientifold sucede algo análogo, pues podría ser la explicación de la equivalencia planar que se observa a nivel perturbativo.

Universidad Autónoma de Madrid

Facultad de Ciencias

Departamento de Física Teórica

Large N methods applied to holography and planar equivalence

Memoria de Tesis Doctoral realizada por

D. Carlos Hoyos Badajoz,

presentada ante el Departamento de Física Teórica
de la Universidad Autónoma de Madrid
para la obtención del Título de Doctor en Ciencias.

Tesis Doctoral dirigida por

Dr. D. José Luis Fernández Barbón,

Científico Titular del C.S.I.C.

Tutor de la Tesis en el Departamento

Dr. D. Enrique Álvarez Vázquez,

Catedrático de la Universidad Autónoma de Madrid

Madrid, Abril 2006.

Contents

1	Introduction	5
I	Multitrace deformations	7
2	Motivation	8
2.1	Master field and AdS/CFT correspondence	8
2.2	Multitrace deformations	9
3	Mean field expansion	11
3.1	Multitrace boundary conditions	11
3.2	Systematics of the mean field approximation	12
3.3	Stability of the Master Field	16
3.3.1	Stability and the Master Equation	18
4	Explicit Examples	21
4.1	Multitraces and Topology-Changing Phase Transitions	23
4.1.1	Review of the Single-Trace Case	23
4.1.2	The Multitrace Case	25
5	Conclusions	29

II	The holographic axial anomaly	31
6	Motivation	32
6.1	Holographic QCD-like models	33
6.2	Large N chiral dynamics	36
6.2.1	Chiral anomaly	38
6.2.2	Witten-Veneziano formula	40
7	Holographic QCD model	43
7.1	A confining supergravity dual	43
7.2	A model with flavor	45
7.3	Introducing the θ angle	51
8	$1/N$ physics of the holographic η'	53
8.1	The anomaly relation in the UV regime	53
8.2	String contributions to the potential	55
8.3	A quantitative check to order $1/\sqrt{N}$	58
9	Conclusions	61
III	Planar equivalence in finite volume	63
10	Motivation	64
10.1	Orbifold and orientifold field theories	65
10.1.1	Orbifold theories	66
10.1.2	Orientifold theories	67
11	Gauge theories in the box	68
11.1	Physical setup	68

11.2	Moduli space and boundary conditions	68
11.3	One-loop potential over moduli space	71
11.3.1	Generalizations	76
12	Planar equivalence in the box I	78
12.1	Planar equivalence and the “planar index”	78
12.2	Effective potentials and planar equivalence	80
12.2.1	Orientifold effective potential	82
12.2.2	Orbifold effective potential	85
13	Planar equivalence in the box II	88
13.1	Twisted boundary conditions and orbifold field theories.	89
13.2	Vacuum structure.	92
13.2.1	Ground states in the daughter theory.	92
13.2.2	The mapping of vacua.	94
13.2.3	Electric fluxes and vacuum angles.	95
13.2.4	Fermionic zero modes.	96
13.2.5	Potential over moduli space.	98
13.3	Tunneling effects.	100
13.3.1	Tunneling in parent theory.	101
13.3.2	Tunneling in daughter theory.	103
13.3.3	Semiclassical dependence on the vacuum angles.	107
13.4	D-brane interpretation.	110
14	Conclusions	114

Appendix	115
A Examples of multitrace deformations	116
A.1 Binomium Perturbation	118
A.2 More Exotic Perturbations	119
B One-loop potential in the torus	121
B.1 Non-analytic behavior	123
C Landscape features of the potential	124
C.1 Effective potentials for flat connections	125
C.1.1 Effective potentials	126
C.2 The Cartan–Weyl landscape	128
C.2.1 Examples	131
C.2.2 The general rules	131
D Mass of bifundamental fields in toron background	134
Bibliography	136

Chapter 1

Introduction

The equivalence between gauge and gravitational theories is one of the most fascinating proposals in the field of mathematical and theoretical physics. In the original formulation, type IIB string theory in $AdS_5 \times S^5$ background with N units of RR 5-form flux is equivalent to $\mathcal{N} = 4$ $SU(N)$ Super-Yang-Mills in four-dimensional space. In principle, the equivalence is valid in the large- N limit, $N \rightarrow \infty$. When the curvature is small and the supergravity approximation is reliable, the gauge theory is at strong coupling. The extension to more general and less symmetric gravity backgrounds and field theories has generated a large number of examples, sometimes more interesting from a physical point of view, but usually the validity of the correspondence is less clear for them.

We can distinguish three main topics in the works on the correspondence, although as any classification is arbitrary and many times the topics are related and cannot be separated within some works. The first topic is the elaboration of a dictionary between both sides of the correspondence. In this line we can include the computation of dynamical quantities that may provide a non-trivial test. Notice that usually Yang-Mills is well-known only at weak coupling, while the opposite is true for supergravity. This characteristic is what makes the correspondence so difficult to prove (or disprove), and so useful. Although the correspondence has been proved to be robust under any kind of test, we lack a systematic matching procedure whenever there is nothing as supersymmetry that protects the computation.

The second topic treats the usual concerns about gravity as a quantum theory, specially when black holes are involved. If a gravitational background is equivalent to a gauge theory, then unitarity must be ensured (unless we are dealing with a pathological case). Although

the understanding of black holes in AdS space seems to have advanced, the situation for Schwarzschild black holes or for cosmological issues like de Sitter space is still highly unclear, and progress appears to be difficult.

The third topic is about the strong coupling regime of gauge theories. According to the correspondence, supergravity can be used to make analytic computations, otherwise technically intractable, specially if the theory is non-supersymmetric. This line of work has been extensively explored, with many successes. However, asymptotically free theories (such as QCD) are still out of reach, because they involve highly curved backgrounds, where analytical control over supergravity computations is lost.

The variety of aspects of the correspondence is somehow reflected in the first and second parts of this work. In the first part we investigate the extension of the AdS/CFT dictionary to include multitraces, which implies to go beyond the large N limit. The analysis is made using the properties of the master field of the gauge theory, and the effect on the gravitational phase diagram is investigated. In the second part we study the $U(1)_A$ axial anomaly in a gravitational background dual to a non-supersymmetric gauge theory with flavor. In the classification above, the first part will be somewhere in between the first and second classes, while the second part will be more related to the third class, although some aspects are also related to the first class.

The third part of this work is not directly related to the correspondence, but it is a by-product of it. AdS/CFT provides a new vision over gauge (and gravity) theories, and as such it can help to find new unsuspected relations among them. That is the case of planar equivalence. There are some theories that can be obtained by projecting a supersymmetric parent theory in a definite way. It was realized thanks to the correspondence that the projected (or daughter) theory and its parent are equivalent in the large- N limit. We will investigate this subject defining the gauge theories in finite volume, but our analysis will have other applications, as we will see.

Part I

Multitrace deformations

Chapter 2

Motivation

2.1 Master field and AdS/CFT correspondence

It is hard to review [1–15] the AdS/CFT correspondence [16–18] making justice to it. Instead, we will try a partial and slightly different point of view. In the original formulation we have a conformal $SU(N)$ gauge theory in four dimensions. At strong coupling, and in the large- N limit [19, 20], we expect that the theory is described by free singlet-states. However, all the degrees of freedom of the theory should contribute to vacuum amplitudes, so they are proportional to N^2 . Then, any correlation function will be dominated by vacuum contributions. Notice that the large- N vacuum is not the usual one on top of which the perturbative expansion on the 't Hooft coupling is made. Instead, all possible corrections on the coupling have been included in a resummation at each order in N . In the path integral formalism, the large- N vacuum configuration is known as the 'master field' [21].

The master field can be treated as a classical configuration [22–24]. Uncertainties, in the sense of deviations from the mean expectation values of operators, are minimized on master field configurations, and vanish in the strict $N \rightarrow \infty$ limit. According to the correspondence, the master field that arises in the large- N limit of a gauge theory has a geometrical description. The global symmetries of the gauge theory map to isometries of the dual space and there is a correspondence between gauge operators and dual fields of the same representation. The complete statement relates the gauge theory to a quantum gravitational theory, a string theory. The strong-coupling classical configuration can receive stringy and quantum corrections. Stringy or α' corrections come with powers of the AdS

curvature. In the field theory, they are suppressed by powers of the inverse of the 't Hooft coupling. Quantum corrections, proportional to the string coupling, correspond in the gauge theory to $1/N$ corrections. The duality has two directions, weakly coupled gauge theory will describe strings in highly curved backgrounds.

2.2 Multitrace deformations

Let us make a few more comments about the map between the dual theories. AdS space has a conformal time-like boundary at infinite proper distance. However, light rays can travel to and from the boundary in finite proper time as seen by an inertial observer, so boundary conditions must be specified. On the other hand, the direction orthogonal to the boundary corresponds to a renormalization group scale of the gauge theory, with the boundary at an ultraviolet fixed point. Different boundary conditions change the background fields in AdS. In the field theory Lagrangian, they introduce new terms involving the dual operators, with bare couplings given by the boundary values.

In all this picture, we are able to map all the fields of AdS to single-trace gauge-invariant operators. For instance, the scalar dilaton field maps to the operator $\mathcal{O} = N^{-1} \text{tr} F^2$. Multitrace operators would correspond to multi-particle (or multi-string) states. When N is very large but finite, the number of independent single-trace operators is also finite. This suggests a “stringy exclusion principle” according to which the number of strings we can introduce is limited to be of order $\sim N$ [25]. On the other hand, when we try to deform the Lagrangian with a multitrace, a puzzle arises because there is no obvious parameter in string theory that can correspond to it. It has been proposed that there can be non-local interactions on the worldsheet, with a coupling associated to the multitrace coupling [26]. For the classical regime, a multitrace deformation is translated to non-linear boundary conditions, so it can be reduced to the case of a single-trace deformation. This makes multitrace deformations quite interesting, because they are easily manageable when the effect of the single-trace is known and at the same time introduce novel features that will be reflected in non-linearities in the background dependence on the couplings.

We can resume the effect of multitraces in two points: breaking of conformal invariance and non-local modifications of the geometry. The first point has been examined under the light of renormalization group flows for double-trace deformations. The double-trace induces a flow of the central charge, that in some cases drives the theory to a different

fixed point, related to the ultraviolet theory by a Legendre transformation [27–30]. In the bulk theory, the background interpolates between AdS spaces of different radius. This is not exclusive of multitrace deformations, we expect a similar behavior whenever the dual gauge theory does not develop a mass gap, but has two different fixed points in the infrared and the ultraviolet. Similar results have been found for holographic duals of non-critical string backgrounds [31]. Double-trace operators have been also used to study the conformal symmetry of orbifolded generalizations of the AdS correspondence [32], a subject that we will also encounter in the sections on planar equivalence.

Non-local deformations are perhaps more interesting. Multitrace terms induce boundary conditions such that the dual background contains a bound state. If the deformation renders the gauge theory unstable, this is also reflected in the bulk, even though the dual fields are not tachyonic. For instance, scalar fields satisfying the Breitenlohner-Freedman bound develop a tachyonic mode on Minkowski slices of AdS [33]. From these considerations, it has been proposed that the boundary theory provides a lower bound on the energy of states in AdS [34–36]. Some of the instabilities have been identified with time-dependent backgrounds [37], and in some cases the evolution leads to a big crunch singularity within AdS [38, 39], so a deeper study of gauge theories with unstable multitrace deformations may result in a better understanding of cosmological singularities in string theory.

In the following sections, we will introduce multitrace deformations and show how master field techniques can be used to reduce to the single-trace case. We will also examine the changes on the gravity background that our deformations produce, specially when new instabilities appear.

Chapter 3

Mean field expansion

3.1 Multitrace boundary conditions

The first treatments of multitrace boundary conditions are in [40, 41] and are based on a simple observation. Consider for simplicity a scalar field of mass m in AdS_{d+1} space

$$ds^2 = \frac{dz^2 + \sum_{i=1}^d dx_i^2}{z^2}. \quad (3.1)$$

The asymptotic behavior of the field close to the boundary at $z = 0$ is

$$\phi(x, z) = \alpha(x)z^{d-\Delta} + \beta(x)z^\Delta \quad (3.2)$$

where Δ is the conformal dimension of the dual single-trace operator \mathcal{O} and it is related to the mass through $\Delta(\Delta + d) = m^2$. In the correspondence, $\beta(x)$ is interpreted as a vacuum expectation value of the operator, while $\alpha(x)$ acts as a source. Therefore, a term in the Lagrangian of the form

$$N^2 W(\mathcal{O}) = N^2 \int d^d x f(x) \mathcal{O} \quad (3.3)$$

corresponds to the boundary condition

$$\alpha = f. \quad (3.4)$$

On the other hand, the partition function deformed with the term W coincides with the expectation value of $\exp(-N^2 W(\mathcal{O}))$ in the undeformed theory. Therefore, we can write the boundary coupling as $W(\langle \mathcal{O} \rangle) = W(\beta)$, and the boundary condition as

$$\alpha = \frac{\delta W}{\delta \beta}. \quad (3.5)$$

The last formula allows to generalize to an arbitrary non-linear deformation $W(\mathcal{O})$. From the gauge theory point of view, it is justified by the properties of the master field. At leading order in large N , a n -point correlation function of a single-trace operator is given by its expectation value

$$\langle \mathcal{O}^n \rangle = \langle \mathcal{O} \rangle^n , \quad (3.6)$$

so a non-linear function can be Taylor-expanded and the value of the multitrace operator substituted by powers of the single-trace operator.

The master field is a saddle point configuration of the path integral. If $\Gamma_0(\mathcal{O}_{cl})$ denotes the effective action of the theory, evaluated over some classical configuration \mathcal{O}_{cl} , then the saddle point equation is

$$\frac{\partial \Gamma_0}{\partial \mathcal{O}_{cl}} = 0 . \quad (3.7)$$

When we add a multitrace deformation, and we apply the property of factorization of the master field, we end up with

$$\left\langle \exp\left(-\int W(\mathcal{O})\right) \right\rangle \sim \exp\left(-\Gamma_0(\mathcal{O}_{cl}) - W(\mathcal{O}_{cl})\right) , \quad (3.8)$$

and the saddle point equation is

$$\frac{\partial \Gamma_0}{\partial \mathcal{O}_{cl}} + \frac{\partial W(\mathcal{O}_{cl})}{\partial \mathcal{O}_{cl}} = 0 . \quad (3.9)$$

So the master field configuration with a multitrace deformation is reduced to the single-trace case with an effective coupling

$$\alpha = \frac{\partial W(\mathcal{O}_{cl})}{\partial \mathcal{O}_{cl}} , \quad (3.10)$$

equivalent to the generalized boundary conditions.

3.2 Systematics of the mean field approximation

Let us consider a gauge-theory model specified by a single-trace action S_0 and a multitrace perturbation by a general function of a single-trace operator of the form

$$\mathcal{O} \sim \frac{1}{N} \text{tr} F^n + \dots \quad (3.11)$$

where the dots stand for other terms in gauge or matter fields. The complete action is

$$S = S_0 + N^2 \int d^d x \zeta \mathcal{O} + N^2 \int d^d x f(\mathcal{O}) , \quad (3.12)$$

where we have separated explicitly the linear part of $f(\mathcal{O})$. We shall assume that operator condensates in this theory, $\langle \mathcal{O} \rangle$, are determined in terms of the microscopic couplings, with at most a discrete degeneracy. In particular, this means that we will only consider theories whose single-trace limit $f \rightarrow 0$ has isolated vacua with a mass gap, separated from any possible moduli spaces of vacua.

The coupling ζ will be promoted to a source for the operator \mathcal{O} , although the large N master field will be assumed translationally invariant on \mathbf{R}^d , and ζ will be evaluated as a constant in all expectation values.

In the Hartree approximation, the expectation value $\langle \mathcal{O} \rangle$ may be calculated at $N = \infty$ from the single-trace effective theory with action

$$\bar{S} = S_0 + N^2 \int d^d x \bar{\zeta} \mathcal{O} , \quad (3.13)$$

with $\bar{\zeta}$ determined from the master equation:

$$\bar{\zeta} = \zeta + f' \left(\langle \mathcal{O} \rangle_{\bar{\zeta}} \right) . \quad (3.14)$$

The consideration of large N phase transitions requires comparing the values of the full partition function

$$\mathcal{Z}[\zeta, f] = \int DA e^{-S} \quad (3.15)$$

at different large N master fields. The path integral measure over the gauge field A may contain various other fields as well, although we use the notation DA for simplicity.

The effective single-trace partition function

$$\bar{\mathcal{Z}}[\bar{\zeta}] = \int DA e^{-\bar{S}} \quad (3.16)$$

can be used to compute the single-trace expectation values, but it is in general different from (3.15) at the saddle points.

In order to derive a useful expression for $\mathcal{Z}[\zeta, f]$ it is convenient to introduce appropriate auxiliary fields. First, we insert a delta-functional constraint by the identity

$$\mathbf{1} = \int \prod_x d\sigma_x \delta[\sigma - \mathcal{O}] , \quad (3.17)$$

which defines $\sigma(x)$ as a classical interpolating field for the local operator $\mathcal{O}(x)$. We can further exponentiate the delta-functional by means of a second auxiliary field

$$\delta[\sigma - \mathcal{O}] = \int \prod_x \frac{d\chi_x}{2\pi} e^{i \int \chi(\sigma - \mathcal{O})} . \quad (3.18)$$

It will be convenient to distribute democratically the factor of $(2\pi)^{-1}$ between the σ and χ measures. Defining

$$D\sigma = \prod_x \frac{d\sigma_x}{\sqrt{2\pi}} \quad (3.19)$$

and analogously for $D\chi$, we can write

$$\mathbf{1} = \int D\sigma D\chi e^{i \int \chi(\sigma - \mathcal{O})}, \quad (3.20)$$

which defines a formal path integral representation of the full partition function,

$$\mathcal{Z}[\zeta, f] = \int D\sigma D\chi \mathcal{Z}_0 \left[\zeta + i \frac{\chi}{N^2} \right] \exp \left[-N^2 \int f(\sigma) + i \int \chi \sigma \right]. \quad (3.21)$$

In this expression \mathcal{Z}_0 denotes the single-trace partition function that results by setting $f = 0$.

The connected functionals of the full and single-trace theory are given by

$$W[\zeta, f] = -\frac{1}{N^2} \log \mathcal{Z}[\zeta, f], \quad W_0[\zeta] = -\frac{1}{N^2} \log \mathcal{Z}_0[\zeta]. \quad (3.22)$$

In these definitions, ζ is treated as a spacetime-dependent source. At the saddle points we will assume translational invariance on \mathbf{R}^d and it will be useful to define the volume densities

$$W[\zeta, f] = \int d^d x w(\zeta, f), \quad W_0[\zeta] = \int d^d x w_0(\zeta), \quad (3.23)$$

as a function of the microscopic couplings.

Both W_0 and all its functional derivatives have a $1/N^2$ expansion with leading term of $O(1)$. They generate the set of connected correlators of $\mathcal{O}(x)$ in the single-trace theory. For example, the one-point function is of $O(1)$,

$$\langle \mathcal{O} \rangle_\zeta = \frac{\delta W_0}{\delta \zeta} = w'_0(\zeta), \quad (3.24)$$

while the connected two-point function is of $O(1/N^2)$,

$$\langle \mathcal{O}(x_1) \mathcal{O}(x_2) \rangle_{c, \zeta} = -\frac{1}{N^2} \frac{\delta W_0}{\delta \zeta(x_1) \delta \zeta(x_2)}. \quad (3.25)$$

In order to derive a $1/N$ expansion for $\mathcal{Z}[\zeta, f]$ we evaluate the path integral over the auxiliary fields in the saddle-point approximation. We write $\sigma = \sigma_c + \sigma'/N$ and $\chi = \chi_c + N\chi'$, and we determine σ_c and χ_c requiring the cancellation of the $O(N)$ terms. This leads to the equations

$$\sigma_c = \frac{\delta W_0}{\delta \zeta} \Big|_{\zeta + i\chi_c/N^2}, \quad i\chi_c = N^2 f'(\sigma_c). \quad (3.26)$$

Defining an effective coupling

$$\bar{\zeta} = \zeta + \frac{i\chi_c}{N^2} \quad (3.27)$$

we see that $\sigma_c = \langle \mathcal{O} \rangle_{\bar{\zeta}}$, and the saddle-point equations (3.26) are equivalent to the master equation (3.14). These equations imply that the saddle point of the χ integral lies in the imaginary axis for real values of the one-point function. In this case, one must deform the contour of integration of the zero mode of χ accordingly.

The leading term in the $1/N$ expansion of the partition function is given by

$$w(\zeta, f) = w_0(\bar{\zeta}) + f \left(\langle \mathcal{O} \rangle_{\bar{\zeta}} \right) - \langle \mathcal{O} \rangle_{\bar{\zeta}} f' \left(\langle \mathcal{O} \rangle_{\bar{\zeta}} \right) + O(1/N^2). \quad (3.28)$$

This shows that the partition function at large N is not just the partition function of the effective single-trace model.

The local stability of a given master field is controlled by the functional quadratic in the perturbation fields σ', χ' , of $O(1)$ in the large N expansion around the saddle point. This term contributes

$$-\log \mathcal{Z}[\zeta, f] = O(N^2) + \frac{1}{2} \log \text{Det}[\mathcal{K}] + O(1/N^2), \quad (3.29)$$

where \mathcal{K} is a nonlocal operator acting on the field-space (χ', σ') as

$$\mathcal{K} = \begin{pmatrix} \bar{G}_2 & -i \\ -i & f_c'' \end{pmatrix}, \quad (3.30)$$

The higher-order functional derivatives of W_0 , together with the higher derivatives of the multitrace potential $f(\sigma)$, define effective vertices for the $1/N$ expansion of (3.21). The connected single-trace correlators define nonlocal vertices of the χ' field,

$$V_W = \sum_{n \geq 3} \frac{1}{N^{n-2}} \frac{i^n}{n!} \int d^d x_1 \cdots d^d x_n \frac{\delta^n W_0}{\delta \zeta(x_1) \cdots \delta \zeta(x_n)} \Big|_{\bar{\zeta}} \chi'(x_1) \cdots \chi'(x_n), \quad (3.31)$$

where each functional derivative of W_0 has a separate expansion in powers of $1/N^2$ with leading term of $O(1)$.

Both the saddle-point equations (3.26) and the propagator (3.30) depend implicitly on the full single-trace connected functional W_0 , which itself has a $1/N^2$ expansion with leading term of $O(1)$. In principle, we have the choice of keeping this implicit $1/N$ expansion in the value of the saddle point σ_c, χ_c and the effective propagator \mathcal{K} . However, we often ignore the explicit form of W_0 beyond the planar approximation and, in practice, we solve

for σ_c, χ_c just at the leading (planar) order. In this case we may include the nonplanar dependence of (3.26) and (3.30) via a series of explicit tadpole and mass insertions. These new vertices have the form (3.31) with $n = 1, 2$ and W_0 replaced by its “non-planar” part with leading scaling of $O(1/N^2)$. This means that the tadpoles form a series with leading term of $O(1/N)$, whereas the mass insertions start at $O(1/N^2)$.

Finally, the vertices for the σ' field are local,

$$V_\sigma = \sum_{m \geq 3} \frac{1}{N^{m-2}} \frac{1}{m!} \int d^d x f^{(m)}(\sigma_c) (\sigma'_x)^m. \quad (3.32)$$

Using \mathcal{K} as a propagator and (3.31), (3.32) as vertices, we can calculate the $1/N$ corrections to the master field in a systematic diagram technique. For quadratic perturbations, $f''' = 0$, the σ field is free and can be explicitly integrated out, leaving only the diagram technique of the χ field, as in the treatment of [27, 28].

Regarding the NLST interpretation, if the single-trace model is associated to some string background X_0 via AdS/CFT or a deformation of it thereof, the perturbation expansion in powers of the multitrace vertices $f^{(m)}(\sigma_c)$ defines the nonlocal worldsheet interactions, according to [26]. The content of the Hartree approximation is simply that one-point functions and partition functions may be calculated at large N by working in a modified single-trace background \bar{X} , characterized by effective single-trace couplings $\bar{\zeta}$. However, the physics of the NLST goes much beyond the one-point functions and the large N vacuum energy. In particular, the stability of the NLST cannot be inferred directly from the stability of \bar{X} in the single-trace theory, but instead requires a specific analysis.

3.3 Stability of the Master Field

The global stability properties of the perturbed model depend to a large extent on the global properties of the function $f(\sigma)$ for large values of σ . If this function is unbounded from below we can expect a globally unstable model. In this section we shall concentrate on the local stability properties of a given saddle point, characterized by a solution of the master equations (3.26).

In momentum space the operator \mathcal{K} has the block form (3.30) for each value of the momentum. The naive stability conditions demand positivity of the eigenvalues

$$\lambda_k^\pm = \frac{1}{2} (f_c'' + \bar{G}_2(k)) \pm \frac{1}{2} \sqrt{((f_c'' - \bar{G}_2(k))^2 - 4)}. \quad (3.33)$$

This amounts to the reality condition

$$|f_c'' - \overline{G}_2(k)| > 2, \quad (3.34)$$

together with the positivity conditions

$$f_c'' + \overline{G}_2(k) > 0 \quad \text{and} \quad 1 + f_c'' \overline{G}_2(k) > 0. \quad (3.35)$$

In ordinary field theories we expect $\overline{G}_2(k) > 0$ for Hermitian $\mathcal{O}(x)$, so that the violation of the stability conditions can only occur for sufficiently negative values of f_c'' . When these conditions are not met, we can still define the integrals by analytic continuation in f_c'' or, equivalently, by an appropriate contour rotation of the σ', χ' integrals around the saddle point. However, in this process physical quantities will pick up complex phases that change their physical interpretation. One simple example of this phenomenon is the imaginary part of the vacuum energy, which should be interpreted as the total decay width of the unstable saddle point.

Since χ is a formal auxiliary field, it is not obvious that all the conditions $\lambda_k^\pm > 0$ have the same physical status. For example, the contribution to the vacuum energy coming from each momentum mode is given by

$$\frac{1}{2} \log (\lambda_k^+ \lambda_k^-) = \frac{1}{2} \log [1 + f_c'' \overline{G}_2(k)], \quad (3.36)$$

and simply demanding that this contribution be real imposes the less restrictive condition

$$1 + f_c'' \overline{G}_2(k) > 0, \quad (3.37)$$

In fact, to the extent that we are interested in the exact correlation functions of the operator $\mathcal{O}(x)$, we must focus on the propagation properties of the $\sigma(x)$ field after $\chi(x)$ has been integrated out, since we have

$$\langle \mathcal{O}(x_1) \cdots \mathcal{O}(x_n) \rangle = \langle \sigma(x_1) \cdots \sigma(x_n) \rangle \quad (3.38)$$

as an exact statement in the complete theory. Therefore, we first integrate over χ' and obtain an effective action for σ' of the form

$$\exp(-\Gamma_{\text{eff}}[\sigma']) = \text{Det}^{-1/2} [\overline{G}_2] \exp \left[-\frac{1}{2} \int \sigma' (\overline{G}_2^{-1} + f_c'') \sigma' + O(1/N) \right], \quad (3.39)$$

where we have omitted the interaction terms that are suppressed by powers of $1/N$. Integrating now over σ' in the gaussian approximation we obtain the previous result for the total determinant (3.36),

$$\text{Det}^{-1/2} [\overline{G}_2] \cdot \text{Det}^{-1/2} [\overline{G}_2^{-1} + f_c''] = \text{Det}^{-1/2} [1 + f_c'' \overline{G}_2], \quad (3.40)$$

where we assume a convenient regularization procedure to make sense of these manipulations. More generally, the $1/N$ expansion of the correlators (3.38) can be calculated using Feynman rules with effective kinetic term

$$\mathcal{K}_\sigma = \overline{G}_2^{-1} + f_c'' . \quad (3.41)$$

Hence, the physical stability condition demands positivity of this (Euclidean) kinetic term for all momenta. Assuming $\overline{G}_2(p) > 0$, this condition is equivalent to (3.37) above.

In order to give a more physical characterization of the stability conditions let us consider the spectral representation of the single-trace two-point function

$$\overline{G}_2(p) = \int dz \frac{\rho(z)}{z + p^2} , \quad (3.42)$$

with $\rho(z) > 0$ the spectral density (for simplicity, we assume that $\mathcal{O}(x)$ is scalar and Hermitian). Expanding \overline{G}_2^{-1} near $p^2 = 0$ we have

$$\overline{G}_2(p) \approx \frac{Z_0(\mathcal{O})}{p^2 + M_0^2} , \quad (3.43)$$

where the wave-function rescaling, $Z_0(\mathcal{O})$, and the mass gap, M_0^2 , of the single-trace theory are assumed to be positive,

$$Z_0(\mathcal{O}) = \frac{(\int dz \rho(z)/z)^2}{\int dz \rho(z)/z^2} , \quad M_0^2 = \frac{\int dz \rho(z)/z}{\int dz \rho(z)/z^2} . \quad (3.44)$$

Hence, the physical stability condition (3.37) boils down to

$$1 + f_c'' \frac{Z_0(\mathcal{O})}{M_0^2} > 0 . \quad (3.45)$$

The single-trace mass gap gets renormalized and this defines an effective mass gap,

$$M_0^2 \longrightarrow M_{\text{eff}}^2 = M_0^2 + Z_0(\mathcal{O}) f_c'' \geq 0 , \quad (3.46)$$

that must be positive for stability.

3.3.1 Stability and the Master Equation

We can relate (3.37) to the master equation by evaluating $\overline{G}_2(0)$. The integrated two-point function at zero momentum can be formally written as

$$\int d^d x \overline{G}_2(0) = N^2 \int d^d x \int d^d y \langle \mathcal{O}(x) \mathcal{O}(y) \rangle_{c, \overline{\zeta}} = - \int d^d x w_0''(\overline{\zeta}) . \quad (3.47)$$

Hence, the stability condition (3.37) becomes

$$1 - f_c'' w_0''(\bar{\zeta}) > 0 . \tag{3.48}$$

On the other hand, the master equation can be written as $\zeta = H(\bar{\zeta})$, where

$$H(\bar{\zeta}) = \bar{\zeta} - f'(w_0'(\bar{\zeta})) . \tag{3.49}$$

This function satisfies

$$H'(\bar{\zeta}) = 1 - f_c'' w_0''(\bar{\zeta}) , \tag{3.50}$$

which is the expression appearing in the stability condition (3.48). Therefore, $H(\bar{\zeta})$ is monotonically increasing (decreasing) for stable (unstable) solutions of the master equation. We can thus determine the stability of the solutions by a simple glance at the plot of the function $H(\bar{\zeta})$ (c.f. Fig. 3.3.1). In particular, the solutions of $H'(\bar{\zeta}) = 0$ mark the stability boundary of a given branch and correspond to the onset of the nonlocal tachyons.

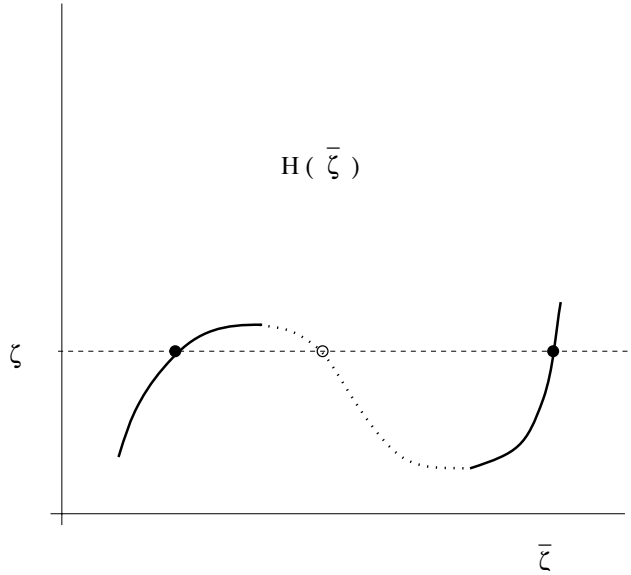


Figure 3.1: Sketch of a function $H(\bar{\zeta})$ leading to various solutions of the master equation. Stable branches are indicated in solid lines, separated by locally unstable branches in dotted lines. At the extrema of $H(\bar{\zeta})$ we have the onset of the tachyonic instabilities.

The function $H(\bar{\zeta})$ also controls the monotonicity of the vacuum energy with respect to the effective coupling $\bar{\zeta}$. Starting from the general expression (3.28) we can write the vacuum energy density as

$$w = w_0 + f(w_0') - w_0' f'(w_0') , \tag{3.51}$$

where all functions depend implicitly on $\bar{\zeta}$. Taking the derivative with respect to $\bar{\zeta}$ and using the definition of $H(\bar{\zeta})$ in (3.49) we find

$$w'(\bar{\zeta}) = w'_0(\bar{\zeta}) H'(\bar{\zeta}) . \quad (3.52)$$

If the condensate of the single-trace theory, $\langle \mathcal{O} \rangle \sim w'_0$, is a monotonic function of $\bar{\zeta}$ there is a correlation between the monotonicity of $H(\bar{\zeta})$ and that of the total vacuum energy.

Chapter 4

Explicit Examples

A simple model is the standard “approximation” of QCD in terms of Dp -branes (with $p < 5$) at finite temperature [42]. One starts by engineering a non-supersymmetric version of Yang–Mills theory in $d = p$ Euclidean dimensions by considering the low-energy limit of a hot Dp -brane.

The important expansion parameter is the effective 't Hooft coupling of the YM_d theory at the energy scale set by the temperature T of the SYM_{d+1} theory on the hot D-brane (c.f. [43, 44]),

$$\lambda_d \sim g_s N \left(\sqrt{\alpha'} \right)^{d-3} T^{d-3} , \quad (4.1)$$

where g_s is the string coupling and α' the string's Regge slope. For $\lambda_d \ll 1$ perturbative Feynman diagrams give a good description, whereas for $\lambda_d \gg 1$ we can use the AdS/CFT dual in terms of the near-horizon metric of the black D-branes [43].

The single-trace action is given by

$$S_0 = \frac{N^2}{\lambda_d} \int d^d x \mathcal{L}_d , \quad \mathcal{L}_d = \frac{T^{d-4}}{2N} \text{tr} F^2 + \dots , \quad (4.2)$$

where the dots stand for regularization artefacts at the temperature scale T or above (superpartners, higher-dimensional modes or string excitations). In what follows we shall simplify the notation by adopting units in which $T = 1$.

At $\lambda_d \gg 1$ the supergravity approximation yields an explicit value for the vacuum energy in terms of the free energy of the hot D-branes,

$$w_0 = -(5 - d) C_d \lambda_d^{\frac{d-3}{5-d}} , \quad (4.3)$$

where C_d is a positive constant. From here one finds

$$\langle \mathcal{L}_d \rangle = w'_0 = (d-3) C_d \lambda_d^{\frac{2}{5-d}}, \quad G_2(0) = -w''_0 = \frac{2(d-3)}{5-d} C_d \lambda_d^{\frac{7-d}{5-d}}. \quad (4.4)$$

Hence, we have all the ingredients needed to consider multitrace deformations by a non-linear function of the operator $\mathcal{L}_d(x)$,

$$S = S_0 + N^2 \int d^d x f(\mathcal{L}_d). \quad (4.5)$$

Defining

$$\zeta = \frac{1}{\lambda_d}, \quad H(\bar{\zeta}) = \bar{\zeta} - f' \left((d-3) C_d \bar{\zeta}^{\frac{2}{d-5}} \right), \quad (4.6)$$

we have an effective single-trace model determined by the inverse 't Hooft coupling $\bar{\zeta}$, which acts as a curvature expansion parameter of the black Dp -brane metric. From this model we can calculate the condensate $\langle \mathcal{L}_d \rangle$ as a function of $\bar{\zeta}$, which in turn is determined by the master equation $\zeta = H(\bar{\zeta})$.

The multitrace deformation is trivial for $d = 3$ in agreement with the fact that the D3-brane free energy is independent of the dilaton in the leading supergravity approximation. Incidentally, we notice that $G_2(0) = -w''_0 < 0$ for $d < 3$. This violation of the positivity of the two-point function at zero momentum is presumably due to the non-Hermiticity of the effective Lagrangian operator (4.2), which would be dominated at $\lambda_d \gg 1$ by the regularization artifacts. This fact renders the $d < 3$ models rather unphysical for the matters discussed here. Therefore, in the following we restrict attention to $d = 4$ and drop the d -dimensional subscript from all quantities. We also simplify the formulas by setting $C_4 = 1$ with an appropriate choice of coupling parameters.

The transition between the perturbative and supergravity descriptions occurs at the “correspondence line” of [45]. For the single-trace model it is given by $\zeta \sim 1$, which is perturbed by multitraces to $\bar{\zeta} \sim 1$ or, in terms of the original coupling

$$\zeta = H(1) = 1 - f'(1). \quad (4.7)$$

We see that, depending on the sign of $f'(1)$, the multitraces increase or decrease the supergravity domain in ζ -space. We discuss in the Appendix A some specific choices for the multitrace perturbation.

4.1 Multitraces and Topology-Changing Phase Transitions

Large- N phase transitions induced by multitrace couplings arise from the many possible solutions of the master equation $\zeta = H(\bar{\zeta}_i)$. However, in most cases considered so far the different solutions $\bar{\zeta}_i$ are continuously connected and the corresponding string backgrounds have the same topology when studied in the supergravity approximation. Large- N phase transitions with change of spacetime topology are known in the AdS/CFT framework, the most famous example being the Hawking–Page transition [42, 46], corresponding to a CFT on a finite-radius sphere. From the CFT point of view, the phase transition arises as a finite-size effect.

The interplay between multitrace-induced and topology-changing transitions is an interesting question that we address in this section. Fortunately, the example model based on hot D-branes does show topology-changing transitions when the Yang–Mills theory is compactified on a torus, so that we can carry on our study in a rather direct way. We start with a short review of the topology-changing transitions corresponding to finite-size effects of SYM models on toroidal compactifications.

4.1.1 Review of the Single-Trace Case

Let us consider the compactification of the hot D4-brane on a $(4 - p)$ -dimensional torus of size L . In the perturbative description, the Euclidean spacetime of the SYM model at finite temperature has the topology $\mathbf{R}^p \times \mathbf{S}_\beta^1 \times (\mathbf{S}_L^1)^{4-p}$, with $\beta = 1/T$ and we take the supersymmetric spin structure on the torus of size L .

In the perturbative regime, $\lambda \ll 1$, the thermodynamics of the SYM_{4+1} theory changes character at $TL \sim 1$, from five-dimensional scaling of the entropy $S \sim T^4$ at $TL > 1$ to a p -dimensional scaling $S \sim T^{p-1}$ at $TL < 1$. At strong coupling $\lambda \gg 1$, the AdS/CFT correspondence incorporates this change of behavior by a transition between topologically distinct backgrounds, both with the same asymptotic boundary conditions [44]. The first background is the near-horizon geometry of the original black D4-brane wrapped on the $(4 - p)$ -torus. This metric is T-dual to that of black Dp -branes, localized on the torus, but distributed uniformly over its volume, i.e. the so-called black brane “smeared” over $4 - p$ transverse dimensions.

The vacuum energy per unit volume in \mathbf{R}^p is the same for both T-dual metrics and is given by the thermodynamic free energy of the five-dimensional theory, i.e. we can write

$$w_0 = -\frac{1}{N^2 V_p} \log \mathcal{Z}_0(T), \quad (4.8)$$

where V_p is the volume in the noncompact \mathbf{R}^p directions. In general, for a $(d + 1)$ -dimensional SYM theory at finite temperature T on a spatial volume V_d we have (c.f. [43, 44])

$$-\log \mathcal{Z}_0(T) = -N^2 V_d C_d (g_{\text{eff}}^2 N)^{\frac{d-3}{5-d}} T^{\frac{9-d}{5-d}}, \quad (4.9)$$

where g_{eff}^2 is the effective SYM coupling constant of mass dimension $3 - d$. Considering now the particular case of D4-branes wrapped on the \mathbf{T}^{4-p} torus, the effective coupling is $g_{\text{eff}}^2 N = \lambda/T$ and

$$w_{0,s} = -L^{4-p} C_4 \lambda T^4. \quad (4.10)$$

With the same quantum numbers and asymptotic behavior, one can consider the metric of Dp-branes fully localized on the $(4 - p)$ -torus. The corresponding vacuum energy is related to the thermodynamic free energy of the effective SYM theory in p Euclidean dimensions, with effective coupling $g_{\text{eff}}^2 N = \lambda L^{p-4}/T$,

$$w_{0,\ell} = -N^2 C_p (\lambda L^{p-4}/T)^{\frac{p-3}{5-p}} T^{\frac{9-p}{5-p}}. \quad (4.11)$$

The smeared metric dominates for large temperatures, whereas the localized metric takes over at low temperatures. The cross-over temperature is given by

$$1 = \frac{w_{0,s}}{w_{0,\ell}} = \frac{C_4}{C_p} (\lambda L T)^{\frac{2(p-4)}{p-5}}, \quad (4.12)$$

which defines the ‘‘localization curve’’

$$\lambda \sim \frac{1}{LT}. \quad (4.13)$$

The transition between the smeared and the localized geometry is reminiscent of the Gregory–Laflamme instability [47]. They are, however, very different, since both backgrounds are locally stable in the near-horizon regime (they both have positive specific heat [48]). Thus, we have a first-order phase transition between locally stable backgrounds.

We plot in Fig. 4.1.1 a phase diagram of the single-trace theory as a function of $\zeta = 1/\lambda$ and the dimensionless combination LT . The localization curve (4.13) continues at weak coupling as $LT = 1$. The correspondence lines separating the perturbative and the supergravity regimes are $\zeta = 1$ for large LT and $\zeta = (LT)^{p-4}$ for smaller values of LT .

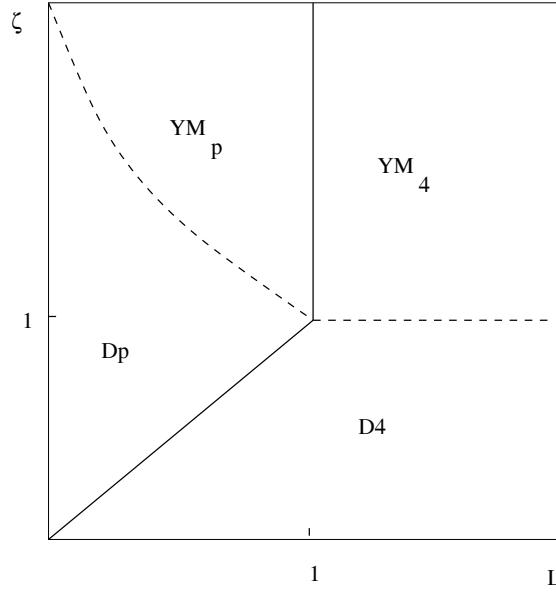


Figure 4.1: Phase diagram of the finite-temperature D4-brane at large N , as a function of the effective dimensionless coupling $\zeta = 1/\lambda$ and the size of the torus LT , in units of the temperature. Full lines denote finite-size localization transitions and dashed lines correspond to correspondence regions between supergravity and perturbative descriptions.

4.1.2 The Multitrace Case

Since the multitrace deformation modifies the vacuum energy through (3.28) the phase transition curves change accordingly. Let us consider the simple case of a monomium perturbation of the form (A.1) in the $d = 4$ case. The “smeared” phase over the $(4 - p)$ -torus of size L has vacuum energy density

$$w_s = -L^{4-p} \bar{\zeta}_s^{-1} - L^{4-p} \xi \frac{n}{n+1} \left(\bar{\zeta}_s^{-2} \right)^{n+1}, \quad (4.14)$$

where we have chosen couplings so that $C_4 = 1$ and we use units with $T = 1$ throughout this section. $\bar{\zeta}_s$ denotes the selfconsistent coupling in the smeared phase, obeying the master equation

$$\zeta = \bar{\zeta}_s - \xi \bar{\zeta}_s^{-2n}. \quad (4.15)$$

On the other hand, the phase of localized black Dp -branes yields similar expressions after dimensional reduction to \mathbf{R}^p . The effective dimensionless coupling arising through the standard rule

$$\frac{1}{\lambda} \int d^4x \longrightarrow \frac{L^{4-p}}{\lambda} \int d^p x \quad (4.16)$$

is given by

$$\zeta_{\text{eff}} = L^{4-p} \zeta , \quad (4.17)$$

and similarly for $\bar{\zeta}$. The master equation of the localized phase is then

$$\zeta = \bar{\zeta}_\ell - \xi \left[(p-3) C_p (\bar{\zeta}_\ell L^{4-p})^{\frac{2}{p-5}} \right]^n . \quad (4.18)$$

The resulting vacuum energy is given by

$$w_\ell = -(5-p) C_p (L^{4-p} \bar{\zeta}_\ell)^{\frac{3-p}{5-p}} - \xi \frac{n}{n+1} \left[(p-3) C_p (\bar{\zeta}_\ell L^{4-p})^{\frac{2}{p-5}} \right]^{n+1} . \quad (4.19)$$

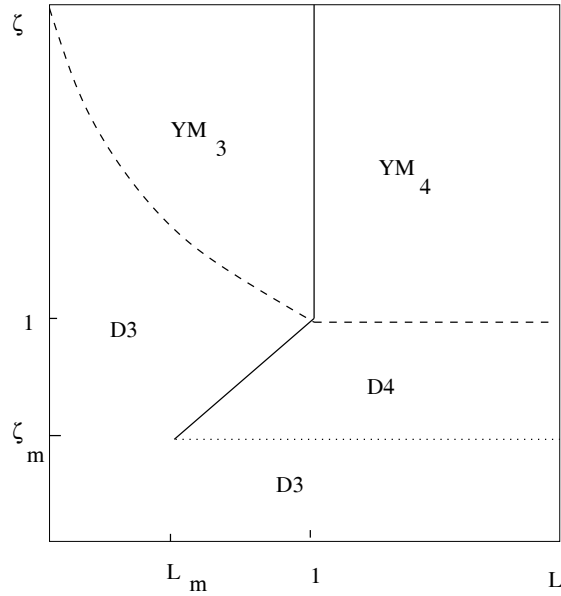


Figure 4.2: Phase diagram for the localization transition between D4-branes and D3-branes with a multitrace perturbation $\xi < 0$. The localization line terminates at (ζ_m, L_m) and the dotted line signals the local instability of the D4-branes, induced by the multitrace couplings.

In general, we see that the multitrace perturbation is not qualitatively significant for

$$\zeta \gg |\xi|^{\frac{1}{2n+1}} \quad (4.20)$$

in the smeared phase. In the localized phase, the qualitative features are standard for

$$\zeta \gg L^{p-4} |\xi|^{\frac{5-p}{5-p+2n}} . \quad (4.21)$$

We shall further simplify the analysis by choosing $p = 3$, i.e. compactification on a single circle of size L . In this particular case the equations (4.18) and (4.19) governing the localized phase collapse to very simple expressions:

$$\zeta = \bar{\zeta}_\ell, \quad w_\ell = -C_3. \quad (4.22)$$

The transition curve between the smeared and the localized phases in the supergravity regime follows from the equation

$$1 = \frac{w_s}{w_\ell} = \frac{L}{2C_3 \bar{\zeta}_s} \left[1 + \frac{n}{n+1} \frac{\xi}{\bar{\zeta}_s^{2n+1}} \right]. \quad (4.23)$$

For $\xi < 0$ we have a minimal value of $\bar{\zeta}_s$ for which the smeared solution is locally stable:

$$\bar{\zeta}_m = (2n |\xi|)^{\frac{1}{2n+1}}. \quad (4.24)$$

The main effect of this in the (ζ, L) phase diagram is the abrupt termination of the localization line (4.23) at the point (ζ_m, L_m) , with

$$\zeta_m = \frac{2n+1}{2n} (2n |\xi|)^{\frac{1}{2n+1}}, \quad L_m = \frac{2C_3 (n+1)}{2n+1} (2n |\xi|)^{\frac{1}{2n+1}}. \quad (4.25)$$

Hence, part of the supergravity regime that was dominated by D4-branes is now covered by the D3-brane phase due to the local instabilities induced by the multitrace coupling (see Fig. 4.1.2).

For $\xi > 0$ the D4-brane phase is locally stable, but the condition $\zeta > 0$ still enforces a minimum value of $\bar{\zeta}_s$, given by $\bar{\zeta}_c^{2n+1} = \xi$. The critical length at this point is

$$L_c = \frac{n+1}{2n+1} 2C_3 \bar{\zeta}_c. \quad (4.26)$$

Expanding the master equation (4.15) and the localization equation (4.23) near the point $(\zeta = 0, L_c)$ we find

$$\zeta \approx \frac{2n+1}{n+1} \bar{\zeta}_c \left(1 - \frac{L_c}{L} \right) \quad (4.27)$$

in the vicinity of the $\zeta = 0$ axis. The resulting phase diagram is depicted in Fig. 4.1.2.

Thus, comparing with Fig. 4.1.1, we see that the multitraces tend to modify the structure of topology-changing phases in the extreme supergravity regime (low values of the effective coupling $\bar{\zeta}$).

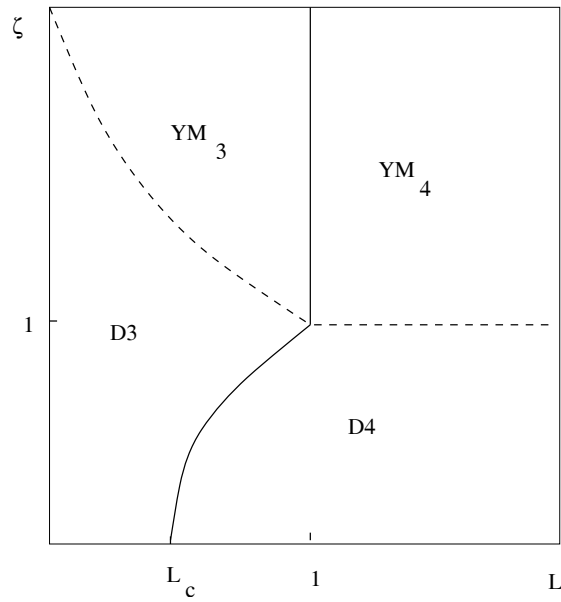


Figure 4.3: Phase diagram for the localization transition between D4-branes and D3-branes with a multitrace perturbation $\xi > 0$. The localization line intersects the $\zeta = 0$ axis at $L = L_c$, cutting off part of the D4-brane phase. In this case, there are no local instabilities.

Chapter 5

Conclusions

We have shown that AdS/CFT treatment of multitraces is equivalent to the leading Hartree approximation. We have applied mean field methods to study multitrace deformations of gauge theories in the large- N limit. The deformation has been seen to be equivalent to a single-trace deformation with a coupling that depends on the master field and that has to be evaluated self-consistently, in a Hartree approximation. The global properties of the self-consistent master equation, concretely the properties of monotonicity of the function $H(\bar{\zeta})$ in (3.49), are related to the local stability of the master field. These properties of the master field, and a systematic formal $1/N$ expansion can be discussed using auxiliary fields. Since multitrace deformations correspond to non-local string theories, we have found new classes of tachyonic instabilities of these models, induced by the multitrace couplings. The instabilities appear even though one can compute operator condensates in the effective single-trace background. It would be interesting to find the connection with the "stringy exclusion principle".

As a concrete application, we have studied the deformation of the thermodynamic phase diagram of hot D4 branes in finite volume under the effect of multitraces. We have found that large- N phase transitions are strongly affected when the coupling is $O(1)$ in dimensionless units. The analytic deformations we have introduced affect to the gravitational region of the phase diagram. If the deformation were non-analytic, it would affect to the Yang-Mills region (App. A).

Further work can be directed towards a better understanding of the tachyonic instabilities of the master field from the dual gravitational background point of view and the relation to supersymmetry breaking (in our examples supersymmetry is already broken at

the single-trace level to generate a mass gap). It would also be interesting to calculate the $1/N$ effects.

Part II

The holographic axial anomaly

Chapter 6

Motivation

Since the beginning of the AdS/CFT correspondence [16–18] a main goal has been to find similar dictionaries for non-supersymmetric and non-conformal theories, and to go beyond the large- N limit. The motivation is to find a holographic dual of QCD. Hopefully, the correspondence would allow to compute many of the strong-coupling properties that arise at low energies. This would be a great accomplishment of the correspondence, since our present understanding on these matters is at best qualitative or it is based on numerical lattice computations.

The first success of this approach is the insight we gain by having a geometrical formulation of a plethora of non-perturbative effects as anomalies, confinement, the appearance of a mass gap, monopoles, instantons, baryons, phases, etc (see the reviews [1, 49, 50] and references therein). More quantitatively, full spectra of glueballs [51, 52] and mesons [53–59] have been computed and sometimes compared with lattice simulations, with not bad agreement, once the parameters have been fixed appropriately. Recall that the spectrum is found by solving field equations of motion on a higher-dimensional AdS space, so the coincidence is remarkable. A different application has been to extract hydrodynamic properties of high-temperature phases of the gauge theory from bulk correlation functions, with many interesting results [60–68]. The great difficulties found in theoretical and numerical treatments of hydrodynamical properties of plasma phases makes the holographic approach remarkably useful.

An interesting issue is how the $U(1)_A$ -axial anomaly is realized in holographic models with flavor. The axial anomaly in the large- N limit is a subtle matter. The reason is that although we expect any dependence on the vacuum angle θ to disappear when we introduce

massless flavors, their contributions are subleading in the 't Hooft expansion [19]. It was proposed that the would-be Goldstone boson of the axial symmetry (η') has a mass that is suppressed by N according to the Witten-Veneziano formula [69, 70]. This assumes a θ/N dependence on the path integral, but θ must be an angle, so there should be a sum over branches $\theta + 2\pi k$, $k \in \mathbf{Z}$ in order to be consistent [71, 72]. Gauge/gravity dual models provide a new arena to test these ideas. We will see that the picture above is confirmed.

6.1 Holographic QCD-like models

According to the AdS/CFT correspondence, a string theory in $AdS_{d+1} \times X^{9-d}$ ($d = 2, 3, 4, 6$) spacetime is equivalent to a conformal gauge theory in flat spacetime. The isometries of AdS space map to the conformal group of flat space, while the isometries of the compact space X^{9-d} map to global symmetries of the gauge theory. Once we have identified the symmetries, the map extends to representations, where fields on the gravity side map to operators on the gauge side. If the theories are supersymmetric, then the supercharges match accordingly. In the map there are three points to remark

1. The radial coordinate of AdS corresponds to the energy scale of the gauge theory. Moving from the conformal boundary of AdS at infinity to the origin is equivalent to follow the renormalization group flow from high to low energies.
2. Boundary values of the fields in AdS determine the background and correspond to insertion of dual operators in the bare Lagrangian of the gauge theory.
3. The parameters on both sides are related. Roughly speaking, the string coupling and the curvature radius of AdS map to $1/N$ and the 't Hooft coupling $\lambda_t = g_{\text{YM}}^2 N$. For $d \neq 4$ the gauge coupling is dimensionful, so string tension factors have to be included. The effective coupling runs with the scale and this is reflected on the radial dependence of the curvature and the dilaton.

In principle, the correspondence could be generalized to any (super)gravity background and dual field theory, as long as there is a coordinate that could be identified with the energy scale of the theory. And we should be able to construct a map between fields and operators, of course. If we define the correspondence through a near-horizon limit of a brane, we should take care that the closed and open string sectors decouple. For D-branes, they must have codimension greater than two. The duality has also been considered

for theories that are neither gravity (higher spin theories) nor field theories (little string theories).

On the way towards QCD, usually a ten-dimensional background of critical strings is the starting point. The geometry will include an AdS factor, whose radial coordinate plays the role of the energy scale of the theory. Any radial dependence will have the meaning of an RG flow of the quantities involved, with the boundary at spatial infinity corresponding to the UV of the gauge theory. Therefore, if we deform the AdS geometry far away from the boundary, the dual theory will flow from a conformal UV fixed point to a non-conformal low-energy effective theory. The deformation will correspond to the insertion of a relevant operator in the gauge theory Lagrangian.

For QCD considerations, the interesting deformations of the geometry are such that they effectively induce a “wall” at some value of the radial coordinate, so excitations coming from the boundary will stop there. In the gauge theory, the interpretation is that there is a mass gap, below which there are no propagating degrees of freedom. The “wall” also implies that the theory is confining, so we can identify the radial position of the “wall” with the strong coupling scale Λ_{YM} .

In ten-dimensional backgrounds, there is a compact part of the geometry, so there are Kaluza-Klein modes with a mass characterized by the size of the compact space. These modes are charged under the global internal symmetries of the field theory, so they do not correspond to any pure Yang-Mills state. They are related to supersymmetric degrees of freedom, so we can break supersymmetry with an appropriate election of the compact space. The scale of SUSY breaking Λ_{UV} will be given by the size of the compact space.

In order to have a good theory of QCD, we would like to have a hierarchy between the high-energy scale and the strong-coupling scale $\Lambda_{YM} \ll \Lambda_{UV}$. The hierarchy will be induced by a small value of the 't Hooft parameter at the high energy scale $\lambda(\Lambda_{UV}) \ll 1$, so that the dual low-energy effective theory is asymptotically free (Fig. 6.1)

$$\Lambda_{YM} \sim \Lambda_{UV} e^{-C/\lambda} \ll \Lambda_{UV} . \quad (6.1)$$

In this case, the observables at scales $\leq \Lambda_{YM}$ will be determined by this scale. For instance, the quark condensate $\langle \bar{\psi}\psi \rangle \sim \Lambda_{YM}^3$, the vacuum energy $\sim \Lambda_{YM}^4$, etc.

However, in the dual theory a small 't Hooft coupling is equivalent to large curvatures. In principle, this will induce large stringy corrections over quantities computed using the supergravity approximation. Since we still lack a comprehensive formulation of sigma

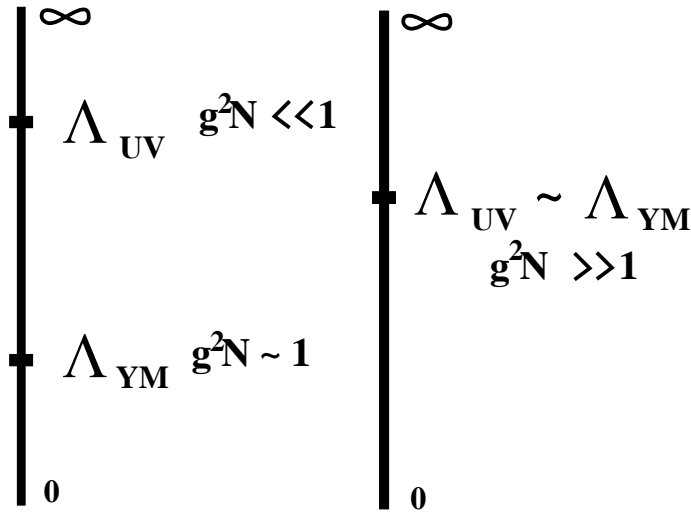


Figure 6.1: On the left, the RG flow corresponding to the confining dual of a highly curved geometry $g^2 N \ll 1$. On the right, the RG flow corresponding to small curvatures $g^2 N \gg 1$. Supersymmetric modes start to decouple below the high-energy scale Λ_{UV} , while the mass gap associated to confinement is given by Λ_{YM} .

models in the background we are considering, we will lose analytical control over the results. If we keep the geometry with small curvatures, then we do not know any model where the strong coupling scale decouples from the high energy scale (Fig. 6.1). Therefore, our model of QCD will be contaminated with spurious modes. Observables will depend on the high-energy scale Λ_{UV} , and will also have a parametric dependence with the 't Hooft coupling.

At this point there are two ways to proceed, the first one is to live with it and hope that the properties of the theories we can study will not change too much compared with the theories we are interested in study. A second possibility is to get ride of unwanted modes from the beginning. In this line, non-critical strings are good candidates since they are defined on lower dimensional spaces. However, in the end they share the problem of stringy corrections, since they live on highly curved spaces [73–81]. In any case, until we are able to deal with string theory in highly curved backgrounds, we will lack a completely realistic model of QCD. However, we can go on and study the non-perturbative properties of our model. Since they are related to QCD-like realistic models by a continuous change of parameters, it is not unplausible that some properties remain qualitatively unchanged.

The next step is to add flavors to the gauge theory. The easiest procedure is to embed N_f probe branes in the geometry [82, 83], where N_f is the number of flavors. We can neglect the backreaction as long as the number of colors is much larger than the number of flavors $N \gg N_f$, so it corresponds to a quenched approximation. In some sense, we are taking the 't Hooft limit of the gauge theory, compared to the limit of Veneziano [84] where the number of flavors is comparable to the number of colors. On the gravity side, the non-quenched setup will correspond to a geometry with extra fluxes turned on and the backreaction properly taken into account. We will concentrate on constructions with probe branes in a geometry with conformal boundary, where we should remark:

1. Mesons in the dual theory correspond to open string excitations of the probe brane.
2. The embedding of the brane must fill the directions associated to the field theory, so the quarks in the dual theory are not restricted to lower-dimensional domains.
3. The embedding must be regular and identifiable with an RG flow. So it must go from the conformal boundary to finite (or zero) radius and have no defects as conical singularities.
4. The asymptotic conditions of the embedding are related to the bare quark mass, while the bending of the brane near the origin is related to the formation of a quark condensate.
5. There is a $U(1)$ symmetry that can be identified with the $U(1)_A$ symmetry. It can be a global symmetry of the embedding or a gauge symmetry on the flavor branes. The formation of a quark condensate is reflected in the spontaneous breaking of this symmetry by the embedding. When this happens, there is a massless open string mode that can be identified with the large- N massless Goldstone boson of axial symmetry.

6.2 Large N chiral dynamics

In this section we will review the main features of the physics we try to describe with supergravity. An introduction to chiral effective Lagrangians in the context of the Standard Model can be found in [85].

A gauge theory with N_f massless fermions has a global $U(N_f)_L \times U(N_f)_R$ symmetry.

$$Q_L \rightarrow LQ_L \quad , \quad Q_R \rightarrow RQ_R \quad (6.2)$$

At strong coupling, the theory is expected to confine and form a quark condensate, so the symmetry is spontaneously broken to a diagonal $U(N_f)$.¹ At low energies the dynamics can be described in terms of an effective Lagrangian for the N_f^2 Goldstone bosons (pions) of the broken symmetry, with all the other fields integrated out.

The Goldstone bosons can be grouped in a $N_f \times N_f$ matrix U belonging to $U(N_f)$

$$U = e^{i\eta'/f_{\eta'}} e^{i\pi \cdot \tau / f_{\pi}} \quad (6.3)$$

where f_{π} has dimension of mass and τ are the generators of $SU(N_f)$. Essentially U is the vev of the quark condensate $\langle \bar{Q}Q \rangle$ which we promote to a field. Under a global transformation

$$U \rightarrow LUR^\dagger \quad (6.4)$$

The effective Lagrangian contains all possible terms compatible with the symmetry. The coefficients depend on the details of the microscopic theory. Since $U^\dagger U = \mathbf{1}$, all terms contain derivatives, and we can organize them by the number of derivatives, so an expansion in powers of the energy can be developed. The first term (two derivatives) is

$$\mathcal{L}_2 = \frac{f_{\pi}^2}{2} \text{Tr} (\partial_{\mu} U \partial^{\mu} U^{\dagger}) \quad (6.5)$$

Notice that in order to have a canonically normalized η' field

$$f_{\eta'}^2 = N_f f_{\pi}^2 \quad (6.6)$$

to leading order in $1/N$, there can be an OZI suppressed contribution from a term $\sim (\text{tr} (U^\dagger \partial_{\mu} U))^2$ that modifies this relation.

If the symmetry is only approximate because the quarks are not exactly massless, we should introduce a symmetry-breaking term. The simplest possibility is

$$\mathcal{L}_m = \frac{f_{\pi}^2}{2} \text{Tr} (MU + M^\dagger U^\dagger) \quad (6.7)$$

where M is the quark mass matrix.

¹And this symmetry cannot be spontaneously broken [86], this result is known as the Vafa-Witten theorem.

6.2.1 Chiral anomaly

We have presented the η' as a Goldstone boson of the broken $U(1)_A$ symmetry, but as a matter of fact, the η' particle is massive due to the chiral anomaly, that breaks explicitly the $U(1)_A$ symmetry at the quantum level. This is the present understanding of the $U(1)$ -problem [87,88].

The chiral current

$$J_5^\mu = \bar{Q}_i \gamma^\mu \gamma_5 Q_i \quad (6.8)$$

is conserved classically because in the QCD Lagrangian with massless fermions $U(1)_A$ is a global symmetry. If the fermions had a mass, the symmetry is lost. Quantum mechanically the chiral current is not conserved, its divergence being equal to the anomaly.

It can be computed perturbatively, through triangle diagrams (ABJ anomaly) or as the non-invariance of the path integral measure under chiral rotations.

$$\partial_\mu J_5^\mu = \frac{N_f g^2}{16\pi^2} F_{\mu\nu}^a \tilde{F}^{a\mu\nu} \quad (6.9)$$

where $\tilde{F}^{a\mu\nu} = \frac{1}{2}\epsilon^{\mu\nu\sigma\rho} F_{\sigma\rho}^a$.

The matrix element of the chiral current operator to annihilate a η' state is

$$\langle 0 | J_{5\mu}(x) | \eta'(p) \rangle = i f_{\eta'} p_\mu e^{ipx} \quad (6.10)$$

Therefore, the η' mass is

$$m_{\eta'}^2 = -p^2 = \frac{N_f g^2}{16\pi^2 f_{\eta'}} \langle 0 | F_{\mu\nu}^a \tilde{F}^{a\mu\nu}(0) | \eta' \rangle \quad (6.11)$$

The anomaly is related to the θ -term of the Lagrangian

$$\frac{g^2 \theta}{16\pi^2} \int d^4x F \tilde{F}(x) \quad (6.12)$$

but

$$F \tilde{F} = \text{tr}(F_{\mu\nu} F^{\mu\nu}) = \partial_\mu K^\mu = \partial_\mu \left(2\epsilon^{\mu\nu\rho\sigma} \text{tr}(A_\nu \partial_\rho A_\sigma - \frac{1}{3} g A_\nu A_\rho A_\sigma) \right) \quad (6.13)$$

is a total derivative so we can define a *gauge variant* conserved chiral current $\tilde{J}_{5\mu} = J_{5\mu} - \frac{N_f g^2}{8\pi^2} K_\mu$ with the corresponding conserved chiral charge $\tilde{Q}_5 = \int d^3x \tilde{J}_{50}$.

\tilde{Q}_5 generates chiral transformations that change the value of the vacuum angle. The QCD vacuum is labelled by the θ parameter, that we can interpret as a 'Bloch momentum' between gauge vacua $|n\rangle$ of different topological charge n .

$$|\theta\rangle = \sum_n e^{in\theta} |n\rangle \quad (6.14)$$

The large gauge transformation that increase the topological charge simply changes the phase of the θ -vacuum

$$U_1 |n\rangle = |n+1\rangle \Rightarrow U_1 |\theta\rangle = e^{-i\theta} |\theta\rangle \quad (6.15)$$

The conserved chiral charge is not gauge-invariant, and under this transformation

$$U_1 \tilde{Q}_5 U_1^\dagger = \tilde{Q}_5 - 2N_f \quad (6.16)$$

If we perform a chiral rotation over the theta vacuum

$$U_1 e^{-i\phi \tilde{Q}_5} |\theta\rangle = U_1 e^{-i\phi \tilde{Q}_5} U_1^\dagger U_1 |\theta\rangle = e^{-i(\theta - 2N_f \phi)} e^{-i\phi \tilde{Q}_5} |\theta\rangle \quad (6.17)$$

the change in the theta angle is

$$\theta \rightarrow \theta - 2N_f \phi \quad (6.18)$$

So when there are massless fermions, the theta dependence of the theory disappears.

We can implement the chiral anomaly in the Lagrangian by making the substitution [71, 72]

$$\theta \rightarrow \theta - i \log \det U \quad (6.19)$$

The multivalued character of the logarithm has been the subject of some controversy (see [89], for instance). But it fits quite well with large N considerations because, as we will see (eq. 6.24) the partition function of the theory should present a multibranched structure on theta dependence. At each branch, the energy has a minimum at a value of θ that is displaced an integer multiple of 2π respect to the other branches. The branch that has less energy is dominating. If we could change θ , there will be a value $\theta = (2k+1)\pi$ where the dominating branch changes, so the potential will be non-analytic at that point. This is reflected in the chiral Lagrangian through the logarithm.

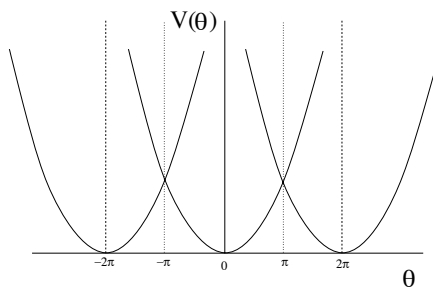


Figure 6.2: Multibranched structure of the energy depending on θ .

6.2.2 Witten-Veneziano formula

Historically, the motivation to introduce the logarithm was compatibility with the large N expansion. 't Hooft proposed that the anomaly was generated by instantons [89–91], which in the chiral Lagrangian will induce a term $\sim \det U$.

At $N = \infty$ there is no anomaly (it scales as $\sim g^2 = \lambda_t/N$) but if it were produced by instantons, the scaling will be $\sim e^{-N}$, while the large N expansion seems to indicate that the true scaling is $1/N$. From the point of view of the quark model [92], the splitting of the η' is explained by a quark-antiquark annihilation diagram, which is not present for the pions. In the large N limit, it is a $1/N$ OZI-suppressed diagram, because there are two fermion loops. Also, the potential $\det U$ contains arbitrary powers of the η' not suppressed by factors of N , which is in contradiction with the large N expansion.

There was also the question of how physics depends on θ for large values of N . If the instantons were the only contribution that can produce a theta dependence, then the dependence would be exponentially suppressed, as e^{-N} . However, two dimensional models [93] suggested that the suppression was only $\sim 1/N$. If we assume dependence on θ at order $1/N$, then massless quarks should eliminate it. This problem can be solved [69, 70] assuming a $1/N$ scaling of the anomaly.

From the partition function of the theory

$$Z = \int dA_\mu \exp \left(i \int d^4x \operatorname{tr} \left(-\frac{1}{2} F^2 + \frac{\lambda_t \theta}{16\pi^2 N} F \tilde{F} \right) \right) \quad (6.20)$$

differentiation with respect to θ is equivalent to insertion of $F \tilde{F}$ at zero momentum

$$\left. \frac{d^2 E}{d\theta^2} \right|_{\theta=0} = \frac{1}{N^2} \left(\frac{\lambda_t}{16\pi^2} \right)^2 \lim_{k \rightarrow 0} U(k) \quad (6.21)$$

where

$$U(k) = \int d^4x e^{ikx} \langle F \tilde{F}(x) F \tilde{F}(0) \rangle \quad (6.22)$$

We know this quantity as the topological susceptibility

$$\chi_t \equiv \frac{1}{N^2} \left(\frac{\lambda_t}{16\pi^2} \right)^2 \lim_{k \rightarrow 0} \int d^4x e^{ikx} \langle F \tilde{F}(x) F \tilde{F}(0) \rangle \quad (6.23)$$

Notice that $dE/d\theta|_{\theta=0} = 0$, because when $\theta = 0$ the theory is CP-conserving, so the vacuum expectation value of a CP-odd operator like $F \tilde{F}$ must vanish. It is also important to point that $\left. \frac{d^2 E}{d\theta^2} \right|_{\theta=0}$ is order one in the large N expansion, because of the scaling of glueballs

operators. However, the vacuum energy is $O(N^2)$, so the dependence of the energy with θ should be such that

$$E(\theta) = N^2 f(\theta/N) \quad (6.24)$$

where $f(x)$ is some function of order one in N . Any analytical function can be at most periodic under $\theta \rightarrow \theta + 2\pi N$. In order to restore periodicity under $\theta \rightarrow \theta + 2\pi$, we need a multibranch structure of the partition function.

There is no θ dependence in ordinary perturbation theory. Diagram by diagram $U(k)$ vanishes at $k = 0$. However, if we sum all the planar diagrams to get the first order in the large N expansion and then consider the $k \rightarrow 0$ limit it is possible that the limit is nonzero. Although individual diagrams vanish, each order vanishes more slowly than the one before

$$U(k) = ak^2 + b\lambda_t k^2 \log k^2 + c\lambda_t^2 k^2 \log^2 k^2 + \dots \quad (6.25)$$

It is plausible that the whole sum does not vanish at $k = 0$.

When we introduce fermions, there are suppressed corrections

$$U(k) = U_0(k) + \frac{1}{N}U_1(k) + \frac{1}{N^2}U_2(k) + \dots \quad (6.26)$$

$U_0(k)$ controls the θ dependence of the gauge theory without quarks. When we introduce quarks there are $1/N$ contributions that should eliminate the θ dependence when the quarks are massless. To see more clearly how this can happen is better to write this formula in a different way. $U_0(k)$ is the two-point correlation function of the $F\tilde{F}$ operator. In the large N expansion the intermediate states are one-hadron states, which can be glueballs or mesons. Therefore, we may write

$$U(k) = \sum_{\text{glueballs}} \frac{\left| \langle 0 | F\tilde{F} | n^{\text{th}} \text{ glueball} \rangle \right|^2}{k^2 - M_n^2} + \sum_{\text{mesons}} \frac{\left| \langle 0 | F\tilde{F} | n^{\text{th}} \text{ meson} \rangle \right|^2}{k^2 - m_n^2} \quad (6.27)$$

The sum in glueballs is of order N^2 while the sum in mesons is of order N . When $k \rightarrow 0$ the only way to make both terms of the same order is to have a meson with a mass that scales as $1/N$, and that is precisely the η' . If we look carefully at the formula, we will realize that both terms are of the same sign, so a cancellation seems impossible in principle. The reason is that when we have written $U_0(k)$ as a sum over glueball states, we have forgotten a contact term that should make $U_0(0)$ positive so the cancellation is possible. Nobody has computed the contact term, and in fact the problem is ambiguous [94] since no physical principle is known that should fix the contact terms so that $\chi_t \geq 0$. However, in the

lattice regularization with Ginsparg-Wilson fermions [95–97] a proof can be given of the positivity of the topological susceptibility, up to corrections that are expected to vanish in the continuum limit.

A possible physical explanation for the positivity of $U_0(0)$ [92] comes from the interpretation of the confining vacuum as a condensate of color magnetic monopoles. Introducing a small theta angle gives to the monopoles a small fraction of electric charge [98], which makes the energy of the condensate to increase. Then, the CP conserving vacuum ($\theta = 0$) is a minimum of the energy, which implies that the topological susceptibility ($\sim U_0(0)$) is positive.

So

$$U_0(0) = \frac{\left| \langle 0 | F \tilde{F} | \eta' \rangle \right|^2}{m_{\eta'}^2} \geq 0 \quad (6.28)$$

Using the formulas of the anomaly and the matrix element of the Goldstones (eq. 6.11), the equation (6.21) and the fact that $f_{\eta'} = \sqrt{N_f} f_\pi$ (eq. 6.6) to leading order, we find the Witten-Veneziano formula

$$m_{\eta'}^2 = \frac{4N_f}{f_\pi^2} \left(\frac{d^2 E}{d\theta^2} \right)_{\theta=0}^{\text{no quarks}} \quad (6.29)$$

f_π is of order \sqrt{N} , because the current-current correlator, which is of order N has a term f_π^2/k^2 . $d^2 E/d\theta^2$ is of order one because of the normalization used, so the formula is consistent with the claim $m_{\eta'}^2 \sim 1/N$. When $N = \infty$, the anomaly vanishes and the η' is a Goldstone boson, with $m_{\eta'}^2 = 0$. The generalization of this formula is that the potential of the η' is given by the θ dependence of the energy with no quarks

$$E_0(\theta) \rightarrow E_0 \left(\theta + \frac{2\sqrt{N_f}\eta'}{f_\pi} \right) \quad (6.30)$$

Moreover, it can be further generalized to change every quantity in the pure gauge theory that depends on θ by $\theta + 2\frac{\sqrt{N_f}\eta'}{f_\pi}$ [70]. We can read the η' -glueball couplings directly from the θ -dependence of the glueball fields.

Chapter 7

Holographic QCD model

7.1 A confining supergravity dual

A non-supersymmetric, non-conformal model is given in [42]. We introduce a finite temperature in order to break both kind of symmetries. There are two possible phases, a hot gas of gravitons at low temperature and a black hole at higher temperatures. Those phases were shown to be respectively related to a confining and a screening phase in the gauge theory.

A supergravity model dual of a confining theory is an Euclidean continuation of a black hole, that can be constructed taking the near-horizon limit of a set of hot D4 branes. In the Euclidean formulation, we wrap the D4 branes around a S^1 of radius $\beta = 1/T$ and impose anti-periodic boundary conditions on fermions, thus breaking supersymmetry. We can continue to Minkowski space taking the compactified coordinate as time, and the resulting metric is the *AdS* black hole [42]. If we continue to Minkowski space but with the compactified coordinate as a spatial coordinate, then we will recover a solitonic solution. The near-extremal, near-horizon solution of the Euclidean hot D4-branes is

$$ds^2 = \left(\frac{u}{R}\right)^{3/2} (f(u)^2 d\tau^2 + \sum_{i=1}^4 (dx^i)^2) + \left(\frac{R}{u}\right)^{3/2} \left(\frac{du^2}{f(u)} + u^2 d\Omega_4^2\right) \quad (7.1)$$

The radius is

$$R^3 = \pi g_s N l_s^3, \quad (7.2)$$

the dilaton is

$$e^\phi = g_s \left(\frac{u}{R}\right)^{3/4} \quad (7.3)$$

There are N units of four-form flux on the S^4 . The deviation from extremality is given by the function

$$f(u) = 1 - \frac{u_0^3}{u^3} \quad (7.4)$$

where u_0 is the radius at the event horizon or where the space ends, depending if τ is continued to time or space coordinate. The period of τ can be related to R and u_0 . Changing variables

$$u = u_0(1 + c\rho^2) \quad (7.5)$$

and going close to the 'horizon' $\rho \ll 1$, the metric can be written as

$$ds^2 \simeq d\rho^2 + \rho^2 d\sigma^2 + \dots \quad (7.6)$$

if

$$c = \frac{3}{4} \left(\frac{u_0}{R} \right)^{3/2} u_0^{-2} \quad (7.7)$$

and

$$\sigma = \frac{3}{2} u_0^{1/2} R^{-3/2} \tau \quad (7.8)$$

This shows that the geometry is regular and behaves as flat two-dimensional space when we are close to $u = u_0$. In order to avoid conical singularities, the period of σ must be 2π , which means that the period of τ is

$$\frac{1}{T} \equiv \frac{2\pi}{M} = \frac{4\pi}{3} R^{3/2} u_0^{-1/2} \quad (7.9)$$

M is the Kaluza-Klein mass of the excitations around the τ direction.

We can express the string coupling constant in terms of the Yang-Mills coupling constant. From the Dirac-Born-Infeld action of the D4 branes

$$g_5^2 = (2\pi)^2 g_s l_s \quad (7.10)$$

The four dimensional coupling constant can be read from this expression integrating on the τ coordinate

$$g_{YM}^2 = g_5^2 \frac{M}{2\pi} = (2\pi) g_s l_s M \quad (7.11)$$

From this formula and equations (7.9) and (7.2) we can extract the following relations

$$g_s = \frac{1}{2\pi} \frac{g_{YM}^2}{M l_s}; \quad u_0 = \frac{2}{9} g_{YM}^2 N M l_s^2; \quad R^3 = \frac{g_{YM}^2 N l_s^2}{2M} \quad (7.12)$$

and express all quantities in terms of gauge parameters only.

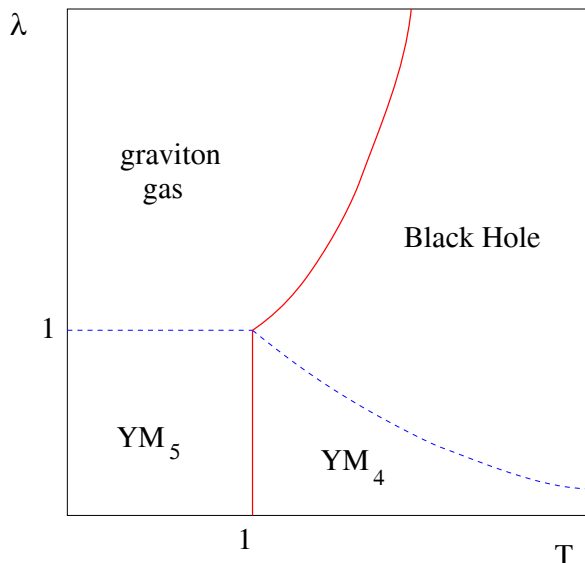


Figure 7.1: Phase diagram in the correspondence. At low temperatures and small 't Hooft coupling, the theory is five-dimensional Yang-Mills. At large couplings it can be described as a hot gas of gravitons in AdS . When we increase the temperature, there is a phase transition. The small coupling theory is effectively four-dimensional Yang-Mills, while the large coupling can be described as a black hole in AdS .

7.2 A model with flavor

The physical interpretation of a brane in the dual gauge theory depends crucially on the properties of its embedding. We are interested in embeddings that can be interpreted as RG flows for the fermions and that do not present singularities, like conical points. The first condition implies that at fixed AdS radial coordinate, there is a unique connected section of the brane. The second condition is a regularity condition that can be imposed on the solution of the embedding equations.

The dynamics of the brane are described by the Dirac-Born-Infeld action (DBI). From the DBI action we can extract the classical equations of motion of the D-brane in the background. The solutions that satisfy the boundary conditions and minimize the energy are the embeddings we are looking for.

Before taking the near-horizon limit, let us consider a plane centered on the correspondence branes and where the flavor branes extend along one direction. The separation between the flavor and correspondence branes gives the minimal amount of energy that is necessary to create an open string extended between both. Thus, this distance is associated

to the bare quark mass. If we substitute the correspondence branes by its SUGRA solution, the flavor branes will deviate from their flat asymptotic form near the throat, falling inside it. When we take the near-horizon limit, the asymptotically flat part is dropped and substituted by conditions at the boundary. The separation between correspondence and flavor branes becomes a boundary condition. There is another boundary condition, that is how fast the brane approaches its flat limit, but it turns out that when we impose regularity conditions, it is determined by the brane separation.

Different flavor embeddings have been computed in AdS [82] and deformations [53, 54, 56]. Typically, the probe brane expand the four dimensional space where the gauge theory is supposed to live. The other dimensions are wrapping some homologically-trivial cycle of the internal manifold (a loop on it can slide off), that is fibered along the radial coordinate of the AdS -like space. The shape is that of a 'cigar' or a 'trumpet' (fig. 7.2).

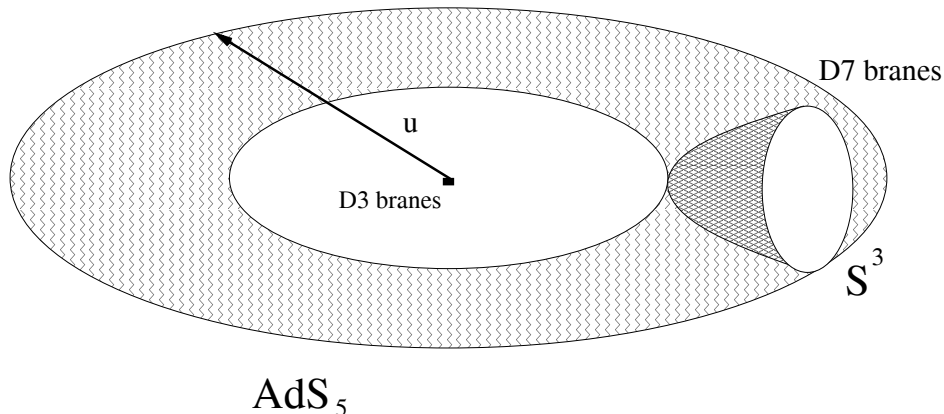


Figure 7.2: Flavor D7 branes embedded in a D3 background. The D7 wrap a S^3 around the S^5 and expand the AdS_5 space. the embedding ends at finite AdS radial coordinate because the wrapped cycle collapses.

It may happen that the cycle that is wrapping the probe brane collapses before reaching the origin of the AdS -like coordinate. It can be shown that as we decrease the separation boundary condition, the branes fall deeper into the AdS -like space. What happens when the separation boundary condition is zero depends on the concrete background we are working in, it may reach the origin of the space or stop at a finite distance from it.

To understand what is happening, is better to go to another set of coordinates where the origin of the AdS -like space is at the origin of a three-dimensional space and the embedding of the brane can be drawn as a curve along the vertical direction. Pure AdS

will be just like that, but deformations like a black hole [42], a AdS soliton or even a naked singularity [99] will have a “ball” centered at the origin. The brane tends asymptotically to a straight vertical line. The separation boundary condition is the separation of the asymptotic vertical line from the vertical line passing through the origin. The horizontal plane can be identified with a plane transverse to both correspondence and flavor branes.

When we rotate the flavor branes around the correspondence branes, the fields suffer a ten-dimensional geometrical rotation

$$\psi_L \rightarrow e^{i\phi}\psi_L \ , \ \psi_R \rightarrow e^{-i\phi}\psi_R \ , \ X \rightarrow e^{-i2\phi}X \quad (7.13)$$

where X is the complex field associated to the position of the brane in the transverse plane.

From the four dimensional point of view, this is a chiral rotation $U(1)_A$. So we can identify rotations around the origin of the transverse plane as chiral rotations in the field theory. Then, we can make the following identifications:

The embedding breaks spontaneously the $U(1)$ symmetry, except if it is a straight embedding through the origin. If the separation boundary condition is non-zero, then we must associate this breaking with the explicit breaking of the chiral symmetry by non-zero fermionic masses. If the separation is zero, it may happen that the deformation of the geometry at the origin of AdS repels the brane so there is no flat solution. The brane will be curved outwards and the $U(1)$ symmetry will be spontaneously broken again. This is what happens for the AdS soliton and the naked singularity backgrounds. For the pure AdS and black hole backgrounds, the flat solution exist, in the first case because there is no obstruction and in the second, the brane is attracted to the black hole and can reach the event horizon and fall into it (Fig. 7.2).

So the $U(1)$ -breaking solutions of zero separation are associated to a non-zero asymptotic slope. By the field-operator correspondence, it can be shown that we can identify it with a non-zero fermion condensate. So in the field theory we must interpret these solutions as spontaneous breaking of the chiral $U(1)_A$ symmetry.

Rotations of the embeddings around the origin are rotations in the phases of the fermion masses. Rotation of the embeddings around their symmetry axes are rotations in the phase of the condensate, therefore, the rotations of the brane around itself can be identified with the η' meson.

Notice that if quarks are massive, when we rotate the solution around itself, the energy of the embedding increases because of the repulsive action of the geometry, so the η'

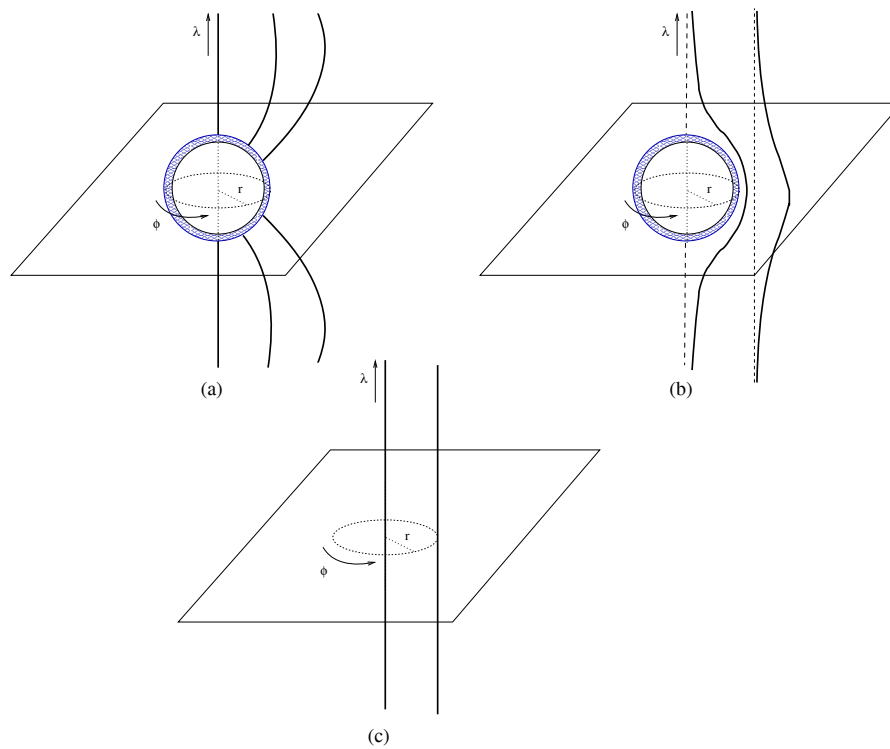


Figure 7.3: (a) Embedding of the flavor branes in the black hole background. The branes can fall into the horizon. (b) Flavor branes in the bubble of nothing or the Constable-Myers background. The branes are repelled by the geometry. (c) Embedding in a supersymmetric background.

has a mass. We might rotate the whole embedding around the origin, passing through configurations of the same energy. This is equivalent to perform a rotation on the fermion masses **and** the condensate at the same time, in such a way that the effective Lagrangian (eq. 6.7) remains unchanged. But a rotation on the fermion masses is not really physical, they are given parameters of the theory.

When the quark masses are zero there is a true massless mode [54, 56, 58] of the broken $U(1)$ symmetry because we are rotating the brane around its symmetry axis, changing the boundary conditions. Therefore, we are in the $N = \infty$ limit of the theory, where the η' is a Goldstone boson.

We will work with the explicit example of [56]. We introduce D6 branes in the background of the hot D4 branes. The D6 branes are parallel to the four Minkowskian coordinates of the hot D4 branes and expand three directions perpendicular to the D4s.

$$\begin{array}{cccccccccccc} \text{D4} & 0 & 1 & 2 & 3 & 4 & \times & \times & \times & \times & \times & & \\ \text{D6} & 0 & 1 & 2 & 3 & \times & 5 & 6 & 7 & \times & \times & & \end{array} \quad (7.14)$$

The embedding is easier to work out in isotropic coordinates. If z^a are the coordinates transverse to the D4 branes, and $|z| \equiv \rho$, then

$$u = \left(\rho^{3/2} + \frac{u_0^3}{4\rho^{3/2}} \right)^{2/3} \quad (7.15)$$

where the metric is

$$ds^2 = \left(\frac{u}{R} \right)^{3/2} (\eta_{mn} dx^m dx^n + f(u) d\tau^2) + K(\rho) (d\rho^2 + \rho^2 d\Omega_4^2) \quad (7.16)$$

with

$$K(\rho) = \left(\frac{R}{u} \right)^{3/2} \frac{1}{f(u)} \frac{\partial U}{\partial \rho} = \frac{R^{3/2} u^{1/2}}{\rho^2} \quad (7.17)$$

The D6 are wrapping a S^2 of the S^4 , which can be seen as the polar part of the “567” coordinates. The two sets of branes are separated on the “78” plane, we can denote r as their separation and ϕ as the angle. Then, we can rewrite the metric as

$$ds^2 = \left(\frac{u}{R} \right)^{3/2} (\eta_{mn} dx^m dx^n + f(u) d\tau^2) + K(\rho) (d\lambda^2 + \lambda^2 d\Omega_2^2 + dr^2 + r^2 d\phi^2) \quad (7.18)$$

where $\rho^2 = \lambda^2 + r^2$ and λ is the radial coordinate in the “567” space.

The embedding is chosen to be at a fixed τ and fixed in ϕ . The D6 are wrapping the S^2 and expand along λ , so the embedding is determined by a function $r(\lambda)$, that must be a solution of the equations of motion given by the DBI action.

The induced metric on the D6 worldvolume is

$$ds_{D6}^2 = \left(\frac{u}{R}\right)^{3/2} \eta_{mn} dx^m dx^n + K(\rho)((1 + \dot{r}^2)d\lambda^2 + \lambda^2 d\Omega_2^2) \quad (7.19)$$

The analytic expression of $r(\lambda)$ is not known, but it can be computed numerically and in the limit $\lambda \rightarrow \infty$

$$r(\lambda) \simeq r_\infty + \frac{c}{\lambda} \quad (7.20)$$

The quark bare mass is given by the asymptotic separation

$$m_q = \frac{u_0 r_\infty}{2\pi l_s^2} \quad (7.21)$$

the condensate can be deduced from the dependence of the energy with the quark mass in the gauge theory, that we relate through the correspondence with the energy of the D6 branes

$$\frac{\delta \mathcal{E}_{YM}}{\delta m_q} = \langle \bar{\psi} \psi \rangle \leftrightarrow \frac{\delta \mathcal{E}_{DBI}}{\delta r_\infty} \sim \langle \bar{\psi} \psi \rangle \quad (7.22)$$

Using the relations (7.12)

$$\frac{1}{N} \langle \bar{\psi} \psi \rangle = -g_{YM}^2 N M^3 c \quad (7.23)$$

Regularity of the solution at $\lambda = 0$ implies that $c = c(r_\infty)$. When the quark mass is large ($1 \ll r_\infty$), $c \sim 1/2r_\infty$. So $\langle \bar{\psi} \psi \rangle \sim 1/m_q$. There is a short heuristic argument for this in QCD. The trace of the energy-momentum tensor is

$$T_\mu^\mu = m_q \bar{\psi} \psi - \frac{\alpha_s(11N_c - 2N_f)}{24\pi} \text{Tr} F^2 \quad (7.24)$$

In the limit $m_q \rightarrow \infty$, the theory behaves as pure Yang Mills, for which

$$T_\mu^\mu = -\frac{11N_c \alpha_s}{24\pi} \text{Tr} F^2 \quad (7.25)$$

Taking vevs and equating both expressions

$$\langle \bar{\psi} \psi \rangle = \frac{\alpha_s N_f}{12\pi m_q} \langle \text{Tr} F^2 \rangle \quad (7.26)$$

so if $\langle \text{Tr} F^2 \rangle \neq 0$, we can conclude that $\langle \bar{\psi} \psi \rangle \sim 1/m_q$.

The spectrum of fluctuations of the D6 embeddings in the ϕ and r coordinates has been calculated. It shows a massless mode for ϕ fluctuations, that we identify with the η' . The other modes exhibit a mass gap, proportional to M .

As happened with the glueball spectra [51, 52], meson physics is not really decoupled from Kaluza-Klein modes [53, 54, 56], and there is no regime where we are left with pure

QCD alone. However, at energies much lower than M , all the dynamics are frozen but those of the massless mode. As we have argued, it is a Goldstone boson in the probe approximation, so the shape of the action is determined by the symmetry breaking and the high energy physics are encoded in the coefficients.

7.3 Introducing the θ angle

The couplings of the gauge theory are usually associated to non-normalizable modes of the AdS fields. The θ angle is identified with RR or sometimes the NSNS forms when there is a coupling in the correspondence branes like

$$\sim \int_{\mathcal{M}_{p+1}} G_{p-3} \wedge (\text{Tr } F \wedge F) \quad (7.27)$$

where G_{p-3} is the form field to be identified with the θ angle and F is the gauge field strength of the brane. In order to have a low-energy four dimensional theory, the extra dimensions should be compactified on some $(p-3)$ -dimensional manifold (K_{p-3}), so

$$\theta \simeq \int_{K_{p-3}} G_{p-3} \quad (7.28)$$

Let us consider again the hot D4 branes. The low energy worldvolume effective action of the D4 branes has a term

$$\frac{1}{l_s} \int_{D4} C_1 \wedge \frac{\text{Tr } F \wedge F}{8\pi^2} \quad (7.29)$$

We can modify the type IIA vacuum so that $G_2 = dC_1 = 0$ but

$$\theta = \int_{S^1} C_1 \quad (7.30)$$

is possibly non-zero. The right hand side is gauge invariant modulo $2\pi\mathbf{Z}$, so we can interpret θ as an angle. At low energies in four dimensions, (eq. 7.29) reduces to a theta term in the gauge theory action, with θ as the vacuum angle. In the holographic description, the parameters of the theory are determined far from the branes, that is at large u . The analogous statement is that the integral of C_1 does not vanish when $u \rightarrow \infty$ even if G_2 does. But (u, τ) parametrize a disk, so we can apply Stokes theorem

$$\int_D G_2 = \lim_{u \rightarrow \infty} \int_{S^1} C_1 \quad (7.31)$$

the left hand side is a real number but θ is an angle, hence

$$\frac{1}{l_s} \int_D G_2 = \theta + 2\pi k \equiv \theta_k \quad (7.32)$$

We introduce as ansatz a G_2 with only one non-vanishing component

$$G_{u\tau} = \partial_u C_\tau \quad (7.33)$$

From the IIA SUGRA action in the metric given by (7.1), the equations of motion are

$$\partial_u(u^4 \partial_u C_\tau) = 0 \quad (7.34)$$

with the solutions

$$C_\tau = C_\infty \left(1 - \frac{u_0^3}{u^3}\right) \rightarrow G_{u\tau} = 3C_\infty \frac{u_0^3}{u^3} \quad (7.35)$$

Evaluating (7.32) gives

$$C_\infty = \theta_k \frac{M l_s}{2\pi} \quad (7.36)$$

The energy of the gauge theory depends on θ . We can see this holographically by introducing this solution in the supergravity action.

$$E = \frac{1}{4\kappa_0^2} \int d^{10}x (-g)^{1/2} g^{uu} g^{\tau\tau} (\partial_u C_\tau)^2 \quad (7.37)$$

where $\kappa_0^2 = (2\pi)^7 l_s^8 / 2$. Performing the integrals over τ , u and the four-sphere, and using the relations (7.12), the energy density is

$$\mathcal{E} = \frac{1}{2} \chi_t \theta_k^2 \quad (7.38)$$

And the topological susceptibility is

$$\chi_t = \frac{\lambda_t^3 M^4}{2^2 3^6 \pi^6} \quad (7.39)$$

The holographic derivation of the theta dependence was first performed by Witten [100], while the topological susceptibility in this background (but with different coordinates) was computed in [101] (the 't Hooft coupling was $1/2\pi$ times the one used here).

The theta dependence is in agreement with the multibranch structure of the large N analysis, each branch labelled by an integer k .

Chapter 8

$1/N$ physics of the holographic η'

Probe branes and a background RR form flux realize holographically flavor and theta dependence in the *AdS/CFT* correspondence. In a gauge theory, the theta angle and quarks are related through the $U(1)_A$ anomaly. We will now show, following [102] that the same relations can be extracted from the supergravity dual.

8.1 The anomaly relation in the UV regime

The $U(1)_A$ symmetry is described as rotations in the ϕ angle (see eq. 7.18). Since this symmetry is anomalous, the rotation of the D6-brane fields by an angle α must be equivalent to a shift in the effective theta angle

$$\int_{S^1} C_1 \rightarrow \int_{S^1} C_1 + N_f \alpha \quad (8.1)$$

so that the dependence on the microscopic θ -angle and the phase on the “89” plane comes in the combination $\theta + N_f \phi$.

In the supergravity description this behavior is encoded in the topological properties of the RR fluxes generated by the D6. The D6 is a magnetic source of RR two-form flux, the total flux on a S^2 surrounding the D6 branes (in the “489” space) being

$$\int_{S^2} G_2 = 2\pi N_f \quad (8.2)$$

The UV limit of the gauge theory corresponds to the boundary of the supergravity construction. As we approach it, the D6 are placed at the origin of the (r, ϕ) plane. Since τ is

periodically identified, a two sphere surrounding the D6 can be continuously deformed to a cylinder as in the figure 8.1.

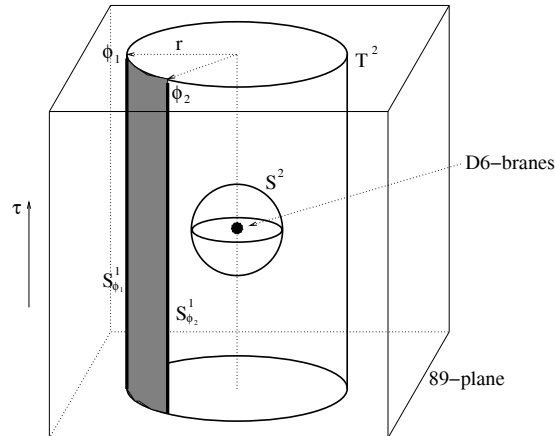


Figure 8.1: Asymptotically, the D6 brane lie at the origin of the (8,9)-plane and are localized in the τ -direction.

The topology is that of a two-torus, parametrized by (τ, ϕ) . Since G_2 is a closed form, the total flux remains the same

$$\int_{T^2} G_2 = 2\pi N_f \quad (8.3)$$

Since rotations in ϕ are isometries of the background, and the D6 lies asymptotically at the origin of the “89”-plane, it follows that the flux through any strip lying between two angles ϕ_1 and ϕ_2 must be proportional to the area of the strip

$$\int_{\text{Strip}} G_2 = N_f (\phi_2 - \phi_1) \quad (8.4)$$

Since locally $G_2 = dC_2$, we can apply Stokes’ theorem

$$\int_{\text{Strip}} G_2 = \int_{S^1_{\phi_1}} C_1 - \int_{S^1_{\phi_2}} C_1 \quad (8.5)$$

where $S^1_{\phi_i}$ is parametrized by τ at $\phi = \phi_i$. Combining these results we deduce that the Wilson line of C_1 at a given angle ϕ , as induced by the D6-branes is

$$\int_{S^1_{\phi}} C_1 = N_f \phi \quad (8.6)$$

where we have set to zero a possible additive constant by choosing the origin of the polar coordinate ϕ appropriately. If, in addition there is a background value for this Wilson line

(an asymptotically flat connection defining the θ -angle) then the total value of the Wilson line is

$$\int_{S^1_\phi} C_1 = \theta + N_f \phi \tag{8.7}$$

Under a rotation of $\Delta\phi = \alpha$ in the background, the 'Dirac sheet' singularity that is used to define C_1 (extending as a string in (r, ϕ) at $\phi = 0$) rotates by minus the same angle and shifts the theta angle according to (8.7). So physics is independent of the microscopic θ -angle when the D6 are asymptotically located at the origin of the "89"-plane, *i.e.*, in the chiral limit. Supersymmetry breaking at a scale M implies that a shift of the θ -angle by a change of the RR two-form G_2 costs energy. Therefore, a potential for the D6-brane coordinate ϕ must somehow be generated, so the complete potential energy is only a function of the $U(1)_A$ -invariant combination $\theta + N_f \phi$.

8.2 String contributions to the potential

The θ -dependence computed by Witten in the pure glue sector plus the anomaly argument, constrain the leading potential of the η' field in the k -th branch of the potential to be

$$V(\phi)^{(k)} = \frac{1}{2} \chi_t (\theta + 2\pi k + N_f \phi)^2 \tag{8.8}$$

We would like to know how this potential is generated for the ϕ field. The stringy diagrams can be compared with the OZI-suppressed diagrams of the quark annihilation.

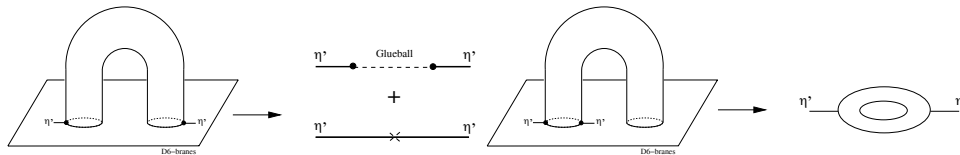


Figure 8.2: Basic stringy diagrams of order N_f/N_c . The left one correspond to quark-antiquark annihilation, while the right one describes the meson propagator with a quark loop.

Remember that those diagrams distinguish the flavor singlet meson from non-singlet fields, so it suggests that they give the most important contribution at the quantitative level, although other diagrams can contribute to the self-energy as well.

In order to give a mass to the η' , those contributions must shift the zero-momentum pole of the η' propagator. Unfortunately, no direct calculation of the full string diagrams

is possible in the background in question, since we are restricted by the supergravity approximation. We can separate then the exchange of supergravity modes from a stringy 'contact term' coming from the exchange of the infinite tower of closed string modes and possible contributions at the boundary of the worldsheet moduli space, where the cylinder becomes infinitesimally short. The contribution of a *finite* number of low-lying glueball modes with mass M_n shifts the η' mass-pole by

$$\delta m_{\eta'}^2 = - \sum_n \frac{g_n(0)^2}{M_n^2} \quad (8.9)$$

where $g_n(0)$ stands for the zero-momentum limit of the glueball- η' mixing, which must non vanish for this contribution to be non-trivial. The shift in (eq. 8.9) has the 'wrong' sign, so the string contact term must be positive and all-important at the quantitative level.

Any closed-string field Φ that is sourced by the D6-branes and have a non-trivial wave function with respect to the ϕ angle is subject to mixing with the η' meson. Expanding Φ in Fourier modes

$$\Phi(\phi) = \sum_n \mathcal{G}_n e^{-in\phi} \quad (8.10)$$

where the normalizable modes \mathcal{G}_n , when pulled back to the \mathbf{R}^4 factor in the D6 brane worldvolume represent glueballs of $U(1)_A$ charge n . These kind of modes give non-derivative couplings, but are in fact Kaluza-Klein artifacts, since there are no $U(1)_A$ -charged glueball fields in QCD. Furthermore, the kind of couplings they provide do not break the $U(1)_A$ symmetry. In chiral notation, we will have terms of the form

$$N \sum_n \int_{\mathbf{R}^4} \mathcal{G}_n \text{Tr} U^n \quad (8.11)$$

After integrating out the glueball fields, the tree level potential they will generate will be of the form $\text{Tr} U^n \cdot \text{Tr} U^{-n}$ because the glueball propagator couples \mathcal{G}_n and \mathcal{G}_{-n} (n being the KK-momentum). The global phase drops from these expressions, so such coupling does not generate a potential for the η' , which is just as well, since such contributions seem completely independent of the θ -dependence, in agreement with Witten-Veneziano formula.

The kind of glueballs whose couplings with the η' meson can contribute to the potential should show the characteristic multivaluedness of the θ -dependence at large N . We expect the coupling to be a function of $-i \log \det U \sim N_f \phi$, linear in the angular coordinate, so angular periodicity will require the sum over different branches. The relation with θ -dependence suggest that we should study the RR sector of the closed-string theory.

The D6 branes couple electrically to the eight-form flux $G_8 = dC_7$, through a Wess-Zumino term

$$S_{WZ} = N_f \mu_6 \int_{D6} C_7 \quad (8.12)$$

In terms of C_7 this coupling is both local and can be defined off-shell. For on-shell configurations this coupling can be reexpressed in terms of the one-form potential C_1 , but off-shell there is no local expression for C_1 . The reason is that, on-shell, the vacuum equations are

$$dG_8 = 0, \quad d^*G_8 = dG_2 = 0 \quad (8.13)$$

hence, both G_2 and G_8 can be expressed in terms of a local potential. However, if the seven-form glueballs are off-shell, the Bianchi identity of the two-form field is no longer satisfied, so no local one-form potential can be defined. If we were working with one-form glueballs we would not be able to define off-shell local couplings with the Wess-Zumino term.

In order to induce a linear coupling in ϕ , we will need to show that fluctuations of the form $C_7 = (\phi + \phi_0)W_7$ exist and can couple to the D6-branes. Our ansatz is inspired in the Hodge dual of the background two-form giving the θ -dependence (eq. 8.26)

$$W_7 = -G(x)h(u)\lambda^2 r(rd\lambda - \lambda dr) \wedge d\omega_2 \wedge dV_4 + \tilde{h}(u)\lambda^2 r d\lambda \wedge dr \wedge d\Omega_2 \wedge i_{N(x)}dV_4 \quad (8.14)$$

where $G(x)$ is a pseudo-scalar field, $N(x)$ is a vector field, $h(u)$ and $\tilde{h}(u)$ are radial profiles to be determined and

$$i_{N(x)}dV_4 = \frac{1}{3!}N_\mu(x)\epsilon_{\mu\nu\alpha\beta}dx^\nu \wedge dx^\alpha \wedge dx^\beta \quad (8.15)$$

Note that C_7 can be multivalued because is not gauge invariant, but G_8 is, so $dW_7 = 0$ for G_8 not to be multivalued. This implies

$$\partial_\mu N^\mu = -G \quad (8.16)$$

as well as an equation relating $h(U)$ with $\tilde{h}(U)$

$$\tilde{h} = 5h + \rho \frac{dU}{d\rho} h' . \quad (8.17)$$

The pseudo-scalar glueball field is not constrained, but if we impose the on-shell condition $d^*G_8 = 0$, then

$$N_\mu = -\frac{1}{M^2}\partial_\mu G \quad (8.18)$$

for some constant M^2 . With (8.16) it implies the on-shell condition for the glueball field

$$\partial_\mu \partial^\mu G = M^2 G, \quad (8.19)$$

M^2 is determined from an eigenvalue equation involving the radial profiles.

$$H' = M^2 \tilde{H} \rho \left(\frac{dU}{d\rho} \right)^{-1}, \quad (8.20)$$

where

$$\begin{aligned} \tilde{H}(U) &= - \left(\frac{U}{R} \right)^{-9/4} K(\rho)^{-3/2} f(U)^{-1/2} h(U), \\ H(U) &= \left(\frac{U}{R} \right)^{-3/4} K(\rho)^{-5/2} f(U)^{-1/2} \tilde{h}(U). \end{aligned} \quad (8.21)$$

We can write the non-derivative couplings $\phi - \mathcal{G}_n$ that arise from the Wess-Zumino term by pulling back C_7 onto the D6-brane worldvolume and integrating over the S^2 and radial directions. We are interested only in the η' , so the pullback of ϕ will depend only on the \mathbf{R}^4 coordinates and the D6 embedding will be in the ground state. Setting $\phi_0 = 0$

$$S_{WZ} \rightarrow \frac{N_f f_\pi}{2\sqrt{N}} g_n \int_{\mathbf{R}^4} \phi(x) G(x) = \sqrt{\frac{N_f}{N}} g_n \int_{\mathbf{R}^4} \eta'(x) G(x) \quad (8.22)$$

where

$$\frac{f_\pi}{2\sqrt{N}} g_n = \mu_6 \text{vol}(S^2) \int_0^\infty d\lambda h_n(u) r \lambda^2 (r - \lambda r) \quad (8.23)$$

This shows that there are non-vanishing couplings of the η' meson to the glueballs, so the cylinder diagram in figure 8.2 can generate a potential for the η' with the right properties.

8.3 A quantitative check to order $1/\sqrt{N}$

In the previous sections, we have computed the energy dependence with θ (eq. 7.38) in the closed string sector. The anomaly argument tell us that we must substitute θ by $\theta + N_f \phi$ when the D6-brane probes are introduced. This leads to the η' potential

$$V(\eta') = \frac{1}{2} \chi_t \left(\theta + \frac{2\sqrt{N_f}}{f_\pi} \eta' \right)^2 \quad (8.24)$$

which realizes the Witten-Veneziano formula for the η' mass with χ_t given by (7.39). If we expand around $\eta' = 0$ instead of the true minimum of the potential, there is a tadpole term

$$\mathcal{T} = \chi_t \theta_k N_f \phi \quad (8.25)$$

On the other hand, we may read the linear term directly from the Wess-Zumino action for the particular seven-form that is induced by the θ -angle background (eq. 7.35). In the metric (7.18) the two-form is

$$G_2 = \frac{C}{u^4 \rho} \frac{\partial u}{\partial \rho} (\lambda d\lambda + r dr) \wedge d\tau \quad (8.26)$$

The G_2 couples magnetically to the D6 branes, so in order to calculate the coupling we need to compute first the Hodge dual form

$$G_8 = {}^*G_2 = C \frac{\lambda^2 r}{\rho^5} (r d\lambda - \lambda dr) \wedge d\phi \wedge d\Omega_2 \wedge dV_4 \quad (8.27)$$

where we have used the equation (7.17) and the determinant of the metric $\sqrt{|g|} = (u/\rho)^5 \lambda^2 r f(u)^{1/2}$.

The form potential that couples to the D6s is

$$C_7 = C \frac{\lambda^2 r}{\rho^5} \phi (r - \lambda \dot{r}) d\lambda \wedge d\Omega_2 \wedge dV_4 \equiv \phi \omega_7 \quad (8.28)$$

After integrating over the two sphere, the energy density given by the tadpole is

$$\mathcal{T} = N_f \mu_6 \int_{D6} C_7 = N_f \frac{\lambda_t^3 M^4}{2^2 3^5 \pi^6} \theta \phi \int_0^\infty d\lambda \frac{\lambda^2 r}{\rho^5} (r - \lambda \dot{r}) = N_f 3 \chi_t \theta \phi \int_0^\infty d\lambda \frac{\lambda^2 r}{\rho^5} (r - \lambda \dot{r}) \quad (8.29)$$

where we have used formula (7.39). Remarkably the integral gives the precise value to recover the tadpole

$$\int_0^\infty d\lambda \frac{\lambda^2 r}{\rho^5} (r - \lambda \dot{r}) = \int_0^\infty d\lambda \frac{\lambda^2}{\rho^4} (\rho - \lambda \dot{\rho}) = \frac{1}{3} \int_0^\infty \frac{d}{d\lambda} \left(\frac{\lambda^3}{\rho^3} \right) = \frac{1}{3} \quad (8.30)$$

where we have used that $\rho(0) = r(0) \neq 0$ and $r(\infty) = r_\infty < \infty$ in the D6 brane embedding.

The fact that the integral over the worldvolume reduces to a boundary contribution suggests that we can derive the tadpole from a more geometrical computation. We have argued that locally $C_7 = \phi \omega_7$, the tadpole comes just from the integration of ω_7 over Σ_7 , the equilibrium worldvolume of the D6-branes at $\phi = 0$. Define Σ_8 as the hypersurface that results from rotating the D6s around ϕ . Since ω_7 does not depend on ϕ , we can write

$$\int_{\Sigma_7} \omega_7 = \frac{1}{2\pi} \int_{\Sigma_8} d\phi \wedge \omega_7 = \frac{1}{2\pi} \int_{\Sigma_8} G_8 \quad (8.31)$$

In addition, Σ_8 is topologically equivalent to $S^4 \times \mathbf{R}^4$ at fixed u . Since G_8 is closed, we can apply Stokes' theorem so

$$\int_{\Sigma_7} \omega_7 = \frac{1}{2\pi} \int_{S^4 \times \mathbf{R}^4} G_8 \quad (8.32)$$

The latter integral can be evaluated by computing G_8 directly in the original coordinates (eq. 7.1)

$$G_8 = {}^*G_2 = C d\Omega_4 \wedge dV_4 \quad (8.33)$$

so the tadpole is

$$\mathcal{T} = \frac{1}{2\pi} \frac{N_f \phi \theta_k}{(2\pi)^6 l_s^7} \frac{3 M l_s u_0^3}{2\pi} V(S^4) = N_f \chi_t \phi \theta_k \quad (8.34)$$

again in perfect numerical agreement with (eq. 8.25).

This is not the only holographic derivation of Witten-Veneziano formula, a different one in an orbifold model is [103]. The effect of flavor is included in the supergravity background, so the number of flavors is comparable to the number of colors and the correspondence is taken in large N limit of a Veneziano's rather than 't Hooft's expansion. A derivation with D8 branes is presented in [59]

Chapter 9

Conclusions

Many non-perturbative features of gauge theories at strong coupling can be reproduced by gravitational backgrounds. Here, we have selected a holographic dual of a confining theory, the near horizon limit of N_c D4s compactified in a circle with supersymmetry breaking conditions. The circulation of the 2-form RR flux on the circle at the boundary is the vacuum angle of the theory, θ . The model presents a non-zero topological susceptibility and a multibranch structure, according with the physics of large- N chiral dynamics. We add flavor to the model in the form of probe N_f D6 branes, equivalent to a quenched approximation. The embedding of the branes show a zero mode in the chiral limit of zero quark masses, that can be identified with the large- N Goldstone boson of $U(1)$ axial symmetry, the η' . We can deduce the anomaly relation when the RR flux sourced by the D6 branes is taken into account $\theta \rightarrow \theta + 2\sqrt{N_f}\eta'/f_\pi$. We argue that the Witten-Veneziano mechanism should be realized in supergravity as a direct relation between closed and open-closed string amplitudes. We show evidence of non-derivative couplings for the η' , and we are able to compute the first term of the potential generated for the η' and find quantitative perfect agreement with Witten-Veneziano formula. The η' mass should be generated by a cylinder diagram with one insertion of the η' on each boundary, emulating the Isgur-de Rújula-Georgi-Glashow mechanism [104, 105]. However, the non-derivative couplings of the η' to glueballs would make the η' tachyonic, so there should be an important contact term from the stringy completion of the glueball-exchange diagram that gives a positive shift to the mass. This picture is natural when we consider the worldsheet as a cylinder that is long compared to its circumference. In the opposite corner of the moduli space, the diagram is more naturally interpreted from the open string perspective as a meson loop

with twisted η' insertions, providing an UV completion of glueball exchange.

It would be interesting to extend the analysis beyond the probe approximation, in a pure gravitational background. Since the pure-gluon dependence on the θ -angle comes from the energy of RR fluxes, the stringy mechanism would be similar to a Green-Schwarz modification of RR field strengths. It would be interesting to find a ten-dimensional anomaly polynomial that allow for the substitution $\theta \rightarrow \theta + 2\sqrt{N_f}\eta'/f_\pi$ on G_2 field strength, after a reduction on the volume of D6 branes.

We have not discussed non-Abelian flavor issues. In the $D4/D6$ model, the spectrum shows $N_f^2 - 1$ extra light pseudoscalars from independent rotations of the $D6$ branes. We would naturally associate them with the pions of the dual theory. However, there are couplings of the fermions with adjoint scalars that explicitly break the $U(N_f) \times U(N_f)$ flavor group to $U(N_f)_V \times U(1)_A$. Therefore, we expect corrections that lift the mass of the “pions” [99, 102]. Similar results appear in $D3/D7$ models, for instance [54]. However, since the mass of the adjoint field is much larger than the large- N mass of light pseudoscalars, their behavior can have an approximate description in terms of a chiral Lagrangian [58]. In $D4/D8$ models the couplings with scalars are avoided because the global flavor symmetries are identified with residual gauge symmetries of $D8$ branes at the boundary, instead of being geometrical modes of the embedding [59]. Other approaches involving geometries like Klebanov-Strassler or Maldacena-Nuñez seem to have problems to include massless flavors [53, 57].

Part III

Planar equivalence in finite volume

Chapter 10

Motivation

In the original formulation of the AdS/CFT conjecture [16–18], we relate a supergravity theory in $AdS_5 \times S^5$ to a four dimensional $\mathcal{N} = 4$ supersymmetric Yang-Mills theory. An interesting consequence of the duality is that it allows to find new conformal field theories with less supersymmetries. The R-symmetries of the gauge theory are related to the compact space S^5 , while the conformal symmetries are related to the AdS_5 part. Therefore, if we consider spacetimes of the form $AdS_5 \times X^5$, with a compact space X^5 that is less symmetric than the S^5 , the holographic duals will correspond to less supersymmetric conformal theories.

A simple way to proceed is to orbifold the five-sphere by a discrete subgroup of the isometries [106, 107]. In the field theory side, this is equivalent to project the field content of the theory by a subgroup of the R-symmetry group. Depending on the projection, we can have more or less supersymmetries left. In fact, we could define this procedure for any parent supersymmetric theory, so we can even project to a non-supersymmetric daughter theory. We will call them “orbifold field theories”.

For the theories obtained orbifolding the five-sphere, it was shown that the perturbative β -function vanishes to all orders in the planar approximation [108], thus confirming that they are conformal at this level. Actually, the analysis showed that the planar diagrams of parent and daughter theories give the same result, up to a rescaling of the coupling constant. This was pointed out and proven within a pure field-theoretical context in [109]. The perturbative result suggested that the equivalence could be extended to non-perturbative properties, and results for supersymmetric theories showed agreement with this picture [110–114].

An interesting case is when the parent theory is supersymmetric but the daughter is not. If the equivalence held non-perturbatively, then we could apply the methods developed for supersymmetric theories to study the non-perturbative properties of the daughter, that can be closer to realistic physics. In principle, the equivalence between parent and daughter would hold only in the common sector of operators and states that can be related through the orbifold projection. Such ideas have been extensively explored [115–119]. From a different point of view, it was proposed to use orbifold theories in the lattice to describe supersymmetric theories [120].

However, the non-perturbative statement presents some problems [121–123], that could be traced to tachyonic instabilities of the original geometries [124, 125]. Tachyons can be explicitly found in finite volume setups of the field theories [126, 127]. The question of non-perturbative planar equivalence of orbifold field theories has not been settled yet.

A different type of theories are “orientifold field theories” [128, 129]. They are inspired on orientifold constructions of string theory [130–132], and in the extension of the AdS/CFT conjecture to non-critical string theories [133–135]. Orientifolds appear naturally there to avoid tachyons [136, 137].

It was shown that the planar diagrams of orientifold field theories give the same values as for a $\mathcal{N} = 1$ supersymmetric theory, and there is a formal proof of non-perturbative planar equivalence [128, 129]. Many of their non-perturbative properties have been studied [128, 138–142], including an estimate of the quark condensate [138, 139]. In principle, the absence of tachyons in the string dual models would give more confidence in this type of theories. However, we will see that their finite volume behavior is not better than the one of orbifold theories [127]. But before, we will review the theories we want to study.

10.1 Orbifold and orientifold field theories

Although there are many types of planar-equivalent theories, we will deal with a constrained class related to $\mathcal{N} = 1$ theories. The number of fermionic and bosonic degrees of freedom in the large N limit is the same for planar-equivalent theories. This fact accounts for many of their properties, such as the vanishing of the vacuum energy to leading order. Other example with the same property is QCD with equal number of colors and flavors (a Dirac fermion counts twice). The main difference between the last and planar-equivalent theories is that the gauge representation of fermions is not ‘adjoint-like’, a two-index representation

that can be obtained from a projection of the adjoint of a larger or the same gauge group. Indeed, going through the demonstrations of planar equivalence [117, 118, 128, 129] we can check that they heavily rely on the properties of the representations. So we could say that the condition of equality of bosonic and fermionic degrees of freedom is necessary and the question would be whether the second condition is sufficient.

10.1.1 Orbifold theories

In the orbifold case, the parent theory is $\mathcal{N} = 1$ $U(kN)$ supersymmetric Yang-Mills in four dimensions. The field content consists on gauge fields A_μ and Weyl fermions in the adjoint representation λ_α , the last charged under a global $U(1)_R$ group. The orbifold projection is made quotienting the fields by a discrete subgroup $\mathbf{Z}_k \subset U(1)_R$. The orbifold action is a $U(1)_R$ transformation plus a global gauge transformation γ_r , $r = 0, \dots, k - 1$ acting on the fields,

$$\begin{aligned} A_\mu &\rightarrow \gamma_r A_\mu \gamma_r^{-1} \\ \lambda_\alpha &\rightarrow \gamma_r e^{2\pi i r/k} \lambda_\alpha \gamma_r^{-1}, \end{aligned} \tag{10.1}$$

the representation of the orbifold group must be regular $\text{Tr}(\gamma_r) = 0 \ \forall r \neq 0$.

The projected theory is $(U(N))^k$ Yang-Mills A_μ^i , $i = 1, \dots, k$ with Weyl fermions in bifundamental representations $\lambda_\alpha^{i,i+1} \sim (N_i, \overline{N}_{i+1})$ under two adjacent gauge groups. We can represent the action of the orbifold projection as

$$A_\mu \rightarrow \begin{pmatrix} A_\mu^1 & & & \\ & A_\mu^2 & & \\ & & \ddots & \\ & & & A_\mu^k \end{pmatrix}, \lambda_\alpha \rightarrow \begin{pmatrix} 0 & \lambda_\alpha^{1,2} & & \\ & 0 & \ddots & \\ & & \ddots & \lambda_\alpha^{k-1,k} \\ \lambda_\alpha^{k,1} & & & 0 \end{pmatrix}. \tag{10.2}$$

In the daughter theory, the orbifold action \mathbf{Z}_k is seen as permutations of the different gauge factors. Then, the equivalence could work only at the ‘‘orbifold point’’, where all couplings of the different gauge groups are the same.

Planar diagrams of both theories have the same value, when the couplings of parent and daughter are related by a rescaling $kg_p^2 = g_d^2$. The non-perturbative statement depends on both theories having the same vacuum expectation values of ‘untwisted’ (invariant under the orbifold action) operators, related by the orbifold projection. This assumes that the true vacua are ‘untwisted’ and can be mapped between parent and daughter. However,

when $k > 2$, the gaugino condensate of the parent theory breaks spontaneously the orbifold symmetry [119], so the equivalence could work only for the \mathbf{Z}_2 orbifold.

10.1.2 Orientifold theories

Orientifold theories are in some sense simpler than orbifold, since they do not have 'twisted' sectors. The parent theory is $\mathcal{N} = 1$ $SU(N)$ supersymmetric Yang-Mills in four dimensions, and the daughter has the same gauge group but with *Dirac* fermions in two-index symmetric or antisymmetric representations $\Psi_\alpha^{(ij)}$ or $\Psi_\alpha^{[ij]}$. For large N considerations it does not really matter (in principle) which one we choose.

As for orbifold theories, we should map the right operators and states between parent and daughter. Clearly, the pure gauge part will be the same, while for fermions the situation is not completely obvious. Actually, the original arguments for non-perturbative planar equivalence [128] were proposed comparing the parent theory with a *Dirac* fermion in the adjoint representation and the daughter theory with *two* Dirac fermions, in the symmetric and the anti-symmetric representations, respectively. Although this was improved later [129], the map has been established in a somehow heuristic way. Since parent and daughter are similar, their properties are also very similar: formation of a fermion condensate, currents, etc, so a simple identification is possible. For instance, we can split the Dirac fermion Ψ of the daughter theory in two Weyl fermions ξ, η so the bilinear $\lambda\lambda$ of the parent theory will be mapped to $\xi\eta$.

Chapter 11

Gauge theories in the box

11.1 Physical setup

Asymptotically free Yang-Mills theories in (small) finite volume have a (large) mass gap given by the compactification scale L . There are no propagating degrees of freedom below the mass gap, so the coupling constant is frozen at a small value. Since the theory is at weak coupling, it can be studied using analytic methods, as perturbation theory or semiclassical computations, see [143–145] for reviews. Another consequence is that below the mass gap there are only a few degrees of freedom, all the others can be integrated out in a Wilsonian approach.

Our analysis is made in principle in spaces of arbitrary dimensionality D , although for the subject of planar equivalence we will consider only four-dimensional theories. This chapter is dedicated to review the low-energy physics of gauge theories on tori, specially the moduli space and the effective potential that can be generated over it, but we will also introduce twisted boundary conditions that can lift the moduli space.

11.2 Moduli space and boundary conditions

We usually understand the (classical) moduli space as a continuous space of classical configurations of minimal energy that are physically inequivalent. For field theories with scalar degrees of freedom, the moduli space is characterized by flat directions of the potential at the minima. When quantum corrections are considered, the moduli space can change and

eventually disappear.

Pure Yang-Mills theories in Minkowski space do not have a moduli space. The reason is that minimal energy configurations should be flat connections, for which the magnetic field strength vanishes $F_{mn} = 0$. However, all the possibilities are gauge-equivalent to the trivial configuration $A_m = 0$ ¹. In a general space of non-trivial topology the situation may be different. The situation is better described using as variables Wilson loops (holonomies) that are group elements along closed curves \mathcal{C}

$$W(\mathcal{C}) = \mathcal{P} \exp \left(i \oint_{\mathcal{C}} A \right) \quad (11.1)$$

The space of flat connections is formed by Wilson loops of non-trivial homology.

Let us consider the space $\mathbf{R}^d \times \mathbf{T}^n$. Homologically non-trivial Wilson loops wrap the compact directions of the torus, so we have n of them. We will call them Wilson lines for brevity. Flat connections correspond to commuting Wilson lines, and the moduli space is parametrized by their eigenvalues. For an unitary theory (as $SU(N)$), these form a torus T_C^r , where $r (= N - 1)$ is the rank of the group. There is a further discrete Weyl symmetry that permutes the eigenvalues of the Wilson lines and turns the moduli space into an orbifold

$$\mathcal{M} = (\mathbf{T}_C^r)^n / \mathcal{W} \quad (11.2)$$

Up to now, we have considered that the fields obey periodic boundary conditions, but other situations are interesting as well. The fields need to be periodic only up to gauge transformations, but the transformed field must be the same independently of the order in which we make translations along the torus. For gauge fields this imply that the gauge transformations must commute up to a center element. When this element is non-trivial, we are imposing twisted boundary conditions. For $n = 3, d = 1$, the integers mod N that define the twist are grouped in a three-vector called magnetic flux \vec{m} . However, they are not allowed for general representations, the mathematical reason is that we are constructing a $SU(N)/\mathbf{Z}_N$ bundle², so only representations invariant under the center can be consistently introduced. The character that defines the transformation under the center is the N -ality η_R , an integer number defined mod N . The adjoint and all the other center-invariant representations have zero N -ality.

Twisted boundary conditions can be used to lift the moduli space, leaving only a set of

¹Except for a discrete set reached by large gauge transformations and labelled by winding number.

²For $SU(N)$ Yang-Mills theory, the center is \mathbf{Z}_N .

discrete vacua labelled by \mathbf{Z}_N elements. If there are fields of non-zero N -ality, then the twist cannot be maximal, and the moduli space is not completely lifted. Even when the maximal twist \mathbf{Z}_N is possible, we can impose a non-maximal twist $\mathbf{Z}_k \subseteq \mathbf{Z}_N$ if $\gcd(N, k) = l \neq 1$. The moduli space is then reduced to that of a $SU(l)$ theory. So, if $\gcd(N, \eta_R) = 1$, there can be no twist. Twisted boundary conditions were introduced by 't Hooft [146] and successfully applied by Witten to study supersymmetric theories [147, 148]. The topics we review briefly here can be found more thoroughly studied in these references. An extensive classical analysis of twisted boundary conditions in \mathbf{T}^4 can also be found in [145].

Another consequence of having fields of zero N -ality is that we are allowed to make twisted gauge transformations, that are periodic up to an element of the center. These transformations are topologically non-trivial and lie in different homotopy classes that cannot be continuously connected with the identity. Gauss' law only implies invariance under homotopically trivial local gauge transformations, so we can find new physical sectors of the theory using the twisted transformations. This is analogous to the topologically non-trivial vacua associated to instantons, but in this case the vacua are related to the wrapping of the group $SU(N)/\mathbf{Z}_N$ around one-cycles instead of the wrapping of $SU(N)$ around three-cycles.

As we will see, twisted transformations induce shifts along the moduli space, in particular, they move fixed points of the Weyl action among themselves. For $d = 1$, $n = 3$ we can associate the integers \vec{k} that define the twisted transformation and the magnetic flux \vec{m} to an Euclidean twisted configuration in $d = 0$, $n = 4$, determined by the twist tensor $n_{\mu\nu}$

$$\begin{aligned} n_{ij} &= \epsilon_{ijk} m_k \\ n_{0i} &= k_i \end{aligned} \tag{11.3}$$

The twist tensor (11.3) defines the gauge bundle on \mathbf{T}^4 . In general, the Euclidean gauge bundles will have a curvature. In this case, the action does not vanish, but it has a minimum value given by the Pontryagin number or topological charge. Usually, contributions from ordinary instantons are considered. They come from bundles associated to the wrapping of the gauge group over a S^3 . Then, this contribution is an integer known as the winding number. For gauge bundles associated to the torus, the contribution to topological charge can be fractional, because we are using a representation that is not faithful for $SU(N)/\mathbf{Z}_N$. In the sector of zero winding number, the topological charge is given by

$$\mathcal{Q} = \frac{1}{16\pi^2} \int_{\mathbf{T}^4} \text{tr} F_{\mu\nu}(x) \tilde{F}_{\mu\nu}(x) d^4x = -\frac{1}{4N} n_{\mu\nu} \tilde{n}_{\mu\nu} = -\frac{1}{N} \vec{k} \cdot \vec{m} \tag{11.4}$$

where $\tilde{A}_{\mu\nu} = (1/2)\epsilon_{\mu\nu\rho\sigma}A_{\rho\sigma}$. Notice that when $\vec{m} \neq 0$, other vacua different to $A = 0$ can be reached only by twisted transformations with $\vec{k} \cdot \vec{m} = 0$.

11.3 One-loop potential over moduli space

Quantum corrections can change the classical moduli space. In the weak coupling regime, the first corrections are one-loop contributions to the vacuum energy, in the form of an effective potential depending on the holonomies. The first versions of the potential date from the early eighties, when it was used to show that gauge theories in $\mathbf{R}^3 \times \mathbf{S}_\beta^1$ are deconfined at high temperatures $\beta \ll 1$ [149–151]. A similar version was considered for gauge theories with a compactified spatial direction $\mathbf{R}^d \times \mathbf{S}_L^1$ [152], as a failed tentative to break dynamically the gauge symmetry. That was achieved soon afterwards in $\mathbf{R}^d \times \mathbf{S}^2$ spaces [153], and the potential was later extended to $\mathbf{R}^2 \times \mathbf{S}_L^1 \times \mathbf{S}_\beta^1$ spaces [154]. On a different line, the $\mathbf{R} \times \mathbf{T}_L^3$ version was computed to study non-perturbative properties of four-dimensional Yang-Mills theories at weak coupling [155]. This version was generalized to include arbitrary representations and fermions. Although the field has evolved [156], these are still the main three applications of the potential [126, 127, 157, 158], roughly speaking.

The potential can be computed using a perturbative expansion in the path integral formalism, where moduli configurations enter as background fields. To parametrize the moduli space we will use constant connections in the Cartan subalgebra of the group along the compact directions,

$$A_m = A_m^a H^a \quad , \quad [H^a, H^b] = 0 \quad , \quad a = 1, \dots, N-1 \quad (11.5)$$

They will enter as background fields in the path integral. Before going to the calculation itself, let us change a bit our parametrization. The Cartan matrices are diagonal matrices whose eigenvalues are the components of $N-1$ -dimensional vectors in the weight space. These vectors are the weights of the defining representation ν^i , that form a non-orthogonal basis

$$\nu^i \cdot \nu^j = \frac{1}{2}\delta^{ij} - \frac{1}{2N} \quad , \quad i, j = 1, \dots, N-1 \quad (11.6)$$

Assuming that the torus has the same length in all directions $l_m = L$, $m = 1, \dots, n$, we will define \vec{C}^a through

$$\vec{A} = \text{diag}(\nu^1 \cdot \vec{C}, \dots, \nu^N \cdot \vec{C}) \quad , \quad \sum_{i=1}^N \nu^i = 0 \quad (11.7)$$

These coordinates for the moduli space are equivalent to parametrize the torus with phases

$$W(\mathbf{S}_m^1) = \exp(i\nu \cdot C_m) \quad (11.8)$$

where $\mathbf{S}_m^1 \subset \mathbf{T}^n$. We can use the properties of weight systems to translate the properties of periodicity and Weyl symmetries to the \vec{C} space. They read as

$$\left. \begin{array}{l} \text{Periodicity} \quad \vec{C} \sim \vec{C} + 4\pi\alpha\mathbf{Z}^n \\ \text{Weyl} \quad \quad \quad \vec{C} \cdot \alpha \sim -\vec{C} \cdot \alpha \end{array} \right\} \quad (11.9)$$

where α are the roots, the weights of the adjoint representation. We will see that all quantities depending on \vec{C} obey these symmetries. It might seem a strange parametrization, but it will allow us to make straightforward generalizations to different matter contents.

We can continue now with the path integral computation. We will use the covariant gauge-fixing of the background field,

$$D_M \mathcal{A}_M = \partial_M \mathcal{A}_M + i \left[\frac{1}{L} \nu \cdot C_M, \mathcal{A}_M \right] = 0 \quad (11.10)$$

that makes computations simpler. Notice that it reduces to the Lorentz gauge along the non-compact directions.

The $d = 1$ case deserves an special comment. We will follow the same procedure, but the one-loop contribution to the vacuum energy is actually a Wilsonian effective potential for the zero modes. We can describe the low energy physics of the theory using a kind of Born-Oppenheimer approximation where the degrees of freedom of higher energy have been integrated out and we are left only with the moduli space. This approach has been used as a non-perturbative method to find the lowest energy states of QCD and their masses.

We are ready to compute the partition function at different points of the moduli space $\mathcal{Z}(\vec{C})$. The path integral is a Gaussian in the one-loop approximation, so formally we are left with a determinant over the spectrum of states together with a Faddeev-Popov factor. When zero modes are not included in the determinants we will add a prime.

$$\mathcal{Z}(\vec{C}) = \det'_{\text{FP}} \left(-D^2(\vec{C}) \right) \det' \left(-D^2(\vec{C}) \right)^{-(n+d)/2} \quad (11.11)$$

The vacuum energy density is $V_{\text{eff}}(\vec{C}) = i \log \mathcal{Z}(\vec{C})$, that is proportional to the number of physical polarizations

$$V_{\text{eff}}(\vec{C}) = -i(d+n-2) \text{Tr} \log \left[-\partial_\mu \partial^\mu - \left(\vec{\partial} + i \left[\frac{1}{L} \vec{C}, * \right] \right)^2 \right] \quad (11.12)$$

The trace is made over all possible momentum modes in the non-compact directions p_μ , $\mu = 0, \dots, d-1$ and all Kaluza-Klein modes in the compact directions \vec{k}/L , where \vec{k} are integers. The details of the calculation are in App. B. The final result is

$$V_{\text{eff}}(\vec{C}) = (d+n-2) \sum_{\alpha \in \text{roots}} V(\alpha \cdot \vec{C}) \quad (11.13)$$

the sum over roots can be traced to the commutator term in the covariant derivative, that introduce factors of the form $(\nu^i - \nu^j) \cdot \vec{C}$, where the difference of two weights of the defining representation is precisely a root.

The function V is universal for a given space-time, it does not depend on the Lorentz representation of the modes that give rise to the vacuum energy or on the gauge group representation. The bosonic and vector nature of the fields is in the factor $+(d+n-2)$, the sum over roots appears because the gauge fields are in the adjoint representation.

There are several properties of the function V that will be useful to study the properties of the induced potential over the moduli space. Let us write here its final expression, up to a constant term that has been substracted

$$V(\vec{x}) = \frac{\Gamma\left(\frac{d+n}{2}\right)}{\pi^{\frac{d+n}{2}}} \frac{1}{L^d} \sum_{\vec{l} \neq 0} \frac{\sin^2\left(\frac{1}{2}\vec{l}\vec{x}\right)}{(\vec{l}^2)^{\frac{d+n}{2}}} \quad (11.14)$$

It is positive definite, vanishes at the origin, is periodic under $\vec{x} \rightarrow \vec{x} + 2\pi\mathbf{Z}^n$ and is symmetric under reflections $\vec{x} \rightarrow -\vec{x}$. The minima sit at $\vec{x} = 0 \bmod 2\pi\mathbf{Z}^n$ while the maxima are at $\vec{x} = (\pi, \pi, \dots, \pi) \bmod 2\pi\mathbf{Z}^n$. The behavior at the minima depends on the dimensionality of the non-compact space (App. B),

$$V(\vec{x}) \sim \begin{cases} \vec{x}^2 + (\vec{x}^2)^{d/2} & d \text{ odd} \\ \vec{x}^2 + (\vec{x}^2)^{d/2} \log \vec{x}^2 & d \text{ even} \end{cases} \quad (11.15)$$

Usually, the quadratic analytic term is dominant, but for $d=2$ the logarithmic contribution is comparable, and for $d=1$ the non-analytic contribution is the leading one, giving rise to conical singularities. We will explain the origin of the non-analyticity later on.

We can now investigate the geometric properties of the potential over the moduli space. The potential is a sum of terms of the form $V(\alpha \cdot \vec{C})$. It is easy to check that every term obeys the symmetries (11.9), as we predicted. Each term has its minima at the hyperplanes defined by

$$\alpha \cdot C_m = 0 \bmod 2\pi\mathbf{Z} \quad (11.16)$$

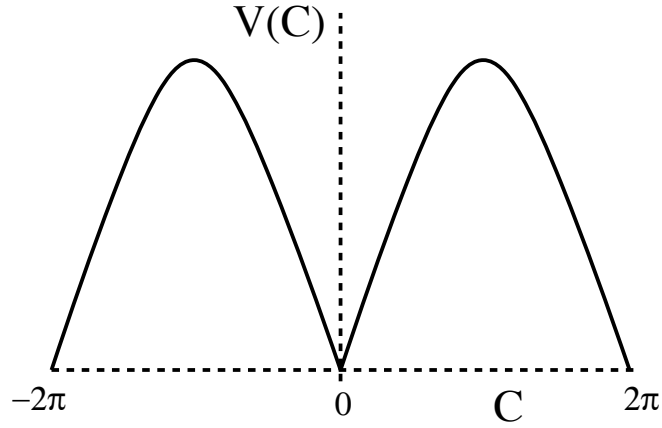


Figure 11.1: $d = 1$ $SU(2)$ bosonic potential along a Cartan direction. Conical minima are located at $C = 0 \bmod 2\pi$, smooth maxima at $C = \pi \bmod 2\pi$.

which are parallel hyperplanes of codimension one, perpendicular to the roots. We can go from one plane to the next by translations along the roots $C_m \rightarrow C_m + 2\pi\alpha/\sqrt{\alpha^2}$. These planes are fixed under the action of Weyl transformations, so we will name them as Weyl (hyper)planes. The local minima of the potential lie at single points where $N - 1$ Weyl planes intersect. For the adjoint representation, the minima are at

$$\vec{C} = 4\pi \sum_i \vec{n}_i \nu^i, \quad \vec{n}_i \in \mathbf{Z}^n \quad (11.17)$$

where all the terms of the potential vanish. Notice that the local minima coincide with the fixed points of Weyl transformations, that is, the orbifold fixed points of the moduli space \mathcal{M} . In order to learn a bit more about these points, let us go out of the moduli space so we can approach a point \vec{C} belonging to the moduli space from a non-Abelian direction. In general, it will have a mass given by the classical potential $([C_m + \mathcal{A}_m, C_n + \mathcal{A}_n])^2 \simeq C^2 \mathcal{A}^2$, but this mass vanishes at $\vec{C} = 0$, leaving a quartic potential. This is the reason of the non-analyticities of the potential at the minima (11.15), we are integrating out degrees of freedom that are effectively massless. Notice also that the local minima are points where the global gauge symmetries are unbroken, while at a generic point of the moduli space, they are broken to the maximal Abelian subgroup (Coulomb branch).

In the previous section we introduced twisted gauge transformations and commented that they induce shifts along the moduli space. This can be seen using the Abelian form

$$U_T(\vec{w}) = \exp\left(\frac{2\pi i}{N} \frac{w_m x_m}{L}\right) \mathbf{1}, \quad w_m \in \mathbf{Z} \quad (11.18)$$

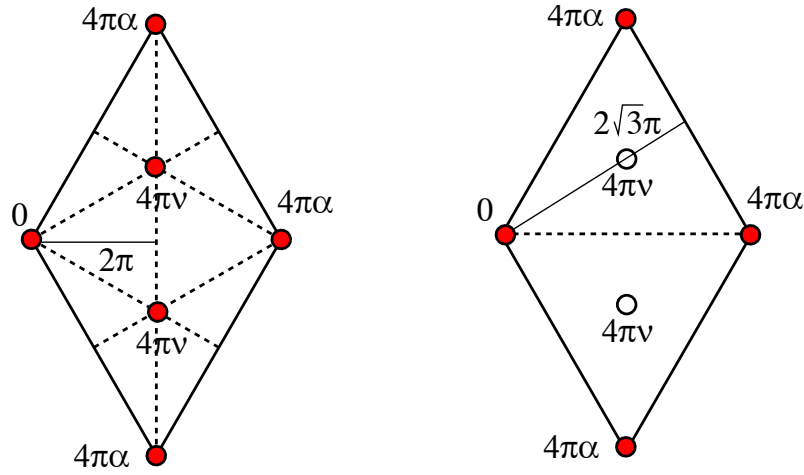


Figure 11.2: The structure of the $SU(3)$ potential for the adjoint representation (on the left) and the defining vector representation (on the right). The Weyl hyperplanes are indicated by dashed lines. We see that the effective Weyl chamber for the vector representation is bigger than the adjoint one by a factor $\sqrt{3}$. The singular points (global minima or maxima) lie on the intersection of Weyl hyperplanes. For the vector representation, we also mark by white circles the smooth critical points of the potential.

The gauge connection transforms as

$$A_m \rightarrow A_m - \frac{2\pi}{NL} w_m \tag{11.19}$$

which is equivalent to a shift of the form

$$C_m \rightarrow C_m + 4\pi\nu^i w_m \tag{11.20}$$

for any ν^i . Notice that as we advanced before, twisted transformations move fixed points (11.17) among themselves. We have found that the local minima of the one-loop potential associated to gauge fields are related by a global $(\mathbf{Z}_N)^n$ symmetry. This can be traced to the invariance of adjoint fields under center transformations. For general representations of non-zero N -ality, this global symmetry will not exist, so we expect that minima associated to the orbifold points will be lifted by different amounts.

11.3.1 Generalizations

The potential can be easily generalized to fields in different representations R under the Lorentz and the gauge group. If it is possible, we can even add a mass for the fields and find the exact result. The complete details are in App. B. Here is the final expression, that we start to explain below

$$V_R(\vec{C}) = (-1)^{F_R} \mathcal{N}_R \sum_{\mu_R} V_{M_R}(\mu_R \cdot \vec{C}) \quad (11.21)$$

As with the gauge fields, the number of physical polarizations \mathcal{N}_R will give a factor in front of the scalar part of the potential, that will include information about the group representation R , the space-time and the mass M_R . Remember that the sign of the potential changes as $(-1)^{F_R}$ depending on the fermionic number of the fields F_R .

The group dependence is derived writing the group representation as a tensor with indices transforming in the fundamental or anti-fundamental representation. The commutator part of the covariant derivative (the adjoint action) is

$$(Ad(A)\psi)_{i_1 \dots i_k}^{j_1 \dots j_l} = \sum_{a=1}^k A_{i_a}^n \psi_{i_1 \dots n \dots i_k}^{j_1 \dots j_k} - \sum_{b=1}^l A_m^{j_b} \psi_{i_1 \dots i_k}^{j_1 \dots m \dots j_l} . \quad (11.22)$$

Writing the Cartan matrices in terms of the defining weights ν^i , we end up with combinations that are the weights μ_R of the group representation. As a comment, the N -ality is given by $\eta_R = k - l$.

As for the mass, it will affect the values of the spectrum, changing the function V (11.14) to

$$V_M(\vec{x}) = \frac{2}{L^d} \left(\frac{ML}{2\pi} \right)^{\frac{d+n}{2}} \sum_{\vec{l} \neq 0} K_{\frac{d+n}{2}} \left(ML \sqrt{\vec{l}^2} \right) \frac{\sin^2 \left(\frac{1}{2} \vec{l} \cdot \vec{x} \right)}{\left(\vec{l}^2 \right)^{\frac{d+n}{4}}} \quad (11.23)$$

where $K_\nu(x)$ is a modified Bessel function of the second kind. We recover the massless potential when $ML \rightarrow 0$ from the limit $K_\nu(x \rightarrow 0) \sim \frac{1}{2} \Gamma(\nu) (2/x)^\nu$. On the other hand, the asymptotics $K_\nu(x \gg 1) \sim e^{-x} \sqrt{\pi/2x}$ implies that the sum over modes is effectively cutoff at $\sqrt{\vec{l}^2} < (ML)^{-1}$. In particular, for large masses $ML \gg 1$, the whole potential is suppressed by a factor $\exp(-ML)$. However, the mass does not modify the symmetry properties of the potential nor its qualitative shape, that is given by the leading modes in the sum.

The main differences with the potential of gauge fields are the sign (if its generated by fermions), the scale factor, given roughly by $\sim \mathcal{N}_R \dim(R) \exp(-ML)$ and the weight dependence. Now the Weyl planes are defined by the weights of R , and not by the roots, so the minima will be in general at different points. The Weyl chamber is also different, its size determined by the highest weight of the representation μ_R^h to be $\sim 2\pi/|\mu_R^h|$ (Fig. 11.3). So the potential has more structure at smaller regions of the moduli space for large representations. If the N -ality is non-zero $\eta_R \neq 0$, then the potential will have different values at the minima of the gauge potential, breaking the global \mathbf{Z}_N symmetries. Indeed

$$\mu_R \cdot 4\pi \sum_i \vec{n}_i \nu^i = \frac{2\pi\eta_R}{N} \sum_i \vec{n}_i + 2\pi (\text{integer}) \quad (11.24)$$

since every weight is a sum of defining weights with positive or negative integer coefficients $\mu_R \simeq k\nu - l\nu$ and the sum of the coefficients is conserved within a representation and equal to the N -ality $\eta_R = k - l$.

Chapter 12

Planar equivalence in the box I

In this section we will study orbifold and orientifold theories in small volume $\mathbf{R} \times \mathbf{T}_L^3$, $L \ll 1$, $g_{\text{YM}}(L)^2 N \ll 1$. We will impose periodic boundary conditions, so low-energy physics are dominated by the moduli space of flat connections and the potential that quantum corrections generate over it. Both are discussed in Chapter 11. We will start identifying the leading $O(N^2)$ behavior of the effective potential as the relevant quantity to test planar equivalence. Then, we will explain the caveats about planar equivalence in finite volume for both orbifold and orientifold theories, and finally we will show that planar equivalence does not hold in finite volume.

12.1 Planar equivalence and the “planar index”

The naturally protected quantity for minimally supersymmetric systems in finite volume is the supersymmetric index, $I = \text{Tr}(-1)^F$, [147, 148]. In the case at hand, we shall be interested in the related graded partition function

$$I(\beta) = \text{Tr} \mathcal{P} (-1)^F e^{-\beta H} , \quad (12.1)$$

where \mathcal{P} is a projector introducing possible refinements of the index with respect to extra global symmetries of the problem. In principle, a judicious choice of \mathcal{P} might be necessary to establish the planar equivalence, but we shall suppress it for the time being. Unlike the analogous object in the parent $\mathcal{N} = 1$ theory, $I(\beta)$ is not independent of β/L or the dimensionless couplings in the Lagrangian. The interesting question is whether we can establish an approximate BPS character of $I(\beta)$.

The strongest possible statement of planar equivalence would have $I(\beta)$ behaving as a supersymmetric index of a rank N supersymmetric gauge theory, at least in some dynamical limit. This would mean a large- N scaling of order

$$I(\beta) = O(N). \quad (12.2)$$

On the other hand, perturbative planar equivalence poses much weaker constraints on the graded partition function, i.e. it only requires

$$\log I(\beta) = O(N), \quad (12.3)$$

since the leading $O(N^2)$ term is a sum of planar diagrams and should vanish as in the supersymmetric parent. Notice that condition (12.3) is exponentially weaker than (12.2). The physical interpretation of the minimal planar equivalence condition (12.3) depends to a large extent on the dynamical regime that we consider. For example, the implications for the structure of the spectrum depend on the value of the ratio β/L . Let us write (12.1) in terms of the spectrum of energy eigenvalues,

$$I(\beta) = \sum_E (\Omega_B(E) - \Omega_F(E)) e^{-\beta E}, \quad (12.4)$$

with $\Omega_{B,F}$ the boson and fermion density of states. The thermal partition function is given by

$$Z(\beta) = \sum_E (\Omega_B(E) + \Omega_F(E)) e^{-\beta E}. \quad (12.5)$$

In the large-volume limit, $\beta/L \ll 1$, these quantities are dominated by the high-energy asymptotics of the spectrum. In particular, for asymptotically free theories, we expect that the free energy can be approximated by that of a plasma phase. Thus, on dimensional grounds,

$$\log Z(\beta) = -N^2 f(\lambda) (L/\beta)^3 + O(N), \quad (12.6)$$

up to a vacuum-energy contribution linear in β , with $f(\lambda)$ a function of the 't Hooft coupling $\lambda = g^2 N$, conveniently renormalized at the scale $1/\beta$. From this expression we infer that the asymptotic high-energy behavior of the density of states is given by

$$\log \Omega_{B,F}(E) = \sqrt{N} s_{B,F}(\lambda) (EL)^{3/4} + O(N). \quad (12.7)$$

Notice that the leading term is of $O(N^2)$ for $E = O(N^2)$. Then, the prediction of planar equivalence boils down to $s_B = s_F$, namely the leading $O(N^2)$ high-energy asymptotics of the density of states is effectively supersymmetric.¹

¹This property is very similar to the so-called “misaligned supersymmetry”, studied in [159], that characterizes non-supersymmetric string theories without classical tachyonic instabilities.

Conversely, in the opposite limit $L/\beta \ll 1$ the graded partition function $I(\beta)$ is dominated by low-lying states. In the classical approximation, the Hamiltonian of gauge theories on \mathbf{T}^3 has states of vanishing potential energy, corresponding to flat connections on the gauge sector and zero eigenvalues of the Dirac operator on the fermion sector. This implies that there is a neat separation of scales, of order $1/L$, between zero modes and the rest of the degrees of freedom in the limit of small volume. The graded partition function may be written as

$$I(\beta) = \text{Tr}_{\text{slow}} (-1)^F e^{-\beta H_{\text{eff}}}, \quad (12.8)$$

with H_{eff} a Wilsonian effective Hamiltonian for the zero modes or “slow variables”. For asymptotically free theories, this Hamiltonian may be estimated in a weak-coupling expansion in the small running coupling $g^2 N$, defined at the scale $1/L$ (c.f. [155, 156, 160–163]).

A characteristic behavior of the supersymmetric index is that the effective Hamiltonian acting on the space of zero modes with energies much smaller than $1/L$ is free, i.e. the Wilsonian effective potential induced by integrating out the non-zero modes vanishes exactly as the result of boson/fermion cancellation. In the non-supersymmetry case, a similar behavior of (12.8) would require that the effective potential be at most of order $V_{\text{eff}} = O(1/N)$, i.e. it would have to vanish in the large N limit. On the other hand, planar equivalence would require the weaker condition that this effective potential vanishes to leading $O(N^2)$ order or, equivalently $V_{\text{eff}} = O(N)$.

Therefore, the existence of a sort of “planar index” seems to be a stronger property than “minimal” planar equivalence, in the sense discussed previously. Understanding this fact in detail is important, given the close relationship between the supersymmetric index in finite volume and the gaugino condensates in the standard $\mathcal{N} = 1$ SYM lore [164, 165].

Now we turn to examine the zero-mode effective potentials for the particular examples of theories in which a form of planar equivalence is expected to hold.

12.2 Effective potentials and planar equivalence

At the level of the effective potentials considered in this work, the property of planar equivalence manifests itself in the cancellation of bosonic and fermionic contributions to leading order in the large- N expansion. Namely, one should find $V_{\text{eff}}(\vec{C}) = O(N)$ instead of the more generic $O(N^2)$ scaling. Alternatively, one relates the given model to its supersym-

metric parent. In many cases, this comparison is rather subtle. For example, in orbifold models the detailed global structure of the toron valleys changes from parent to daughter, since the Weyl groups are clearly different. Hence, the domains of definition of $V_{\text{eff}}(\vec{C})$ differ between parent and daughter theories and a precise comparison would involve a further refinement of the projector that appears in (12.1).

For models with the same configuration space, such as the orientifold field theory, the main property that ensures planar equivalence is the equality, to leading $O(N^2)$ order, of the fermion effective actions between parent and daughter, i.e.

$$\text{Tr}_{\text{Ad}} \log (i\mathcal{D}) - \text{Tr}_{\text{R}} \log (i\mathcal{D}) = O(N). \quad (12.9)$$

In principle, this property may be established in a strong sense, for any sufficiently smooth gauge connection A , provided it belongs to the configuration space of both theories. Within the weak-field expansion, the perturbative version of planar equivalence ensures (12.9) to any finite order in the one-loop Feynman diagram expansion in the background field. To see this, consider the one-loop diagram with n external legs, proportional to $\text{Tr}_{\text{R}} (A/\not{D})^n$. It contains a group-theory factor proportional to $\text{Tr}_{\text{R}} T^{a_1} \dots T^{a_n}$. Reducing this trace to a combination of symmetrized traces, we end up with terms of the form

$$\text{STr}_{\text{R}} T^{a_1} \dots T^{a_n} = I_n(R) d^{a_1 \dots a_n} + \text{lower order products}, \quad (12.10)$$

where $I_n(R)$ denotes the Dynkin index of the representation R , and the symmetric polynomial $d^{a_1 \dots a_n}$ is the symmetrized trace in the fundamental representation.

Then, the Dynkin index for the symmetric and antisymmetric representations, S_{\pm} , is given by $I_n(S_{\pm}) = 2(N \pm 2^n)$ (c.f. [166, 167]), to be compared with $I_n(\text{Ad}) = 2N$ for the adjoint representation. The leading Dynkin index is indeed the same in the large- N limit, so that a given diagram with an arbitrary (but *fixed*) number of legs yields the same contribution in the large- N limit in the parent and daughter theories. So far this is just another way of looking at the statement of perturbative planar equivalence. However, $I_n(S_{\pm})$ has a subleading (non-planar) term that blows-up exponentially with the number of legs of the diagram. Hence, planar equivalence stated diagram by diagram no longer guarantees that the full non-perturbative effective action will satisfy the planar-equivalence property (12.9). In principle, there could be a non-commutativity between the large- N limit and the non-linearities beyond the weak-field expansion, and this question could be a dynamical one, i.e. depending on the particular gauge connection considered as background.

These considerations show that the behavior of the exact one-loop potential (11.13) under planar equivalence is a rather non-trivial issue. The purely perturbative version of the planar equivalence is strictly related to the Taylor expansion of the potential around the origin of moduli space $\vec{C} = 0$, and the behavior at finite distance away from the origin, $|\vec{C}| \sim 1$, remains an open question. In the following subsections we consider in more detail the effective potential in the two main examples of planar equivalence.

12.2.1 Orientifold effective potential

The orientifold model defined by a $SU(N)$ gauge theory with a Dirac fermion in the antisymmetric representation has an effective potential for the flat connections that we may conveniently write as a superposition of the basic $SU(2)$ potentials (11.14), following the general structure of (11.13).

It is convenient to parametrize the weights and roots of the relevant representations as $\nu^i + \nu^j$ with $i < j$ run over the weights of the antisymmetric two-index representation, whereas $\nu^i - \nu^j$ run over the roots of $SU(N)$ as $i, j = 1, \dots, N$, except for the fact that in this way we count one extra vanishing root, which gives no contribution since $V(0) = 0$ in our additive convention for the vacuum energy.² The final form of the potential is

$$V_{\text{ori}}(\vec{C}) = \sum_{i,j} V\left((\nu^i - \nu^j) \cdot \vec{C}\right) - 2 \sum_{i < j} V\left((\nu^i + \nu^j) \cdot \vec{C}\right), \quad (12.11)$$

with an extra term

$$-2 \sum_i V\left(2\nu^i \cdot \vec{C}\right) \quad (12.12)$$

to be added for the symmetric two-index representation. The first two terms are nominally of $O(N^2)$ from the multiplicity of the index sums, whereas the last term is at most of $O(N)$, and thus may be ignored when discussing the property of (minimal) planar equivalence in this model.

The first nontrivial property of the orientifold potential is the instability of the origin of moduli space, $\vec{C} = 0$. To see this, we can explore the potential along the direction of a fundamental weight, say $\vec{C} = \nu^1 \vec{c}$, with very small \vec{c} , so that the $SU(2)$ potential can be approximated by $V(\vec{\xi}) \simeq v|\vec{\xi}|$ with v a positive constant.

²The \vec{C} -independent part of V_{eff} vanishes to $O(N^2)$ in all the models of planar equivalence.

Evaluating the potential in this direction one obtains

$$V_{\text{ori}}(\nu^1 \vec{c}) \approx -N |\vec{c}| \quad (12.13)$$

up to subleading corrections at large N . Hence, we conclude that the zero-holonomy point at the origin of moduli space becomes severely unstable at large N .

The scale over which the bosonic and fermionic contributions vary is roughly the same, since the size of the Weyl chamber for the two-index representations is

$$\ell_{S_{\pm}} = \frac{2\pi}{|\nu^i + \nu^j|} = 2\pi + O(1/N), \quad i \neq j, \quad (12.14)$$

whereas the size of the standard Weyl chamber is $\ell_{\text{Ad}} = 2\pi/|\nu^i - \nu^j| = 2\pi$. On the other hand, the alignment of the bosonic and fermionic potentials is not perfect. We can see this by checking the height of the local conical minima³, that are inherited from the absolute zeros of the bosonic potential. Conical minima of the bosonic potential are determined by the equations

$$(\nu^i - \nu^j) \cdot \vec{C}^{(0)} = 0 \pmod{2\pi \mathbf{Z}^3} \quad (12.15)$$

for all i, j , which have as the general solution the integer lattice generated by the vectors $4\pi \nu^i$. We can now evaluate the fermionic contribution

$$V_{\text{F}}(\vec{C}^{(0)}) = -2 \sum_{i < j} V \left((\nu^i + \nu^j) \cdot \vec{C}^{(0)} \right) \quad (12.16)$$

at a generic zero of the bosonic contribution, given by $\vec{C}^{(0)} = 4\pi \sum_i \vec{n}_i \nu^i$, with $\vec{n}_i \in \mathbf{Z}^3$. Using the properties of the basic weights we have

$$(\nu^i + \nu^j) \cdot 4\pi \sum_k \vec{n}_k \nu^k = 2\pi(\vec{n}_i + \vec{n}_j) - \frac{4\pi}{N} \sum_k \vec{n}_k \quad (12.17)$$

and, by the periodicity properties of the $SU(2)$ potential, we can write

$$V_{\text{F}}(\vec{C}^{(0)}) \sim -N^2 V \left(\frac{4\pi}{N} \sum_k \vec{n}_k \right). \quad (12.18)$$

Hence, as we move around the lattice of conical minima from points with $\sum_k \vec{n}_k = O(1)$ to points with $\sum_k \vec{n}_k = O(N)$, the potential scans on a band of energies ranging from $O(N)$ up to $O(N^2)$, with a typical spacing of $O(N)$. As an example of a set of local minima with

³The conical singularities are smoothed out when considering the effects of the light non-abelian degrees of freedom.

$O(N^2)$ negative energy, we can consider points in the lattice satisfying $\sum_k \vec{n}_k = (N/4, 0, 0)$ at large values of N such that $N/4$ is an integer. On these points, the fermionic contribution is maximal and given by

$$V_F = -N^2 V(\pi) + O(N). \quad (12.19)$$

In an analogous fashion, the conical maxima of the fermionic potential should be lifted up by the smooth portions of the bosonic potential giving us an intricate *landscape* (see App. C) of very narrow valleys and peaks on the $O(N)$ scale of relative heights, with some walls rising up to $O(N^2)$ energies. The conclusion is that nonlinear effects at finite distance away from the origin of moduli space tend to spoil the property of planar equivalence, at least when looking at the potentials with high enough resolution.

In fact, it turns out that planar equivalence is still maintained on the average, since the integral of (12.11) over the toron valley is only of $O(N)$. To see this, we can expand the flat connections in the basis of the simple roots $\alpha_s^i = \nu^i - \nu^{i+1}$, $i = 1, \dots, N-1$, i.e. we write

$$\vec{C} = \sum_{l=1}^{N-1} \vec{c}_l \alpha_s^l \quad (12.20)$$

and the orientifold potential takes the form

$$V_{\text{ori}}(\vec{C}) = \sum_{i,j} [V(\frac{1}{2}(\vec{c}_i - \vec{c}_{i-1} - \vec{c}_j + \vec{c}_{j-1})) - V(\frac{1}{2}(\vec{c}_i - \vec{c}_{i-1} + \vec{c}_j - \vec{c}_{j-1}))] + O(N). \quad (12.21)$$

In this expression, we have neglected terms of $O(N)$ coming from restrictions on the range of the indices. When averaging over the toron valley, the coordinates \vec{c}_j become dummy integration variables, and an appropriate change of variables shows that the bosonic and fermionic terms cancel out upon integration.

We can use similar arguments to show that the average of the squared potential $(V_{\text{ori}})^2$ is at most of $O(N^3)$. This shows that the average cancellation of $O(N^2)$ terms in (12.21) does not come from large “plateaus” of $O(N^2)$ energy occupying different $O(1)$ fractions of moduli-space’s volume. If that would have been the case, all these smooth regions would contribute to $(V_{\text{eff}})^2$ as positive plateaus of $O(N^4)$ energy, producing an average squared potential of $O(N^4)$.

The vanishing of the leading $O(N^4)$ terms in the averaged squared potential suggests that the valleys and peaks of the orientifold potential are localized over small volumes of the moduli space in the large N limit. Still, the wave functions will show strong localization

properties and our analysis sheds no new light on the important question of chiral symmetry breaking in these models (non-trivial expectation values of fermion bilinears in the infinite volume limit).

12.2.2 Orbifold effective potential

For the basic orbifold model with $SU(N) \times SU(N)$ group and a bi-fundamental Dirac fermion we have a potential defined over the direct product of toron valleys parametrized by \vec{C}_1 and \vec{C}_2 flat connections. It has the form

$$V_{\text{orb}}(\vec{C}_1, \vec{C}_2) = \sum_{i,j} V\left((\nu^i - \nu^j) \cdot \vec{C}_1\right) + \sum_{i,j} V\left((\nu^i - \nu^j) \cdot \vec{C}_2\right) - 2 \sum_{i,j} V\left(\nu^i \cdot \vec{C}_1 - \nu^j \cdot \vec{C}_2\right). \quad (12.22)$$

The properties of this potential are similar to those of the orientifold model studied in the

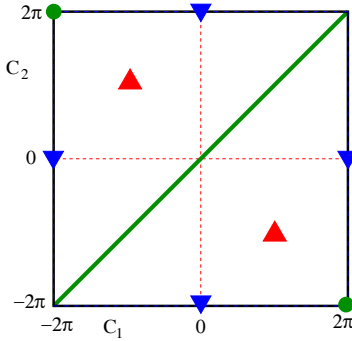


Figure 12.1: Section of the potential for the $SU(2) \times SU(2)$ orbifold field theory. The diagonal line is the region where bosonic and fermionic potentials cancel one another. Global minima of negative energy lie at the points marked by triangles pointing downwards. Global maxima of positive energy are also indicated by triangles pointing upwards.

previous subsection. Conical minima are again distributed in an intricate *landscape* with energy spacings of $O(N)$ but reaching energies of $O(N^2)$. Conical zeros of the bosonic potentials are given by flat connections of the form

$$\vec{C}_{1,2}^{(0)} = 4\pi \sum_l \vec{n}_{1,2,l} \nu^l. \quad (12.23)$$

At these points, the fermionic contribution has the value

$$V_F(\vec{C}_1^{(0)}, \vec{C}_2^{(0)}) = -N^2 V\left(\frac{2\pi}{N} \left(\sum \vec{n}_2 - \sum \vec{n}_1\right)\right) \quad (12.24)$$

and, as before, we have negative minima with energies ranging from $O(N)$ to $O(N^2)$ as $\sum \vec{n}_2 - \sum \vec{n}_1$ ranges from $O(1)$ to $O(N)$.

The global picture is very similar to the case of the orientifold model, including the rough statistical properties of the potential. The same analysis used before also shows that the orbifold potential averages to $O(N)$ energy while the squared potential averages to $O(N^3)$.

The similarity between the orbifold and the orientifold potential is even quantitative along the “antidiagonal” of the moduli space, i.e. the hypersurface defined by $\vec{C}_+ = 0$, where $\vec{C}_\pm = \frac{1}{2}(\vec{C}_1 \pm \vec{C}_2)$ are the eigenvalues of the orbifold \mathbf{Z}_2 action over the moduli coordinates. Along this hypersurface of \mathbf{Z}_2 -odd connections the orbifold potential is identical to the orientifold one, up to $O(N)$ corrections,

$$V_{\text{orb}}(0, \vec{C}_-) = 2 V_{\text{ori}}(\vec{C}_-) + O(N). \quad (12.25)$$

Notice that this argument also implies that the origin of moduli space is unstable along the antidiagonal, in view of the similar behavior of the orientifold potential studied in the previous section. However, there are many other unstable directions, such as $\vec{C}_1 = 0$, $\vec{C}_2 = \nu^1 \vec{c}$, for instance.

The orbifold potential also features negative-energy minima with $O(N^2)$ energy that are not inherited from down-shifting of the bosonic conical zeros. In order to exhibit these special minima, let us focus on one of the “outer rims” of the moduli space, $\vec{C}_2 = 0$, $\vec{C}_1 = \vec{C}$, and points of the form

$$\vec{C}_\epsilon = \left(2\pi \sum_{l=1}^{N-1} \epsilon_l \nu^l, 0, 0 \right) \quad (12.26)$$

where $\epsilon_l = \pm 1$, with $O(N/2)$ terms of each sign. The fermionic potential at these points is

$$V_{\text{F}}(\vec{C}_\epsilon) = -2N \sum_i V(\nu^i \cdot \vec{C}_\epsilon) \sim -2N \sum_i V(\epsilon_i \pi) \sim -2N^2 V(\pi), \quad (12.27)$$

whereas the bosonic contribution is at most of $O(N)$. To see this, notice that

$$2\pi \sum_{l=1}^{N-1} \epsilon_l \nu^l \cdot (\nu^i - \nu^j) = \pi(\epsilon_i - \epsilon_j) \quad (12.28)$$

if $i, j = 1, \dots, N-1$. All these terms are of the form $V(\pm 2\pi)$ or $V(0)$ and thus vanish.

The remaining $N-1$ terms have argument

$$2\pi \sum_{l=1}^{N-1} \epsilon_l \nu^l \cdot (\nu^i - \nu^N) = \pi \epsilon_i \quad (12.29)$$

and contribute $\sum_i V(\pm\pi) \sim NV(\pi)$ to the bosonic potential. We conclude that these minima come from the superposition of N^2 inverted maxima of the $SU(2)$ potential.

A peculiar feature of the orbifold potential is its exact cancellation along the diagonal $\vec{C}_1 = \vec{C}_2$. This is the closest we come to the complete cancellation of the potential over the moduli space, the hallmark of the supersymmetric models. In this case, however, local minima of the potential lie outside the diagonal on the “twisted sector” of the moduli space. Although in finite volume one cannot strictly talk about spontaneous breaking of the orbifold \mathbf{Z}_2 symmetry, minimum energy wave functions are localized near regions with non-zero values of the “twisted fields” $\vec{C}_1 - \vec{C}_2$. In this respect, the status of this result is similar to that in [126], this time in the regime of full spatial compactification.

Chapter 13

Planar equivalence in the box II

The analysis above is not favorable to planar equivalence. However, we should remark that it depends crucially on the properties of finite volume, the moduli space and the effective potential, so one may be concerned about the infinite volume limit of the theory having completely different properties¹. If we impose twisted boundary conditions we can get rid of the moduli space so our results will not depend so much on the finite volume setup. Moreover, in the case of orbifold theories, it is much easier to restrict the analysis to orbifold-preserving vacua and check whether planar equivalence holds for these. This is done comparing topological sectors. Another advantage is that we know how to compute semiclassical amplitudes between these sectors. So it is worth to extend the analysis of orbifold theories to the twisted torus. Orientifold theories will not be considered for two reasons: First, the invariant center is only \mathbf{Z}_2 , that is not enough to significantly lift the moduli space. Second, contrary to the orbifold case there is not a well-defined map between the configurations of parent and daughter.

We will start constructing a map between twisted configurations of parent and daughter orbifold theories and use it to compare the vacuum sector of both theories. The map implies that if we lift the non-Abelian moduli space of the daughter theory, the Abelian moduli space will remain unlifted and the moduli space of the parent theory will be only partially lifted. The effective potential over the Abelian moduli space will break planar equivalence similarly to the case of periodic boundary conditions. In the parent theory, there will be fermionic zero modes that increase the number of vacua respect to the daughter theory. We will also find that semiclassical tunneling amplitudes between orbifold-preserving vacua

¹Indeed, we expect a confinement transition [158].

give different values to orbifold-invariant operators in the parent and daughter theory, so planar equivalence also fails in this construction.

13.1 Twisted boundary conditions and orbifold field theories.

The parent theory is a $U(kN)$ supersymmetric gauge theory. In order to study the relation between parent and daughter theories in this setup, we follow the construction that 't Hooft used to find self-dual solutions of fractional topological charge [168], called torons, and generalize it to our case. The analysis is made in the Euclidean \mathbf{T}^4 .

We should point that the gauge group of the daughter theory is a subgroup of the gauge group of the parent theory *of the same rank*. This is quite useful if we try to establish a map between both theories. For instance, every representation of the parent theory has a unique decomposition in representations of the daughter theory. Notice that if we ignore Abelian groups in the daughter theory, the rank would be different. We will see that Abelian groups play a relevant role in the mapping. We will ignore only the diagonal $U(1)$ group of the daughter theory, that maps to the Abelian part of the parent group. All fields are uncharged under these groups, so they decouple trivially.

We split rows and columns in k diagonal boxes of $N \times N$ size. Then, we work in the subgroup $(SU(N))^k \times U(1)^{k-1} \subset SU(kN)$, which is the orbifold projection on the gauge sector. If we had considered only a $(SU(N))^k$ theory, without the Abelian part, then the possible bundles in the daughter theory would have been characterized by a \mathbf{Z}_N diagonal subgroup of $(\mathbf{Z}_N)^k$. This is so because of the fermions in the bifundamental representations. If twist tensors of different $SU(N)$ groups were different, boundary conditions for fermions will not be consistent. However, Abelian fields can be used to absorb extra phases and enlarge the number of possible bundles. This will be evident in our construction.

Let ω_i , $i = 1, \dots, k$ be the $U(1)$ generators

$$\omega_i = 2\pi \text{diag} (-N\mathbf{1}_N, \dots, N(k-1)\mathbf{1}_N, \dots, -N\mathbf{1}_N) \quad (13.1)$$

where $N(k-1)\mathbf{1}_N$ is located at the i th position and $\mathbf{1}_N$ denotes the $N \times N$ identity matrix. Note that only $k-1$ generators are independent, since $\sum_{i=1}^k \omega_i = 0$.

Define the following twist matrices

$$V_i W_i = W_i V_i \exp \left(\frac{2\pi i}{kN} + \frac{i\omega_i}{kN^2} \right) \quad (13.2)$$

All other pairs commute. Notice that although V_i and W_i are matrices defined in principle to make a $SU(kN)$ twist, in fact the terms in the exponent are such that the non-trivial twist is made only over the i th $N \times N$ box. A possible representation is

$$\begin{aligned} V_i &= \text{diag} \left(\mathbf{1}_N, \dots, P_N^{(i)}, \dots, \mathbf{1}_N \right) \\ W_i &= \text{diag} \left(\mathbf{1}_N, \dots, Q_N^{(i)}, \dots, \mathbf{1}_N \right) \end{aligned} \quad (13.3)$$

where $Q_N^{(i)}$ and $P_N^{(i)}$ are the $SU(N)$ matrices of maximal twist $P_N Q_N = Q_N P_N e^{2\pi i/N}$ associated to the i th gauge group.

Let us try the ansatz

$$\Omega(\mu, x) = \left(\prod_{i=1}^k P_i^{a_\mu^i} Q_i^{b_\mu^i} \right) \exp \left(i \sum_{i=1}^k \omega_i \alpha_{\mu\nu}^i x_\nu / l_\nu \right) \quad (13.4)$$

where summation over ν is understood. The numbers a_μ^i, b_μ^i are arbitrary integers. $\alpha_{\mu\nu}^i$ is an antisymmetric real tensor which will be associated to the Abelian fluxes that are necessary to cancel out phases in the case of non-diagonal twist.

Imposing the twist consistency conditions for the ansatz (13.4), we find that

$$\begin{aligned} n_{\mu\nu} &= \sum_{i=1}^k n_{\mu\nu}^i \\ n_{\mu\nu}^i &= a_\mu^i b_\nu^i - a_\nu^i b_\mu^i \end{aligned} \quad (13.5)$$

and the k conditions

$$\sum_{j=1}^k n_{\mu\nu}^j - k n_{\mu\nu}^i = 2kN^2 \left(k\alpha_{\mu\nu}^i - \sum_{j=1}^k \alpha_{\mu\nu}^j \right), \quad \sum_{i=1}^k \alpha_{\mu\nu}^i = 0 \quad (13.6)$$

which can be used to obtain the $\alpha_{\mu\nu}^i$ tensors from the $n_{\mu\nu}^i$ tensors. The second equation in (13.6) comes from the fact that there are only $k - 1$ independent $U(1)$ groups. Any other linear condition will be valid.

This establishes a map between Euclidean bundles in parent and daughter theories, identifying $n_{\mu\nu}^i$ as the twist tensors of the daughter theory. This implies that many inequivalent twists in the daughter theory map to the same twist in the parent. A second consequence relies on the fact that $\alpha_{\mu\nu}^i$ are constant Abelian field strengths. This implies

that configurations like 't Hooft's torons in the parent theory can be mapped to Abelian electric and magnetic fluxes in the daughter, showing that Abelian groups play a relevant role in the mapping. Generically, physically inequivalent configurations in the daughter theory, like Abelian fluxes and torons, map to the same configuration (up to gauge transformations) in the parent theory. The map can be one-to-many, and it is given by the possible decompositions of the parent twist tensor $n_{\mu\nu}$ (defined mod kN) in k daughter's twist tensors $n_{\mu\nu}^i$ (each defined mod N).

A remark is in order. Although in principle we can turn on arbitrary fluxes of Abelian fields in the daughter theory, we must take into account the presence of charged fermions under these. Since bifundamentals correspond to off-diagonal boxes in a $SU(kN)$ matrix, the value of Abelian fluxes is determined modulo N by consistency conditions of the twist. This implies that fractional contributions of Abelian fluxes to the topological charge are determined completely by (13.6). On the other hand, integer contributions to the topological charge in the parent theory can map to non-Abelian instantonic configurations, Abelian fluxes of order N or a mixture of both. Since the energy of this kind of configurations is a factor N larger than fractional contributions, they are irrelevant in the large N limit and we will not worry about them anymore.

We can be more precise with the map of Abelian configurations. The $U(1)$ groups under consideration follow from the decomposition of $SU(kN)$ gauge connections in boxes $A_\mu = \text{diag}(A_\mu^1, \dots, A_\mu^N)$ so that $U(1)$ connections are given by

$$B_\mu^i = \text{tr} A_\mu^i - \text{tr} A_\mu^{i+1} \quad (13.7)$$

where $i = 1, \dots, k-1$. Then, following [169], we can relate topological invariants of Abelian groups of the daughter theory to the twist tensor of the parent theory. Let $F_{\mu\nu}^i$ be the field strength of the i th Abelian group. We have the following topological invariants

$$c_{\mu\nu}^i = \frac{1}{2\pi} \int dx_\mu \wedge dx_\nu \text{tr} F_{\mu\nu}^i, \quad (13.8)$$

given by the integral of the first Chern class over non-contractible surfaces of the torus and

$$\mathcal{Q}^i = \frac{1}{16\pi^2} \int_{\mathbf{T}^4} \text{tr} (F_{\mu\nu}^i \tilde{F}_{\mu\nu}^i) d^4x \quad (13.9)$$

which is the Pontryagin number and it is related to first and second Chern classes. We can relate \mathcal{Q}^i to the topological charge of the parent theory, while $c_{\mu\nu}^i \pmod{N}$ will be a twist tensor $n'_{\mu\nu}$ for the $SU(N) \subset SU(kN)$ subgroup of gauge connection $A_\mu^i - A_\mu^{i+1} - B_\mu^i$. It contributes to a fractional topological charge through (11.4).

13.2 Vacuum structure.

We have been able to construct a map between configurations of both theories, showing that they are physically inequivalent, although this is not a surprise. As a matter of fact, we are interested only in large N equivalence. According to [117,118], planar equivalence will hold non-perturbatively in the sector of unbroken \mathbf{Z}_k orbifold symmetry. The necessary and sufficient condition is that operators related by orbifold projection, and invariant under orbifold transformations, have the same vacuum expectation values. Therefore, it is enough to check the vacuum sector. In infinite volume it is argued that large N equivalence does not hold for $k > 2$ because of spontaneous breaking of orbifold symmetry by the formation of a gaugino condensate in the parent theory [119]. For $k = 2$ the condensate does not break orbifold symmetry and the question remains open. In finite volume in principle there is no spontaneous breaking, so any failure of large N orbifold equivalence must show itself in a different way. In the following analysis we will restrict to the sector of vanishing vacuum angles for simplicity.

13.2.1 Ground states in the daughter theory.

We will start by comparing the bosonic sector of ground states of parent and daughter theories in a three-torus. The first question we can ask ourselves is what are the relevant configurations we must consider. We assume that the orbifold projection has been made at a scale of energy much larger than the typical scale of the torus $\mu \gg 1/L$. At this point, all the coupling constants of the orbifold theory are equal. The running of coupling constants of non-Abelian groups is given at leading order by the renormalization group of the parent theory, by perturbative planar equivalence. However, the running for Abelian groups is different since they are not asymptotically free. As a matter of fact, the coupling constants of Abelian groups will be smaller than the coupling constants of non-Abelian groups in our torus, and the difference will increase with the volume. We can now consider what are the contributions to energy of Abelian configurations, that depend on electric ($E_i = \alpha_{0i}$) and magnetic ($B_i = \epsilon_{ijk}\alpha_{jk}$) fluxes as

$$H = \int_{\mathbf{T}^3} \left(\frac{e^2(L)}{2} \mathbf{E}^2 + \frac{1}{2e^2(L)} \mathbf{B}^2 \right) \quad (13.10)$$

In the quantized theory \mathbf{B}^2 acts as a potential, while \mathbf{E}^2 plays the role of kinetic energy.

We see that the magnetic contribution is proportional to the inverse of the coupling, so

the ground states of the theory will be in the sectors of zero Abelian magnetic flux. From (13.5), this forces us to introduce equal magnetic flux on all non-Abelian gauge factors,

$$\vec{m}_p = k\vec{m}_d \quad (13.11)$$

where $\vec{m}_{p(d)}$ is the magnetic flux in the parent (daughter) theory. This kind of boundary conditions preserve the orbifold symmetry of interchanging of $SU(N)$ groups.

The twist of the daughter theory is determined by a \mathbf{Z}_N diagonal subgroup. The elements of this group are actually equal to the elements of a \mathbf{Z}_N subgroup of the center of the parent theory

$$Z_l = \bigoplus_k \text{diag} (1, e^{2\pi il/N}, \dots, e^{2\pi il(N-1)/N}) \quad (13.12)$$

We are now interested in imposing twisted boundary conditions in the daughter theory such that the moduli space of non-Abelian gauge groups is maximally lifted. We can introduce a unit of magnetic flux in the same direction for each of the gauge groups, so we are performing a maximal twist of the theory and thus lifting all the non-Abelian moduli space. However, the kind of boundary conditions we are imposing does not prevent the existence of constant connections for Abelian groups. Bifundamental fermions are charged under these $U(1)$ groups, so it is not possible to gauge away constant connections. Moreover, they become periodic variables. Therefore, the Abelian moduli space of the daughter theory is a $(k-1)$ -torus (for each spatial direction).

In the $A_0 = 0$ gauge we have freedom to make gauge transformations depending on spatial coordinates. Abelian gauge transformations must be such that they compensate the phases that can appear on fermionic fields if we make twisted gauge transformations that are not equal for all non-Abelian gauge groups. Only transformations with $\vec{k} \cdot \vec{m} = 0 \pmod N$ lead to a different vacuum, so there are N^k possible non-Abelian vacua. The total moduli space consists on N^k disconnected $\mathbf{T}^{3(k-1)}$ tori. The Abelian part of the vacuum is a wavefunction over the torus.

In our setup, orbifold symmetry is preserved in the vacua that are reached by twisted gauge transformations of the same topological class for all non-Abelian gauge groups. For these, Abelian gauge transformations are trivial. In Sec. 13.2.5 we will see that these vacua are dynamically selected by the physics on Abelian moduli space.

13.2.2 The mapping of vacua.

We would like to study planar equivalence in a physical setup that is equivalent for the parent theory. From (13.11) this corresponds to the introduction of k units of magnetic flux in the same direction as in the daughter theory. In this case we can reach N disconnected sectors making twisted gauge transformations. We would like to see how these vacua can be mapped to the orbifold-preserving vacua of the daughter theory. In order to do that, we should be able to construct the operators associated to twisted gauge transformations in the daughter theory from the corresponding ones in the parent theory. A second condition is that we should be able to identify the moduli spaces of both theories.

Let us examine the first condition. Suppose that we introduce k units of magnetic flux in the x_3 direction in the parent theory:

$$\begin{aligned} A_\mu(x_1 + L, x_2, x_3) &= \tilde{V}_k A_\mu(x_1, x_2, x_3) \tilde{V}_k^{-1} \\ A_\mu(x_1, x_2 + L, x_3) &= \tilde{W}_k A_\mu(x_1, x_2, x_3) \tilde{W}_k^{-1} \\ A_\mu(x_1, x_2, x_3 + L) &= A_\mu(x_1, x_2, x_3) \end{aligned} \quad (13.13)$$

where twist matrices must satisfy $\tilde{V}_k \tilde{W}_k = \tilde{W}_k \tilde{V}_k e^{2\pi i k/kN}$. We can go from one vacuum state to other by making a twisted gauge transformation U , that satisfies the above conditions (13.13), except in the x_3 direction, where

$$U(x_1, x_2, x_3 + L) = e^{2\pi i k/kN} U(x_1, x_2, x_3). \quad (13.14)$$

A good election for the twist matrices is $\tilde{V}_k = \mathbf{1}_k \otimes P_N$, $\tilde{W}_k = \mathbf{1}_k \otimes Q_N$. Moreover, we can use the $SU(k)$ group that is not broken by the boundary conditions to rewrite U as a box-diagonal matrix, that can be mapped to the twisted gauge transformations of the daughter theory, if we arrange them in a single matrix. In general, the transformations in the daughter theory will include Abelian phases, so the map of vacua will be from one in the parent to many in the daughter.

We now turn to the second condition. The twisting is not enough to lift completely the moduli space of the parent theory, but a torus $\mathbf{T}^{3(k-1)}$ remains. As a matter of fact, it is an orbifold, since we should mod out by the Weyl group of $SU(k)$. In the daughter theory, the Abelian moduli space is the same, except that there are no Weyl symmetries acting on this space. However, in the daughter theory there are discrete global symmetries associated to the permutations of factor groups that can be mapped to Weyl symmetries of the parent theory. They do not modify the moduli space, but we can make a projection to the invariant sector of the Hilbert space to study planar equivalence.

There will be a wavefunction over the moduli space associated to the vacuum. In the parent theory, supersymmetry implies that the wavefunction is constant. In the daughter theory there is no supersymmetry, so a potential can be generated that will concentrate the wavefunction at the minima. Another consequence of supersymmetry is that there are fermionic zero modes over the moduli space, which give rise to more zero-energy states. We will investigate both questions in the next sections.

13.2.3 Electric fluxes and vacuum angles.

The vacuum states we have studied in the parent theory are generated from the trivial vacuum $|0_p\rangle$, associated to the configuration of magnetic flux $\vec{m} = (0, 0, k)$ and classical gauge connection $A_\mu = 0$, by operators that implement the minimal twisted gauge transformations on the parent Hilbert space \hat{U}_p , characterized by $\vec{k} = (0, 0, -1)$ as the electric component of the twist tensor (11.3).

$$|l\rangle = \hat{U}_p^l |0_p\rangle \tag{13.15}$$

We can build Fourier transformed states of (13.15) that only pick up a phase when we make a twisted gauge transformation. We must take into account that the operators associated to twisted transformations depend on the vacuum angle θ_p , so we restrict to a sector of the Hilbert space with definite vacuum angle. Then,

$$\hat{U}_p^N = e^{i\theta_p} \hat{\mathbf{1}} \tag{13.16}$$

The states we are considering are labelled by the electric flux $\vec{e} = (0, 0, e)$

$$|e\rangle = \frac{1}{\sqrt{N}} \sum_{l=0}^{N-1} e^{-\frac{2\pi il}{kN} \left(e + \frac{\theta_p}{2\pi} k \right)} \hat{U}_p^l |0_p\rangle \tag{13.17}$$

and transform as

$$\hat{U}_p |e\rangle = e^{\frac{2\pi i}{kN} \left(e + \frac{\theta_p}{2\pi} k \right)} |e\rangle \tag{13.18}$$

Notice that e must be a multiple of k , in order to be consistent with (13.16).

The theory must be invariant under 2π rotations of the vacuum angle $\theta_p \rightarrow \theta_p + 2\pi$. The states (13.17) are not invariant under this transformation, but it generates a spectral flow that moves a state to another one $e \rightarrow e + k$. In our particular case we can define a $e = ke_p$ electric flux such that the spectral flow acts as $e_p \rightarrow e_p + 1$

$$|e_p\rangle = \frac{1}{\sqrt{N}} \sum_{l=0}^{N-1} e^{-\frac{2\pi il}{N} \left(e_p + \frac{\theta_p}{2\pi} \right)} \hat{U}_p^l |0_p\rangle \tag{13.19}$$

In the daughter theory, the vacua are obtained from the trivial vacuum $|0_d\rangle$, associated to magnetic fluxes $\vec{m}^i = (0, 0, 1)$ and zero classical gauge connections $A_\mu^i = 0$, by the set of operators that implement minimal twisted gauge transformations on the daughter Hilbert space \hat{U}_i , characterized by $\vec{k}^i = (0, 0, -1)$

$$|l_1, \dots, l_k\rangle = \prod_{i=1}^k \hat{U}_i^{l_i} |0_d\rangle \quad (13.20)$$

We will concentrate on states that are reached by diagonal twisted transformations, so that they are characterized by a single integer $l_i = l$, $i = 1, \dots, k$. Again, we can build the Fourier transformed states, taking into account that we are in a sector of the Hilbert space with definite vacuum angles θ_i , so

$$\hat{U}_i^N = e^{i\theta_i} \hat{\mathbf{1}} \quad (13.21)$$

The states are labelled by electric fluxes e_i

$$|e_1, \dots, e_k\rangle_D = \frac{1}{\sqrt{N}} \sum_{l=0}^{N-1} e^{-\frac{2\pi i l}{N} \left(\sum_i e_i + \frac{\sum_i \theta_i}{2\pi} \right)} \prod_{i=1}^k \hat{U}_i^l |0_d\rangle \quad (13.22)$$

If we had considered transformations other than diagonal, this would be shown in the exponent, where different combinations of electric fluxes and vacuum angles will appear. If we make a diagonal twisted transformation, these states change as

$$\prod_{i=1}^k \hat{U}_i |e_1, \dots, e_k\rangle_D = e^{\frac{2\pi i}{N} \left(\sum_i e_i + \frac{\sum_i \theta_i}{2\pi} \right)} |e_1, \dots, e_k\rangle_D \quad (13.23)$$

If the twisted transformations are non-diagonal, there are extra phases appearing on the boundary conditions of the fields that must be compensated by Abelian transformations, so the state will change to a different vacuum in the Abelian sector. We can define subsectors of the Hilbert space that are invariant under diagonal transformations and that are shifted to other sectors by non-diagonal transformations. The labels for such sectors will be given by the Abelian part, so there will be N^{k-1} of them.

13.2.4 Fermionic zero modes.

Fermionic zero modes are spatially constant modes that satisfy the Dirac equation with zero eigenvalues. In the parent theory the gaugino has $k - 1$ zero modes

$$\lambda_0^a = \lambda_{k \times k}^a \otimes \mathbf{1}_N \quad (13.24)$$

where $a = 1, \dots, k-1$ runs over the Cartan subalgebra of the unlifted $SU(k)$ subgroup. If we go to a Hamiltonian formulation, as in [147], they do not contribute to the energy. We can define creation and annihilation operators for these modes: $a_a^{*\alpha}$ and a_a^α where $\alpha = 1, 2$ refers to spin and $a = 1, \dots, k-1$ is the gauge index. Physical states must be gauge invariant. For zero modes gauge invariance appears in the form of Weyl invariance, a discrete symmetry that stands after fixing completely the gauge. The set of Weyl-invariant operators that we can construct with creation operators is limited to contract the gauge indices with δ_{ab} . Thus, the only allowed operators that create fermions over the gauge vacuum are powers of

$$\mathcal{U} = \epsilon_{\alpha\beta} a_a^{*\alpha} a_a^{*\beta} \quad (13.25)$$

This operator creates fermionic modes over the bosonic vacuum $|0_B\rangle$. Fermi exclusion principle limits the number of times we can apply \mathcal{U} over the vacuum, so the set of possible vacua is

$$|0_B\rangle, \mathcal{U}|0_B\rangle, \dots, \mathcal{U}^{k-1}|0_B\rangle. \quad (13.26)$$

Some remarks are in order. First, the total number of vacua in the parent theory is kN , in agreement with the Witten index. Second, \mathcal{U} acquires a phase under general chiral transformations, so the chiral symmetry breaking vacua of infinite volume might be constructed from appropriate linear combinations of the states (13.26).

What is the situation in the daughter theory? The only possible candidates to give fermionic zero modes in spite of twisted boundary conditions are the trace part of bifundamental fields. However, those fields are charged under Abelian groups, so it is not possible to find zero modes over the whole moduli space. We are then confronted to the same kind of concern as in [119], the number of vacuum states is different in each theory, even in the sector of vacua that preserve orbifold symmetry.

Even in the case $k = 2$, the mismatch between the number of vacua, which is due to the different fermion content, seems to spoil large N equivalence. In [119], it is argued that we should consider a mapping two-to-one between vacua of the parent and daughter theories. Such mapping is more difficult to justify in this case, because expectation values of operators involving fermions will give different results in vacua with different number of fermionic zero modes. For instance, if we consider the operator

$$\mathcal{O}_p = \text{tr} (\lambda^\dagger \alpha \lambda^\alpha) \sim \left(a_a^{*\alpha} + \sum_{n=1}^{\infty} a_a^{*\alpha}(n) e^{\frac{-2\pi i n x}{L}} \right) \left(a_a^\alpha + \sum_{n=1}^{\infty} a_a^\alpha(n) e^{\frac{2\pi i n x}{L}} \right) \quad (13.27)$$

we are counting the number of fermions in the state, so there is a diagonal non-vanishing contribution

$$\langle 0_B | \mathcal{U}^l \mathcal{O}_p \mathcal{U}^{l'} | 0'_B \rangle \sim 2^{l'} \delta_{l,l'} \delta_{0_B, 0'_B} \quad (13.28)$$

However, the orbifold projection of this operator

$$\mathcal{O}_d = \text{tr} \left(\lambda_{12}^{\dagger\alpha} \lambda_{12}^\alpha + \cdots + \lambda_{k1}^{\dagger\alpha} \lambda_{k1}^\alpha \right) \quad (13.29)$$

will have a vanishing diagonal contribution, since there are no fermionic zero modes over the vacuum state.

13.2.5 Potential over moduli space.

We now turn to the question of whether a potential appears over the Abelian moduli space of the daughter theory due to quantum effects. For simplicity, we will work with $U(1)$ fields $A_\mu = a_\mu \sqrt{1/N} \mathbf{1}_N$. Gauge fields are uncharged, so they cannot give rise to a potential. Fermionic fields do couple through

$$\mathcal{L}_{\lambda a} = \sum_{i=1}^k \sum_{a=1}^{N^2} \bar{\lambda}_{i,i+1}^a (\not{\partial} + e^i \not{\phi}^i - e^{i+1} \not{\phi}^{i+1}) \lambda_{i,i+1}^a \quad (13.30)$$

where e^i is the Abelian coupling. In principle $e^i = e^{i+1} = e$, since all Abelian gauge groups enter symmetrically and we have applied the renormalization group from a point where all couplings were equal. At that point $e^2 = g_t/N^2$, where $g_t = g_{YM}^2 N$ is the non-Abelian 't Hooft coupling.

Let us comment several aspects of the Abelian moduli space. We can scale the fields so that the coupling constants come in front of the action. Then, when we make an Abelian gauge transformation that shifts the gauge field by a constant, the fermionic field charged under that Abelian group picks up a phase depending on the position. For instance, if

$$a_3^i - a_3^{i+1} \rightarrow a_3^i - a_3^{i+1} + c_3 \quad \Rightarrow \quad \lambda_{i,i+1} \rightarrow e^{ic_3 x_3} \lambda_{i,i+1} \quad (13.31)$$

then, when we move a period along the x_3 direction, the phase of the field changes by $e^{ic_3 l_3}$. We conclude that the periods of the \mathbf{S}^1 components of the Abelian moduli space are $2\pi/l_3$. Would be twisted gauge transformations correspond to $2\pi/Nl_3$ translations along the \mathbf{S}^1 , although fixed boundary conditions for charged fields imply that they are no longer a symmetry of the theory.

Since there are no fermionic zero modes with support over the whole moduli space, we can integrate out the fermionic fields in the path integral. The regions of zero measure where fermionic zero modes have support will be localized at conical singularities of the effective potential obtained this way.

We proceed now to give the fermionic potential. At the one-loop level, it comes from the determinant that results in the path integral when we integrate out fermionic fields.

$$V_{\text{eff}}(a^i) = -\log \left(\prod_{i=1}^k \det \left(\not{D} + \not{a}^i - \not{a}^{i+1} \right)^{N^2} \right) \quad (13.32)$$

This potential can be computed using the methods of [155]. The result, after rescaling by the length of the spatial torus $a^i \rightarrow a^i/l$, is

$$V_{\text{eff}}(a^i) = -N^2 \sum_{i=1}^k V(a^i - a^{i+1}) \quad (13.33)$$

where the function V is given by (11.14).

Notice that the potential depends only on the differences $a^i - a^{i+1}$, so no potential is generated for the diagonal $U(1)$, only for the $U(1)^{k-1}$ groups coming from the non-Abelian part of the parent group after the orbifold projection. This potential has its minima at non-zero values of the differences, in the twisted sector. Since it is of order N^2 , it cannot be ignored in the large N limit.

Examining more closely the potential, we can see that there is only one minimum at $a_\mu^i - a_\mu^{i+1} = \pi$. Usually, wavefunctions over the moduli space are characterized by the electric flux, that we can interpret as momentum along the moduli space. However, kinetic energy on the moduli space is proportional to e^2 (13.10), that is very small and becomes smaller as we increase the volume. On the other hand, the effective potential is very large and does not depend on the coupling. Therefore, the wavefunction is very localized, even for translations given by twisted transformations, and it is more convenient to use a position representation over the moduli space. The first consequence of all this is that if we make an Abelian twisted transformation, we are moving the system to a configuration with more energy, see Fig. 13.2.5. Therefore, most of the vacua of the theory are lifted. Only when we make diagonal non-Abelian twisted gauge transformations, the system remains in a ground state. This leaves N vacua.

On the other hand, the wavefunctions over the moduli space of parent and daughter theories are very different. The first one can be seen as a zero-momentum state, while the

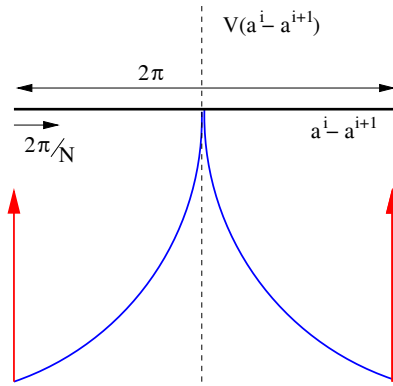


Figure 13.1: *The wavefunction of the ground state is localized at the minimum of the potential in the Abelian moduli space. A translation produced by a twisted transformation will lift the state to a configuration with more energy.*

last is more a position state. This suggests that in the infinite volume limit the daughter theory will fall into an Abelian twisted configuration, breaking orbifold symmetry in that sector. Another difference is that the ground state has a negative energy of order $O(N^2)$. These results are of the same kind as the ones found in [126, 127], although in the other cases the moduli space was non-Abelian for the daughter theory.

We have found many differences between the vacua of parent and daughter theories in finite volume with maximal twist. We were looking to lift the non-Abelian moduli space that in previous works pointed towards non-perturbative failure of planar equivalence. We have seen that properly taking into account the Abelian groups in the daughter theory, the situation does not really improve. Thanks to Abelian groups we are able to map the moduli space of parent and daughter theories, but the generation of a potential by fermionic fields in the daughter theory makes the physical behavior of both theories quite different, although it lifts many of the unexpected non-Abelian vacua. The moduli space of the parent theory is also a problem, because it implies that there are fermionic zero modes that generate vacua that cannot be mapped to the daughter theory.

13.3 Tunneling effects.

We have shown that parent and daughter theories have physically inequivalent vacua in this context due to the potential generated over the moduli space in the daughter theory

and to the mismatch of vacua. However, some quantities do not depend on the moduli space, so the wavefunction will just give a normalization factor that can be chosen to be the same. The orbifold conjecture may still be useful to make some computations in the common vacua, up to kinematical factors.

One of the main applications of twisted boundary conditions is the computation of fermion condensates [164, 165] generated by tunneling between different vacua. These fermion condensates do not depend on the moduli space and tunneling can be studied using self-dual solutions of Euclidean equations of motion. In the case where the tunneling is between vacua related by a twisted gauge transformation, the relevant configurations are of fractional topological charge, which we have associated to the twist tensor (11.4). Notice that to map parent and daughter theories we are using (13.5) and (13.6). If we want to make the mapping between purely non-Abelian configurations, we should take $\alpha_{\mu\nu} = 0$, otherwise we will be introducing self-dual Abelian fluxes in the daughter theory. In this case, all the twist tensors in the daughter theory must be equal because of fermions in the bifundamental representations. This implies that parent and daughter twist tensors are proportional

$$n_{\mu\nu}^p = k n_{\mu\nu}^d \quad (13.34)$$

Under these conditions, the fractional contribution to topological charge (11.4) by tunneling is the same in both theories

$$\mathcal{Q} = -\frac{1}{kN} n_{\mu\nu}^p \tilde{n}_{\mu\nu}^p = k \left(-\frac{1}{N} n_{\mu\nu}^d \tilde{n}_{\mu\nu}^d \right) \quad (13.35)$$

13.3.1 Tunneling in parent theory.

In the $SU(kN)$ parent theory with $n_{\mu\nu}^p = 0 \bmod k$ twist, the solution of minimal charge has $\mathcal{Q} = 1/N$, k times the minimal possible topological charge of the theory. It contributes to matrix elements of the form $\langle 0 | \mathcal{O} \hat{U} | 0 \rangle$ for some operator \mathcal{O} . The operator \hat{U} acts over the trivial gauge vacuum $|0\rangle$ by making a twisted gauge transformation (13.14). We can compute this quantity using a Euclidean path integral

$$\langle 0 | \mathcal{O} \hat{U} | 0 \rangle = -\lim_{T \rightarrow \infty} \frac{1}{T} \langle 0 | \mathcal{O} e^{-HT} \hat{U} | 0 \rangle \rightarrow \int_{\mathcal{Q}=1/N} \mathcal{D}A \mathcal{D}\lambda \mathcal{D}\bar{\lambda} \mathcal{O}_E e^{-S_E} \quad (13.36)$$

Although we do not know the explicit Euclidean solution that contributes in the saddle point approximation, we know what should be the vacuum expectation value of some operators. Because of supersymmetry, only zero modes contribute. There are $4k$ real zero

modes of both bosonic and fermionic fields. The existence of fermionic zero modes implies that the tunneling contributes only to operators involving a product of $2k$ fermionic fields. In particular, there is no contribution to the vacuum energy. Therefore,

$$\mathcal{E} \equiv - \lim_{T \rightarrow \infty} \frac{1}{T} \langle 0 | e^{-HT} \hat{U} | 0 \rangle = 0 \quad (13.37)$$

and

$$\langle \text{tr}_{kN} (\lambda\lambda)^k \rangle \equiv - \lim_{T \rightarrow \infty} \frac{1}{T} \langle 0 | \text{tr}_{kN} (\lambda\lambda)^k e^{-HT} \hat{U} | 0 \rangle = \frac{1}{k!} (\langle \text{tr}_{kN} \lambda\lambda \rangle)^k \quad (13.38)$$

which is a tunneling contribution to a $2k$ -fermionic correlation function. By $\langle \text{tr}_{kN} \lambda\lambda \rangle$ we refer to the value of the gaugino condensate in the parent theory. This does not mean that a gaugino condensate is generated by these configurations, we are just referring to the numerical value of (13.38). This is based on the use of torons to estimate the gaugino condensate [164, 165] and on the coincidence of the instanton measure with the measure of a superposition of torons [170]. The factorial factor comes from considering the configuration of charge $\mathcal{Q} = 1/N$ as a superposition of k equal configurations of charge $\mathcal{Q} = 1/kN$.

Another peculiar fact about this configuration is that it is transformed into itself under a Nahm transformation [171–173]. A Nahm transformation identifies moduli spaces of different self-dual configurations of different gauge theories in different spaces. From a stringy perspective it is a remnant of T-duality [174–178].

We will use techniques developed in [179–183] for Nahm transformations with twisted boundary conditions. Given the rank r , the topological charge \mathcal{Q} , and the twist

$$n = \begin{pmatrix} 0 & \Xi \\ -\Xi & 0 \end{pmatrix} \quad (13.39)$$

where $\Xi = \text{diag}(q_1, q_2)$, the Nahm transformed quantities are given by

$$\begin{aligned} p_1 &= N / \text{gcd}(q_1, N) & p_2 &= N / \text{gcd}(q_2, N) \\ s_1 q_1 &= -\text{gcd}(q_1, N) \bmod N & s_2 q_2 &= -\text{gcd}(q_2, N) \bmod N \\ \mathcal{Q}' &= r / p_1 p_2 & r' &= \mathcal{Q} p_1 p_2 \end{aligned} \quad (13.40)$$

and the twist

$$\Xi' = \text{diag}((p_1 - s_1)p_2 \mathcal{Q}, (p_2 - s_2)p_1 \mathcal{Q}). \quad (13.41)$$

Our tunneling configuration can be determined by $\vec{m} = (0, -k, 0)$, $\vec{k} = (0, 1, 0)$ for instance. Then, we can write the twist tensor as $\Xi = \text{diag}(1, k)$. Using (13.40) and (13.41), it is straightforward to see that $r' = r = kN$, $\mathcal{Q}' = \mathcal{Q} = 1/N$ and $\Xi' = \Xi = \text{diag}(1, k)$.

13.3.2 Tunneling in daughter theory.

Self-dual solutions contributing to tunneling in the daughter theory do not coincide with the projection from the parent theory, as given by (13.34). Tunneling between two adjacent vacua is given by a configuration where each gauge factor contributes by $\mathcal{Q}_d = 1/N$ to the topological charge. Then, the total topological charge is $\mathcal{Q} = k/N$, while the topological charge in the parent theory is $\mathcal{Q}_p = 1/N$, in disagreement with (13.35).

The configurations we are using for tunneling are not related by the map we have proposed, but notice that we are comparing semiclassical contributions of the same order, since the classical Euclidean action in parent $S_{cl}^p = 8\pi^2/g_p^2 N$ and daughter $S_{cl}^d = 8\pi^2 k/g_d^2 N$ theories have the same value according to the orbifold projection $kg_p^2 = g_d^2$. When we examine the moduli space of parent and daughter tunneling configurations, we find further evidence that we are comparing the correct quantities. The bosonic moduli space is $4k$ -dimensional for both theories, and the moduli space of the daughter theory also transforms into itself under a Nahm transformation. This can be seen using (13.40) for each of the gauge factors: $\mathcal{Q}'_d = \mathcal{Q}_d = 1/N$, $r'_d = r_d = N$, $\Xi'_d = \Xi_d = \text{diag}(1, 1)$.

Even using this 'improved' mapping, disagreement emerges from fermionic fields. In the daughter theory there is no supersymmetry in general, because fermions are in a representation different to bosons. However, bifundamental representations of the daughter theory can be embedded in the adjoint representation of the parent theory, and this will be useful.

In order to make an explicit computation, we need a formula for the self-dual gauge configuration of fractional topological charge. We do not have an analytic expression in general, but 't Hooft found a set of solutions [168], called torons, that are self-dual when the sizes of the torus l_μ satisfy some relations. We will assume that we are in the good case and that, although in other cases the relevant configurations will be different, the physics will be the same.

Torons are the solutions of minimal topological charge in a situation with maximal twist. For a $SU(N)$ gauge theory, this means that $\mathcal{Q}_{\text{toron}} = 1/N$. Therefore, they can be used in the daughter theory, where we will have a toron for each of the non-Abelian groups. We can compare torons to the most known self-dual solutions, instantons. Instanton solutions can be characterized by their size, orientation in the algebra and center position. The size of torons is fixed by the size of the spatial torus, and they have a fixed orientation along a

$U(1)$ subgroup. However, they still have a center that can be put at any point of the torus. Therefore, the moduli space of torons is a four-dimensional torus. An explicit expression for torons in the daughter theory in the presence of magnetic flux in the x_3 direction is

$$A_\mu^i = \frac{i\pi}{2gl_\mu l_\nu} \eta_{\mu\nu}^3 (x - z^i)_\nu \omega, \quad i = 1, \dots, k \quad (13.42)$$

where $\eta_{\mu\nu}^a$, $a = 1, 2, 3$ are 't Hooft's self-dual eta symbols [184], ω is a generator of a $U(1) \subset SU(N)$ and z^i are the center positions. Notice that we have chosen to work with anti-hermitian and canonically normalized gauge fields.

Now that we are armed with an analytic expression, we can calculate what happens with fermions in the background of k torons. The Euclidean Dirac operator is

$$\gamma_\mu D_\mu = \begin{pmatrix} 0 & -i\sigma_\mu D_\mu \\ i\bar{\sigma}_\mu D_\mu & 0 \end{pmatrix} \quad (13.43)$$

where $\sigma_\mu = (\mathbf{1}_2, i\vec{\sigma})$, $\bar{\sigma}_\mu = \sigma_\mu^\dagger$ and σ_i are the Pauli matrices. In a self-dual background $F_{\mu\nu}^+$, the square of the Dirac operator is positive definite for negative chirality fields

$$(i\bar{\sigma}_\mu D_\mu)(i\sigma_\nu D_\nu) = -D^2 \mathbf{1}_2 \quad (13.44)$$

while for positive chirality fields, it has a potentially negative contribution

$$(i\sigma_\mu D_\mu)(i\bar{\sigma}_\nu D_\nu) = -D^2 \mathbf{1}_2 - \frac{1}{2} g \sigma_{\mu\nu} F_{\mu\nu}^+ \quad (13.45)$$

where $\sigma_{\mu\nu} = \sigma_{[\mu} \bar{\sigma}_{\nu]}$. This means that there are no fermionic zero modes of negative chirality, although there can be zero modes of positive chirality. In the supersymmetric case, where fermions are in the adjoint representation, there are two zero modes in the background of a single toron.

The covariant derivative acting over bifundamental fields is

$$D_\mu \lambda_{i,i+1} = \partial_\mu \lambda_{i,i+1} + g A_\mu^i \lambda_{i,i+1} - g \lambda_{i,i+1} A_\mu^{i+1} \quad (13.46)$$

Then, introducing (13.42) and (13.46) in (13.45), we find the operator (App. D)

$$\left(-D^2 \mathbf{1}_2 - \frac{1}{2} g \sigma_{\mu\nu} F_{\mu\nu}^+ \right)_{\text{adj}} - 2g \Delta A_\mu^i (D_\mu)_{\text{adj}} \mathbf{1}_2 + M^2 (\Delta z) \omega^2 \otimes \mathbf{1}_2 \quad (13.47)$$

where ‘‘adj’’ denotes that the operator is equal to the case where it acts over the adjoint representation of $SU(N)$. Extra contributions are given by the separation between torons of different groups

$$\Delta z_\mu^i = z_\mu^{i+1} - z_\mu^i, \quad \Delta A_\mu^i = \frac{i\pi}{2gl_\mu l_\nu} \eta_{\mu\nu}^3 \Delta z_\nu^i \omega \quad (13.48)$$

The coefficient of the positive ‘mass’ contribution is

$$M^2(\Delta z) = \frac{\pi^2}{4} \left(\frac{(\Delta z_0^i)^2 + (\Delta z_3^i)^2}{l_0^2 l_3^2} + \frac{(\Delta z_1^i)^2 + (\Delta z_2^i)^2}{l_1^2 l_2^2} \right) \quad (13.49)$$

The physics of fermions is clear now. When two torons of adjacent groups coincide at the same space-time point, there are zero modes for bifundamental fermions transforming under these groups. Zero modes are identical to the case of adjoint representation (supersymmetric case). When we separate the torons, the zero modes acquire a mass proportional to the distance of separation.

Therefore, we can split the moduli space of torons \mathcal{M}_k in sectors where a different number of torons are coincident. We can use quiver diagrams to represent different sectors. Each node is a toron position. Links joining different nodes represent massive fermions, while links coming back to the same node represent fermions effectively in the adjoint representation, so they give rise to supersymmetric contributions. The expansion will look like

$$\begin{aligned} \mathcal{M}_k = & \begin{array}{c} \text{k} \\ \circlearrowleft \\ \text{k} \end{array} + \begin{array}{c} \text{k-2} \\ \circlearrowleft \\ \text{k-1} \rightleftarrows \text{1} \end{array} + \\ & + \begin{array}{c} \text{k-3} \\ \circlearrowleft \\ \text{k-2} \rightleftarrows \text{1} \\ \text{k-2} \rightleftarrows \text{1} \end{array} + \dots \end{aligned} \quad (13.50)$$

A sector with n adjoint links can contribute only to vacuum expectation values of quantities involving at least n factors of the form $\lambda_{i,i+1}\lambda_{i,i+1}$. The contribution is determined by the expectation value of the gaugino condensate of a $\mathcal{N} = 1$ $SU(N)$ supersymmetric gauge theory, $\langle \lambda\lambda \rangle_{\text{susy}}$. As an example, consider the pure supersymmetric contribution

$$\left(\begin{array}{c} \text{k} \\ \circlearrowleft \\ \text{k} \end{array} \right)_{\prod_{i=1}^k \text{tr}_N \lambda_{i,i+1} \lambda_{i,i+1}} = \left(\langle \lambda\lambda \rangle_{\text{susy}} \right)^k \quad (13.51)$$

that receives non-supersymmetric corrections from other sectors of the moduli space, for

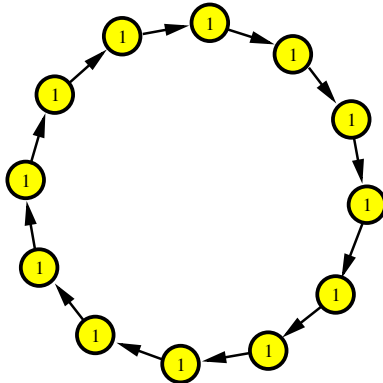


Figure 13.2: *The ring sector produces no supersymmetric factors.*

As a consequence, the first term in (13.55) coincides with (13.38), up to the factorial factor, that in the daughter theory does not appear because torons belonging to different groups are distinguishable.

So we must conclude that there are no simple relations between (13.37) and (13.54) or between (13.38) and (13.55) although both sets of quantities are invariant under orbifold symmetry.

13.3.3 Semiclassical dependence on the vacuum angles.

The results of the previous sections can be used to analyze the dependence on the vacuum angles when we deform the theories adding a mass m for the fermions. This is necessary in order to have such a dependence, otherwise massless fermions will erase it through the chiral anomaly. Notice that we can make the fermions of the daughter theory massive only for the \mathbf{Z}_2 orbifold, so we will restrict to this case.

In the parent theory, when we introduce a mass for the fermions, the states previously associated to fermionic zero modes (13.26) are lifted by an energy that is roughly the mass times the number of fermionic modes. The energy density is obtained dividing by the volume of the box $V = l^3$. So we have $k = 2$ levels, each with N states labelled by the electric flux. As we will see in a moment, tunneling between states of the same level produces a lifting in the energy density of order m^4 . If we are in the small volume (small mass) limit $ml \ll 1$, then the lifting produced by fermionic modes is larger than tunneling contributions, so the states in the highest level decouple. However, as we increase the volume there will be level-crossings between states of different levels.

In the daughter theory, a mass for the fermions modifies the effective potential over the Abelian moduli space (11.14). If $ml \ll 1$, then only high frequency contributions are suppressed, but increasing the volume will exponentially suppress the whole potential, so non-diagonal vacua could become relevant.

We are interested in estimating the dependence of the vacuum energy on the vacuum angles and electric fluxes

$$\mathcal{E}(e, \theta) = \lim_{T \rightarrow \infty} -\frac{1}{T} \ln \langle e, \theta | e^{-HT} | e, \theta \rangle. \quad (13.57)$$

In a semiclassical expansion, the relevant contributions come from fractional instantons that encode tunneling processes between different vacua. We will first study the leading term given by a single (anti)toron of minimal topological charge, and afterwards we will estimate the contribution of infinite many (anti)torons using a dilute gas approximation [185].

In the parent theory, the lowest order contribution is

$$\begin{aligned} \langle 0_p | e^{-HT} \hat{U}_p | 0_p \rangle &= T \int dA(z^1, z^2) m^4 \exp \left(-\frac{8\pi^2}{g_p^2 N} \right) \frac{\det'_F (i\mathcal{D} + m)}{\det'_B (-D^2)^{1/2}} \\ &= T m^4 K_p(m) e^{-2S_{cl}} \end{aligned} \quad (13.58)$$

where $A(z^1, z^2)$ are the zero modes of the $SU(2N)$ gauge field, depending on eight parameters of the $\mathcal{Q} = 1/N$ toron configuration. The fermionic mass is m , so the factor m^4 comes from the would be fermionic zero modes that appear when we turn m to zero. Therefore, they have been subtracted from the determinants \det'_F . The bosonic determinant \det'_B includes only physical polarizations of non-zero modes of vector bosons, so any ghost contribution has been taken into account in it. In the last equality, we have used the orbifold map $g_p^2 = g_d^2/2$. $K_p(m)$ is a m -dependent constant that will be obtained after making the integral over the moduli space of the (anti)toron.

For a general transition amplitude between different twisted vacua, there can be contributions of an arbitrary number of torons and anti-torons, as long as the total topological charge has the correct value. Since we are in a dilute gas approximation, we neglect possible interactions,

$$\langle 0_p | (\hat{U}_p^+)^{l_+} e^{-HT} (\hat{U}_p^-)^{l_-} | 0_p \rangle = \sum_{n=0}^{\infty} \sum_{\bar{n}=0}^{\infty} \frac{1}{n! \bar{n}!} (T m^4 K_p(m) e^{-2S_{cl}})^{n+\bar{n}} \delta_{n-\bar{n}-l_++l_-}. \quad (13.59)$$

We are ready now to compute the vacuum energy in the state (13.19), it is straightforward to see that

$$\mathcal{E}_p(e_p, \theta_p) = -2m^4 K_p(m) e^{-2S_{cl}} \cos \left[\frac{2\pi}{N} \left(e_p + \frac{\theta_p}{2\pi} \right) \right] \quad (13.60)$$

A similar analysis can be done for the daughter theory. The lowest order contribution is, in the diagonal case,

$$\begin{aligned} \langle 0_d | e^{-HT} \hat{U}_1 \hat{U}_2 | 0_d \rangle &= T \int dA_1(z^1) dA_2(z^2) (m + \tilde{M}(\Delta z))^4 e^{-2S_{cl}} \frac{\det'_F(-D_{12}^2 + m^2)}{\det'_B(-D_1^2)^{1/2} \det'_B(-D_2^2)^{1/2}} \\ &= T m^4 K_d(m) e^{-2S_{cl}} \end{aligned} \quad (13.61)$$

We have argued above that it is plausible that the bosonic measures of parent $dA(z^1, z^2)$ and daughter $dA_1(z^1) dA_2(z^2)$ are the same. However, there are extra contributions to the m^4 factor, given by the mass $M(\Delta z)$ (13.49) that bifundamental modes acquire when the two torons are separated. We can also see that the one-loop determinants in (13.58) and (13.61) are different. All this imply that $K_p(m)$ and $K_d(m)$ are not simply related, as we would have expected from the orbifold projection.

Then, a general transition between diagonal vacua is given by

$$\langle 0_d | (\hat{U}_2^+ \hat{U}_1^+)^{l_+} e^{-HT} (\hat{U}_1 \hat{U}_2)^{l_-} | 0_d \rangle = \sum_{n=0}^{\infty} \sum_{\bar{n}=0}^{\infty} \frac{1}{n! \bar{n}!} (T m^4 K_d(m) e^{-2S_{cl}})^{n+\bar{n}} \delta_{n-\bar{n}-l_++l_-}. \quad (13.62)$$

So the vacuum energy of the state (13.22) will be

$$\mathcal{E}_d^D(e_1, e_2, \theta_1, \theta_2) = -2m^4 K_d(m) e^{-2S_{cl}} \cos \left[\frac{2\pi}{N} \left(e_1 + e_2 + \frac{\theta_1 + \theta_2}{2\pi} \right) \right] \quad (13.63)$$

We can study the spectral flows induced by a change in the vacuum angles [144, 186] in both theories and compare the results. In Fig. 13.3.3, we illustrate the discussion with a simple example. In the parent theory, the energy of a state of definite electric flux is invariant only under shifts $\theta_p \rightarrow \theta_p + 2\pi N$. However, the whole spectrum is invariant under a 2π rotation of θ_p , so there is a non-trivial spectral flow that may become non-analytic and produce oblique confinement in the infinite volume limit. Notice also that there are two well-separated levels in the small volume ($ml \ll 1$) limit, where the lifted states have fermionic constant Abelian modes. In the opposite limit, states of the same electric flux number become nearly degenerate. This could be a hint for a two-to-one mapping between parent and daughter states of equivalent electric flux, in a finite volume version of the statement made in [119]. Notice that the parent and daughter “vacuum angles” should be mapped as $2\theta_d = \theta_p$ at the orbifold point $\theta_1 = \theta_2 = \theta_d$, as the orbifold correspondence dictates. Indeed, we find that the spectrum of the daughter theory is invariant under $\theta_d \rightarrow \theta_d + \pi$. However, this does not look as the right transformation for a vacuum angle

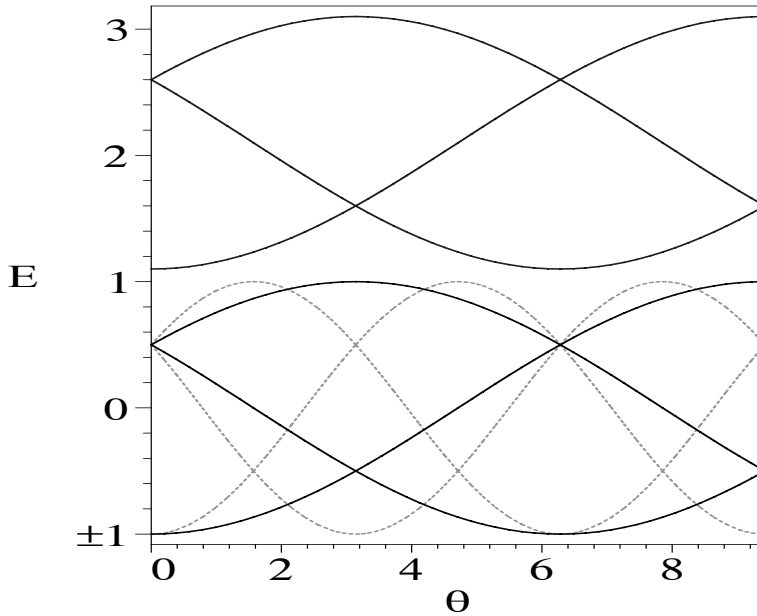


Figure 13.3: We show a picture of the spectral flow of \mathcal{E}_p/K_p (dark lines) and \mathcal{E}_d/K_d (light lines) for different states of electric flux in the case $N = 3$. The horizontal axis corresponds to θ_p for the parent theory and to θ_d for the daughter theory. We assume $ml \ll 1$, so the parent theory presents two separated levels. Notice that the periodicity of the spectral flow of the daughter is half the periodicity of the parent.

and, in view of (13.63), the daughter vacuum angle seems rather to be $\theta_1 + \theta_2$, that has the value $2\theta_d$ at the orbifold point.

On the other hand, the lifted vacua of the parent theory are unsuitable for a correspondence with daughter states because some matrix elements involving fermions will be different, as we have argued before. Regarding the remaining vacua, there is a quantitative disagreement between parent (13.60) and daughter energies (13.63), given by the difference in the values of the tunneling coefficients $K_p(m)$ and $K_d(m)$, so it seems that planar equivalence does not work at this level.

13.4 D-brane interpretation.

We can give a geometrical interpretation of our results based on a construction with D-branes in the torus, as in [187, 188]. In the parent theory we will have a set of kN D4-branes on \mathbf{T}^4 , the “01234” directions including time. The low energy theory is a $U(kN)$ supersymmetric gauge theory. We are interested in study possible vacuum configurations,

that are characterized by different bundles of D-branes over the torus. We will ignore the scalars associated to the transverse dimensions to the torus, anyway, they will be spectators in the analysis below.

The twist of the configuration associated to tunneling in the parent theory, Sec. 13.3.1, is realized diluting D2-brane charge in the worldvolume of D4s. The reason is the coupling of D2 charge with the $U(1)$ first Chern class of D4 gauge group

$$\int_{D4} C_3 \wedge \text{tr} F \quad (13.64)$$

the twist induced in the $U(1)$ must be compensated by the non-Abelian part, in order to have a well-defined $U(kN)$ bundle. So we can introduce k units of magnetic flux in the 3 direction and one unit of electric flux in the same direction by introducing k D2 branes in “34” direction and a D2 brane in “12” directions. Since the intersection number is non-zero we can interpret also this configuration as having D2 branes at some angle inside the torus.

	0	1	2	3	4
kN D4	×	×	×	×	×
k D2	×	•	•	×	×
1 D2	×	×	×	•	•

After making a T-duality along “12” directions

	0	1	2	3	4
kN D2	×	•	•	×	×
k D4	×	×	×	×	×
1 D0	×	•	•	•	•

this configuration is equivalent to an instanton for a $U(k)$ theory with kN units of magnetic flux. However, if the T-duality transformation is made along “34” directions

	0	1	2	3	4
kN D2	×	×	×	•	•
k D0	×	•	•	•	•
1 D4	×	×	×	×	×

we will have k ‘instantons’ in a $U(1)$ theory with kN units of electric flux.

In the daughter theory, we have a set of N D4 branes wrapped around a \mathbf{T}^4 but sitting at an orbifold point in transverse space. The twist associated to the tunneling configuration in the daughter theory, Sec. 13.3.2, is realized diluting a D2-brane both in “34” and “12” directions. The orbifold action is responsible of the multiples copies of the gauge group. So physically we are introducing what in an unorbifolded theory will be N D4 branes and not kN branes, although the field content is constructed projecting the last.

	0	1	2	3	4
(k)N D4	×	×	×	×	×
(k)1 D2	×	•	•	×	×
(k)1 D2	×	×	×	•	•

We can make a T-duality transformation along “12” directions

	0	1	2	3	4
(k)N D2	×	•	•	×	×
(k)1 D4	×	×	×	×	×
(k)1 D0	×	•	•	•	•

so we have an ‘instanton’ in the presence of $(k)N$ units of magnetic flux in a $U(1)^k$ theory. If the T-duality transformation is made along “34” directions

	0	1	2	3	4
(k)N D2	×	×	×	•	•
(k)1 D0	×	•	•	•	•
(k)1 D4	×	×	×	×	×

now the flux is electric instead of magnetic. In this two cases, we can interpret the ‘un-twisted’ fractional instanton as a D0 brane in the presence of a D2 brane. This is the sector where all torons are at the same point. The sectors where torons are at different points correspond to the splitting of the D0 in fractional D0s that can move independently along the torus directions. The gauge group is the same for k fractional D0s as for a regular D0, however the strings joining different fractional D0s acquire a mass proportional to the separation. This is reflected in the mass we have computed for fermionic modes (13.49). So in fact, the quiver diagrams we have used to label different sectors of the moduli space correspond to the gauge theory living in the D0s at different points of the moduli space.

From this point of view we also have a geometric picture of why the configuration of the daughter theory should be mapped to a configuration of the parent theory with k units of both electric and magnetic flux. The matching is between the number of fractional branes in the orbifolded theory and the number of branes of the same dimensions in the ‘parent’.

If we make another T-duality transformation along “1234” directions,

	0	1	2	3	4
(k)N D0	×	•	•	•	•
(k)1 D2	×	×	×	•	•
(k)1 D2	×	•	•	×	×

the D4s become D0s that can move along the torus. The separation in fractional D0s is encoded in the Abelian part of the daughter theory. The diagonal $U(1)$ correspond to the center of mass position, while the $U(1)^{k-1}$ group that form the Abelian moduli space are the relative separations of D0s in this T-dual interpretation. From (13.33) we know that D0s tend to separate, a signal of the orbifold tachyon.

Chapter 14

Conclusions

The analysis of orbifold and orientifold theories in finite volume $\mathbf{R} \times \mathbf{T}^3$ presents some caveats for planar equivalence. With periodic boundary conditions, the holonomies around the compact directions of the torus play the role of low-energy degrees of freedom. For some non-trivial values of the holonomies, there are violations of planar equivalence. This is shown in the non-vanishing at leading order $O(N^2)$ of the one-loop effective potential. This result by itself does not rule out planar equivalence in the strong coupling regime, which is a quite different physical situation. For instance, at strong coupling we expect the formation of a fermion condensate and chiral symmetry breaking. However, the result suggests that when configurations with large gauge field values become important, as one would consider for the strong coupling regime, the equivalence is not obviously fulfilled. Notice that violations of planar equivalence occur only at narrow regions of the moduli space, that become of zero measure as $N \rightarrow \infty$, but still we should be careful before having it for granted.

When we study orbifolds in torus with twisted boundary conditions, we find difficulties in matching parent and daughter. The results, specially semiclassical computations, suggests that the orbifold theory contains a $SU(N)$ supersymmetric subsector, rather than being equivalent to the parent theory. It would be interesting to check whether orientifold theories contain a $SO(N)$ supersymmetric sector, since maybe that sectors are in the root of perturbative planar equivalence.

Appendix

Appendix A

Examples of multitrace deformations

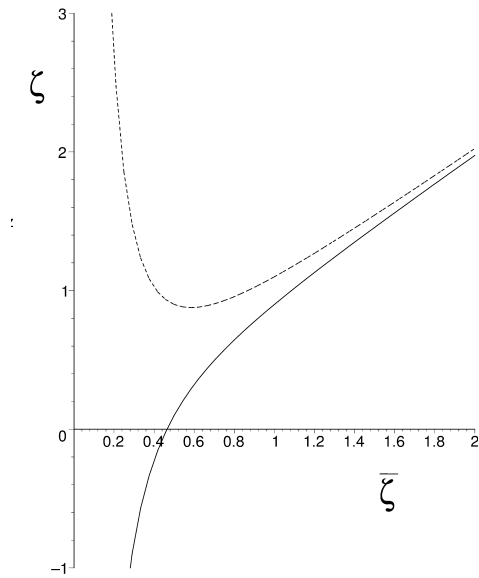


Figure A.1: *The function $H(\bar{\zeta})$ for the monomium perturbation with $n = 1$ and $\xi = 0.1$ (full line), $\xi = -0.1$ (dashed line).*

Choosing a multitrace deformation by a single positive power

$$f(z) = \xi \frac{z^{n+1}}{n+1}, \quad (\text{A.1})$$

we have

$$H(\bar{\zeta}) = \bar{\zeta} - \frac{\xi}{\bar{\zeta}^{2n}} \quad (\text{A.2})$$

and a vacuum energy density

$$w = -\bar{\zeta}^{-1} - \xi \frac{n}{n+1} \left(\bar{\zeta}^{-2} \right)^{n+1}. \quad (\text{A.3})$$

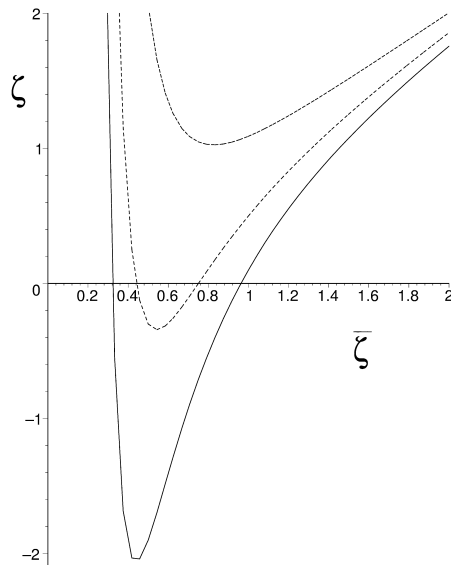


Figure A.2: Binomium perturbation $n = 2$, $l = 1$, $\xi = -0.1$, $\eta = 1, 0.6, 0.01$ (the larger η corresponding to the full line).

For small ξ the behavior is qualitatively equivalent to the single-trace theory near the correspondence line $\bar{\zeta} = 1$. However, there are gross differences deep in the supergravity regime $\bar{\zeta} \ll 1$.

For $\xi > 0$ we have well defined supergravity backgrounds with small curvature ($\bar{\zeta} \rightarrow 0$) and *small* and negative bare 't Hooft coupling ($\zeta \rightarrow -\infty$). Restricting ourselves to positive bare 't Hooft couplings we have a minimum value of $\bar{\zeta}$ given by $\bar{\zeta}_c = \xi^{\frac{1}{2n+1}}$. At this point the bare 't Hooft coupling diverges, i.e. $\zeta = H(\bar{\zeta}_c) = 0$.

On the other hand, for $\xi < 0$ the H -function has a minimum at $\bar{\zeta}_m = (2n|\xi|)^{\frac{1}{2n+1}}$ at which the bare 't Hooft coupling becomes maximal. This is a critical point of the master equation with the onset of a local instability for lower $\bar{\zeta}$. For $\zeta > \zeta_m$ there are two possible solutions of the master equation, but only the more curved one (larger $\bar{\zeta}$) is locally stable.

For either sign of ξ the dynamics differs significantly from the single-trace model when the inverse 't Hooft coupling reaches values of order $\zeta \sim |\xi|^{\frac{1}{2n+1}}$. Hence, for $|\xi| \sim 1$ the single-trace behavior is pushed beyond the correspondence line. In particular, for $\xi \ll -1$ the supergravity regime loses all stable solutions.

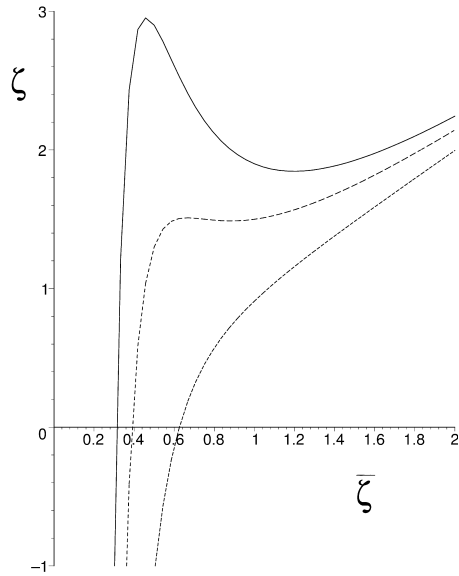


Figure A.3: *Binomium perturbation* $n = 2$, $l = 1$, $\xi = 0.1$, $\eta = -1, -0.6, -0.01$. (the larger η corresponding to the full line)

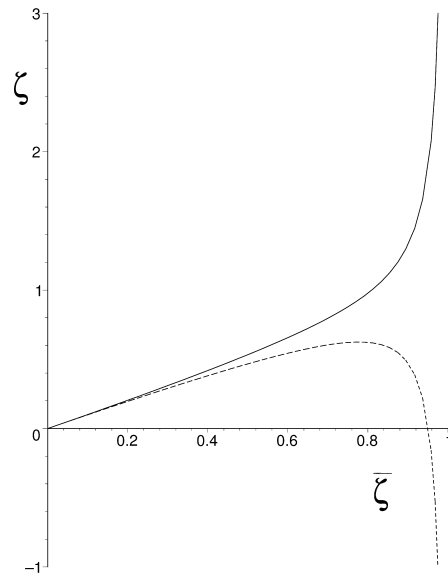


Figure A.4: *Logarithmic perturbation* with $\varepsilon = 1$, $\xi = 0.1$ (dashed lines) and $\xi = -0.1$ (full lines). The branches at $\bar{\zeta} > 1$ are unphysical.

A.1 Binomium Perturbation

For a perturbation of the form

$$f(z) = \xi \frac{z^{n+1}}{n+1} + \eta \frac{z^{l+1}}{l+1}, \quad n > l, \quad (\text{A.4})$$

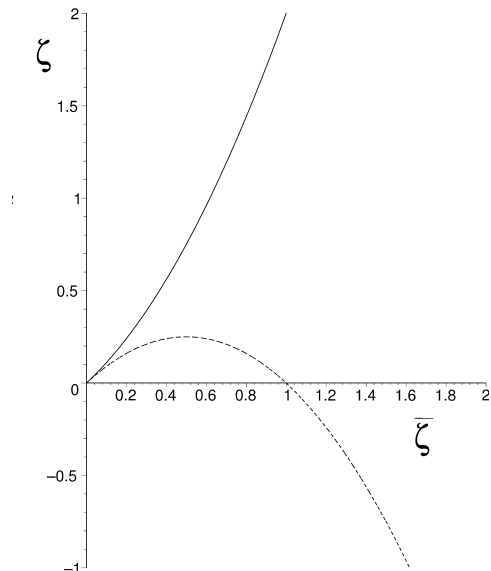


Figure A.5: Simple pole perturbation, $f(z) = \xi/z$, with $\xi = 1$ (full line) and $\xi = -1$ (dashed line).

one has

$$H(\bar{\zeta}) = \bar{\zeta} - \frac{\xi}{\bar{\zeta}^{2n}} - \frac{\eta}{\bar{\zeta}^{2l}}. \quad (\text{A.5})$$

There is no qualitative difference with the monomium if ξ and η have both the same sign. If the sign is different and $\xi < 0$, the shape is the same as in the monomium but the minimum is displaced to lower values of ζ , and can eventually cross the $\zeta = 0$ axis, removing the restrictions on the value of the 't Hooft parameter (c.f. Fig. A.2). The amount of the displacement is related to the ratio $|\eta/\xi|$, growing with it up to a maximum value. If $\xi > 0$ a maximum and a minimum of $H(\bar{\zeta})$ appear if the ratio $|\eta/\xi|$ is large enough. Thus, a new unstable branch develops and there is a phase transition between the low- $\bar{\zeta}$ branch and the high- $\bar{\zeta}$ branch as ζ increases (c.f. Fig. A.3).

A.2 More Exotic Perturbations

In the supergravity approximation one may also study non-polynomial “perturbations” at a formal level. For example, we can consider an analytic logarithmic perturbation

$f(z) = \xi \log(\varepsilon z - 1)$, with $0 < \varepsilon < 1$, leading to

$$H(\bar{\zeta}) = \bar{\zeta} - \xi \varepsilon \frac{\bar{\zeta}^2}{\varepsilon - \bar{\zeta}^2} . \quad (\text{A.6})$$

The function $f(\bar{\zeta})$ develops an imaginary part for $\bar{\zeta} > \sqrt{\varepsilon}$, so that we are led to the restriction $\bar{\zeta} < \sqrt{\varepsilon} < 1$. If $\varepsilon > 1$ this boundary goes beyond the supergravity regime. The $\xi < 0$ branch is locally stable, whereas the $\xi > 0$ branch is only stable up to a maximum value of $\bar{\zeta}$. This determines in turn a maximum value of ζ (or a minimum 't Hooft coupling).

An even more formal perturbation is given by the non-analytic function $f(z) = \xi/z$ with

$$H(\bar{\zeta}) = \bar{\zeta} + \xi \bar{\zeta}^2 . \quad (\text{A.7})$$

In this case, the perturbation by $1/\text{tr} F^2$ does not make much sense in perturbation theory. However, the results are quite smooth in the supergravity approximation, corresponding to the limit of very large 't Hooft coupling. Indeed, from (A.7) we see that these models produce an *analytic* function $H(\bar{\zeta})$, so that they approach the single-trace theory for $\zeta \ll 1$. If $\xi < 0$ there is a maximum of the master equation, which means that the 't Hooft parameter should be higher than $4|\xi|$.

In general, we see that novel qualitative features triggered by multitrace couplings stay well within the supergravity approximation only as long as $|\xi| \ll 1$, with ξ a generic multitrace coupling. Since the master equation takes the form

$$\zeta = H(\bar{\zeta}) = \bar{\zeta} - f'(\bar{\zeta}^{-2}) , \quad (\text{A.8})$$

we find that deformations that have $f'(z)$ analytic around the origin produce important qualitative changes in the deep supergravity regime $\bar{\zeta} \rightarrow 0$. Conversely, singular deformations in perturbation theory, corresponding to singular $f'(z)$ at the origin, approach the single-trace theory in the extreme supergravity regime.

Appendix B

One-loop potential in the torus

In this appendix we give the explicit derivation of the one-loop effective potential over the moduli space of gauge theories in $\mathbf{R}^d \times \mathbf{T}^n$ spacetime. We expand the path integral around a moduli configuration $F_{MN} = 0$ parametrized by a constant connection in the Cartan subalgebra along the compact directions.

$$\vec{C} = \vec{C}^a H^a, \quad [H^a, H^b] = 0, \quad a, b = 1, \dots, r, \quad (\text{B.1})$$

where r is the rank of the gauge group. Assume that we have matter in the gauge representation R and in a Lorentz representation with \mathcal{N}_R physical polarizations, and F_R is the fermion number of the representation. We also consider that the matter can have a mass M_R . Then,

$$\exp(-V_{\text{eff}}(\vec{C})) = \prod_R \det \left(-\partial_\mu \partial^\mu \mathbf{1} - \left(\vec{\partial} \mathbf{1} + \frac{1}{L} \text{Ad}(\vec{C}) \right)^2 + M_R^2 \mathbf{1} \right)^{-(-1)^{F_R} \mathcal{N}_R / 2}. \quad (\text{B.2})$$

Here Ad denotes the adjoint action (11.22). From this expression we get

$$V_{\text{eff}}(\vec{C}) = \frac{1}{2} \sum_R (-1)^{F_R} \mathcal{N}_R \text{Tr} \log \left[-\partial_\mu \partial^\mu \mathbf{1} - \left(\vec{\partial} \mathbf{1} + \frac{1}{L} \text{Ad}(\vec{C}) \right)^2 + M_R^2 \mathbf{1} \right], \quad (\text{B.3})$$

where the trace is over states given by the weights μ_R of the representation and the momentum along \mathbf{R}^d (p) and \mathbf{T}^n ($2\pi \vec{n}/L$). We can use a Schwinger parameter τ to rewrite the logarithm as an integral,

$$V_{\text{eff}}(\vec{C}) = -\frac{1}{2} \sum_R (-1)^{F_R} \mathcal{N}_R \sum_{\mu_R} \int_{\mathbf{R}^d} \frac{d^d p}{(2\pi)^d} \sum_{\vec{n} \in \mathbf{Z}^n} \int_0^\infty \frac{d\tau}{\tau} e^{-\tau(p^2 + M_R^2) - \frac{\tau}{L^2} (2\pi \vec{n} + \mu_R \cdot \vec{C})^2} - [\vec{C} = 0]. \quad (\text{B.4})$$

The last term means that we subtract the same expression evaluated at $\vec{C} = 0$, which is equivalent to eliminate \vec{C} -independent terms.

If we integrate over the time component of the momentum, we get a factor $\sim \tau^{-1/2}$, so after integrating over the Schwinger parameter we end with

$$V_{\text{eff}}(\vec{C}) = \frac{1}{2} \sum_R (-1)^{F_R} \mathcal{N}_R \sum_{\mu_R} \int_{\mathbf{R}^{d-1}} \frac{d^{d-1} \mathbf{p}}{(2\pi)^{d-1}} \sum_{\vec{n} \in \mathbf{Z}^n} \sqrt{\mathbf{p}^2 + M_R^2 + \frac{1}{L^2} (2\pi \vec{n} + \mu_R \cdot \vec{C})^2} - [\vec{C} = 0]. \quad (\text{B.5})$$

which has the form of a sum over the frequencies of infinite harmonic oscillators. The frequency along the compact directions is shifted by the holonomy. Therefore, the potential is of Coleman-Weinberg type.

If we integrate over the whole d -momentum, we get a factor

$$\int_{\mathbf{R}^d} \frac{d^d p}{(2\pi)^d} e^{-\tau p^2} = \frac{1}{(4\pi\tau)^{d/2}} \quad (\text{B.6})$$

The next step is to make a Poisson resummation over the n -momentum,

$$\sum_{\vec{n} \in \mathbf{Z}^n} e^{-\frac{\tau}{L^2} (2\pi \vec{n} + \mu_R \cdot \vec{C})^2} = \frac{L^n}{(4\pi\tau)^{n/2}} \sum_{\vec{l} \in \mathbf{Z}^n} e^{-\frac{L^2}{4\tau} \vec{l}^2 - i\mu_R \cdot \vec{C} \vec{l}} \quad (\text{B.7})$$

that, after the change of variables $t = \vec{l}^2 L^2 / 4\tau$ leaves

$$V_{\text{eff}}(\vec{C}) = \frac{-1}{2\pi^{\frac{d+n}{2}} L^d} \sum_R (-1)^{F_R} \mathcal{N}_R \sum_{\mu_R} \sum_{\vec{l} \in \mathbf{Z}^n} \frac{1}{(\vec{l}^2)^{\frac{d+n}{2}}} \int_0^\infty dt t^{\frac{d+n}{2}-1} e^{-t - \frac{\vec{l}^2 M_R^2 L^2}{4t}} e^{-i\mu_R \cdot \vec{C} \vec{l}} - [\vec{C} = 0]. \quad (\text{B.8})$$

Notice that with the subtraction, the $\vec{l} = 0$ contribution vanishes, as well as the value of the potential at $\vec{C} = 0$. The phases can be arranged in a factor $-2 \sin^2(\mu_R \cdot \vec{C} \vec{l} / 2)$. After making the integration over the Schwinger parameter, we find the final form of the potential

$$V_{\text{eff}}(\vec{C}) = \sum_R (-1)^{F_R} \mathcal{N}_R \sum_{\mu_R} \frac{2}{L^d} \left(\frac{M_R L}{2\pi} \right)^{\frac{d+n}{2}} \sum_{\vec{l} \neq 0} K_{\frac{d+n}{2}} \left(M_R L \sqrt{\vec{l}^2} \right) \frac{\sin^2 \left(\frac{1}{2} \mu_R \cdot \vec{C} \vec{l} \right)}{(\vec{l}^2)^{\frac{d+n}{4}}} \quad (\text{B.9})$$

when $M_R = 0$, it reduces to the massless expression

$$V_{\text{eff}}(\vec{C}) = \sum_R (-1)^{F_R} \mathcal{N}_R \sum_{\mu_R} \frac{\Gamma \left(\frac{d+n}{2} \right)}{\pi^{\frac{d+n}{2}} L^d} \sum_{\vec{l} \neq 0} \frac{\sin^2 \left(\frac{1}{2} \mu_R \cdot \vec{C} \vec{l} \right)}{(\vec{l}^2)^{\frac{d+n}{2}}} \quad (\text{B.10})$$

B.1 Non-analytic behavior

As expected from its definition, the subtracted potential (B.10) gets no contribution from those modes in the Cartan subalgebra that are also constant throughout the torus, corresponding to the $\vec{n} = 0, \alpha = 0$ terms in the sums. Since these modes are precisely given by the background flat connections, $\vec{\phi}$, we can view (B.10) as a Wilsonian potential in which all non-zero modes plus non-abelian constant modes on the torus are integrated out. In fact, the constant non-abelian modes at $\vec{n} = 0$ have an effective mass of order $|\alpha \cdot \vec{\phi}|/L$, and the Wilsonian separation of scales breaks down at points in \mathcal{M} where the Higgs mechanism turns off, i.e. the orbifold points. The extra massless degrees of freedom induce infrared singularities in (B.10). In order to estimate these, we examine the $\vec{n} = 0$ terms, with an ultraviolet cutoff in place,

$$\Delta V(\vec{\xi})_{\text{IR}} = -\frac{1}{(4\pi)^{d/2}} \int_{\epsilon^2}^{\infty} \frac{dt}{t} t^{-d/2} e^{-t\vec{\xi}^2/L^2}. \quad (\text{B.11})$$

In this expression, it is plain that $|\vec{\xi}|/L$ plays the role of an infrared cutoff in the proper time integral, which is itself regularized in the ultraviolet by the length-squared ϵ^2 . We can choose $\epsilon = L$ to consider the contribution of non-abelian constant modes with energies ranging from the compactification scale $1/L$ down to the infrared cutoff $|\vec{\xi}|/L$. Then we may write the previous expression in the form

$$\Delta V(\vec{\xi})_{\text{IR}} = -\frac{1}{(4\pi)^{d/2} L^d} \left(\vec{\xi}^2\right)^{d/2} \Gamma\left(\vec{\xi}^2, -d/2\right), \quad (\text{B.12})$$

in terms of the incomplete Gamma function. For odd values of d we find a non-analytic behaviour of branch-point type, $V_0(\vec{\xi}) \sim (\vec{\xi}^2)^{d/2}$, with a logarithmic correction $V_0(\vec{\xi}) \sim (\vec{\xi}^2)^{d/2} \log(\vec{\xi}^2)$ for even values of d . In particular, we have a conical singularity for $d = 1$. At any rate, as long as $d > 2$ the non-analytic terms are quantitatively subleading to the analytic terms of order $\vec{\xi}^2$, induced by the high-energy modes.

Appendix C

Landscape features of the potential

The landscape in string theory [189–191] could be defined as the set of possible isolated locally stable backgrounds [192–194]. A line of investigation opened by Douglas tries to group the landscape vacua in statistical ensembles in order to deduce properties of the theory [195–198]. Going further, it has been proposed that they are part of a connected space of configurations described by a low-energy effective action [189, 199]. Then, the theory could dynamically explore the different possibilities through some mechanism, as the formation of vacuum bubbles [200–202]. In this case, if we have enough vacua, it is not implausible that our own universe will appear, with the same ‘crazy’ values for the cosmological constant $\sim 10^{-120} M_{\text{Pl}}$ and so on. Remember that the typical energies are of the order of the Plank mass M_{Pl} , so to end in an universe like ours will require a huge amount of vacua exploring a quasi-continuous band of energies. There are two main problems with this picture, a technical and a philosophical one. First, the existence of the landscape in the strong sense or a satisfactory mechanism to realize all the vacua are yet unresolved matters [203]. Second, even if these problems are solved we are not sure of how to falsify the theory, since we expect that different universes are causally disconnected. Let us just avoid these deep questions and come back to the problem of finding and counting vacua.

Usually the landscape refers to the geometric, closed string part, but it may involve the open string sector as well [204]. In this framework, the effective potential of Chapter. 11 can be used to find vacua of brane compactifications. Supersymmetry should be broken much above the compactification scale, and since the spectrum is non-realistic, the construction should be in a hidden sector for a phenomenologically viable model. We will not discuss

these matters, but we will just show that landscape-like features appear in the form of a highly populated band of energies. The most remarkable fact, compared to other landscape constructions [205, 206], is that this is achieved with only a few parameters and a simple field content.

C.1 Effective potentials for flat connections

We begin by reviewing some standard facts about adjoint Higgs fields generated upon toroidal compactification. Let us consider a Yang–Mills model in a $(d + n)$ -dimensional spacetime of the form $\mathbf{R}^d \times \mathbf{T}^n$, a product of a standard flat d -dimensional Minkowski spacetime and an internal torus of size L , which we take orthogonal for simplicity. The classical action

$$S_h = \frac{1}{2g_h^2} \int_{\mathbf{R}^d \times \mathbf{T}^n} \text{tr} |F_{AB}|^2 \quad (\text{C.1})$$

reduces, for distance scales much larger than L , to the effective system

$$S = \frac{1}{2g^2} \int_{\mathbf{R}^d} \text{tr} (|F_{\mu\nu}|^2 + |D_\mu \Phi_a|^2 - |[\Phi_a, \Phi_b]|^2 + \dots) , \quad (\text{C.2})$$

where we have split the $(d + n)$ -dimensional indices (A, B, \dots) into \mathbf{R}^d spacetime indices (μ, ν, \dots) and internal \mathbf{T}^n indices (a, b, \dots) . Each field Φ_a is an adjoint Higgs that originates in the Fourier modes of the gauge field components along the n -torus and the commutator term is their classical potential, coming from the “magnetic” energy density, $F_{ab}F^{ab}$, of field-strengths along the torus directions. The dots stand for higher order terms suppressed by powers of EL in a low-energy expansion with $E \ll 1/L$, and the classical mapping between high and low energy couplings is the standard Kaluza–Klein relation $g_h^2 = L^n g^2$. Only the zero modes of the gauge field on \mathbf{T}^n survive as *massless* adjoint Higgses in the effective theory below the gap $1/L$. These are the flat connections on \mathbf{T}^n , defined by the vanishing of the magnetic energy $F_{ab} = 0$. A gauge-covariant description of these degrees of freedom is given by topologically nontrivial Wilson lines wrapped around the noncontractible cycles of \mathbf{T}^n .

In general, the space of flat connections on \mathbf{T}^n has connected components. These can be the result of specific group-theory properties (e.g. the nontrivial commuting triples for $n = 3$ and particular gauge groups [207]), or be associated to topological structure of the gauge bundles, such as non-Abelian electric and magnetic fluxes through the torus [146]. Each connected component of the moduli space admits a parametrization in terms of

constant commuting gauge connections in some appropriate subgroup of the gauge group. Since most of our results apply to each connected component separately, in the following we focus on the particular case of the single connected component containing the identity Wilson lines, corresponding to bundles admitting periodic boundary conditions on the torus (Chapter. 11). A set of coordinates of \mathcal{M} is provided by the constant commuting connections

$$L\vec{\Phi} \equiv \vec{\phi} = \sum_{i=1}^r \vec{\phi}_i H_i \quad (\text{C.3})$$

with H_i a complete set of generators of the Cartan subalgebra and r the rank of the group.

In the effective gauge theory on \mathbf{R}^d , the moduli space \mathcal{M} is to be regarded as the target space for the Higgs fields. For $d > 2$, it is also the space of their possible “expectation values” in a Coulomb phase, i.e. the gauge group left unbroken by the Higgs mechanism at a generic point on \mathcal{M} is the maximal Abelian subgroup. On submanifolds of higher codimension we have enhanced gauge symmetry, which remains completely unbroken at the origin of moduli space, together with the points on \mathcal{M} that are obtained from $\vec{\phi} = 0$ by the action of twisted gauge transformations [146]. For example, for $SU(N)$ the center is \mathbf{Z}_N . In general, if N is the cardinal of the center, we find N^n vacua that are locally identical to the unbroken vacuum labelled by $\vec{\phi} = 0$.

C.1.1 Effective potentials

The low-energy effective action for fields, $\vec{\phi}$, parametrizing the Cartan torus (i.e. for those with vanishing classical potential [Φ^a, Φ^b] = 0) includes an effective potential induced by integrating out all the high-energy degrees of freedom. Working in perturbation theory in the Yang–Mills coupling, we have a natural expansion parameter at the compactification scale $1/L$. For a rank N gauge group, it is given by the dimensionless 't Hooft coupling $\lambda = g^2(L) N L^{4-d}$, where $g^2(L)$ is the effective d -dimensional Yang–Mills coupling, renormalized at the scale $1/L$. This parameter, defined at the matching scale $1/L$ runs with energy according to

$$\lambda_{\text{eff}}(E) = \lambda (EL)^{d_{\text{eff}}-4}, \quad (\text{C.4})$$

with logarithmic running for $d_{\text{eff}} = 4$. The effective dimension is given by $d_{\text{eff}} = d$ for $EL < 1$, whereas $d_{\text{eff}} = d + n$ for $EL > 1$. Of course, perturbation theory necessarily breaks down at sufficiently high energies for $d + n > 4$. The strong-coupling threshold is

defined by $\lambda_{\text{eff}}(\Lambda_{\text{UV}}) = 1$, or

$$\Lambda_{\text{UV}} = \frac{\lambda^{-\frac{1}{d+n-4}}}{L}, \quad (\text{C.5})$$

and defines the scale beyond which some ultraviolet (UV) completion must be provided. Effects of such UV physics decouple below the compactification scale L as inverse powers of $\Lambda_{\text{UV}} L$, or equivalently, as positive fractional powers of λ .

Keeping in mind these limitations of the perturbative approach, the one-loop effective potential can be defined by the gaussian functional integral over those gauge fields on $\mathbf{R}^d \times \mathbf{T}^n$ that are orthogonal to the flat connections. Since the flat connections $\vec{\phi}$ are not integrated over, they function as a background field and we may use the standard machinery of the background field gauge. We obtain for the one-loop effective potential (11.13)

$$V_{\text{eff}}(\vec{\phi}) = (d+n-2) \sum_{\alpha \in \text{roots}} V(\alpha \cdot \vec{\phi}) \quad (\text{C.6})$$

An interesting property of the one-loop effective potential is its ultraviolet finiteness, after a $\vec{\phi}$ -independent constant is appropriately subtracted. This is actually true to all orders in perturbation theory. The reason is that any counterterm of the $(d+n)$ -dimensional gauge theory must be gauge-invariant and, as such, a polynomial in covariant derivatives and curvature field strengths. All those counterterms vanish on the space of flat connections, and therefore V_{eff} cannot get UV divergences at any order in perturbation theory (see [208, 209] for a recent analysis of counterterms in compactified gauge theories). The error made by extending the momentum integrals and sums beyond the UV threshold Λ_{UV} vanishes as $\Lambda_{\text{UV}} L$ goes to infinity. Therefore, all corrections to V_{eff} from the physics of the UV completion are controlled by the small parameter $\lambda \ll 1$.

The function $V(\vec{x})$ also determines the effective potential induced by integrating out matter fields in an arbitrary representation of the gauge group. For scalar fields or fermions in an irreducible representation R , we find (11.21)

$$V_{\text{eff}}(\vec{\phi}) = \sum_R (-1)^{F_R} \mathcal{N}_R \sum_{\mu \in R} V_{M_R}(\mu \cdot \vec{\phi}), \quad (\text{C.7})$$

Where \mathcal{N}_R is the number of physical polarizations, F_R is the fermion number and μ_R are the weights of the representation. The potential function V_M is the massive generalization of V (11.23).

An interesting particular case concerns models with softly broken supersymmetry, i.e. broken by the mass splittings M_R . In this case, the total potential gets no contribution

from the far UV regime, and the boson-fermion cancellation is complete when the non-supersymmetric mass splittings are removed. In any case, notice that the mass terms do not have a large effect on the qualitative form of the potential function (11.21), which is dominated by small values of $|\vec{\ell}|$ even for the $M = 0$ case. Therefore, the main effect of soft-breaking masses is a global quenching of the associated effective potentials, without major modifications of the qualitative features such as the symmetry properties (i.e. the location of the vacua with unbroken gauge symmetry).

A point of detail concerns the proper Wilsonian interpretation of the effective potentials induced by arbitrary matter representations. In the adjoint representation, all flat connections are zero modes of the adjoint covariant derivative operator. These zero modes were eliminated from the partition sums by the vacuum-energy subtraction. For generic matter representations, zero modes are located on submanifolds of zero measure in the moduli space \mathcal{M} . Therefore, we integrate out all matter degrees of freedom and let singularities of V_{eff} appear on \mathcal{M} , much in the same fashion as the enhanced-symmetry singularities appear for the case of the adjoint representation.

Some further generalizations concern different spin structures for fermions on \mathbf{T}^n (which amount to additive shifts of $\vec{\phi}$ in all formulae, see for example [154]), and twisted boundary conditions for the gauge bundles on \mathbf{T}^n . In this last case, the moduli space of flat connections is partially lifted (see [145] for a review). On the remaining moduli space the analysis is equivalent to what is described here.

C.2 The Cartan–Weyl landscape

The potential (11.21) has “landscape-like” features for generic representations. The overall features are dictated by the crystallographic nature of the compact moduli space \mathcal{M} , in particular the slightly different action of the Weyl group, W , depending on the representation under consideration. Associated to a given weight μ in a general representation, there are codimension n hyperplanes on \mathcal{M} , defined by

$$\mu \cdot \vec{\phi} = 0 \pmod{2\pi\mathbf{Z}^n}, \quad (\text{C.8})$$

that are fixed by W . Such Weyl hyperplanes host local minima of bosonic potentials (along transverse directions) and local maxima of fermionic potentials. Therefore, local minima (maxima) are found at intersections of Weyl hyperplanes, i.e. at the edges of the

so-called Weyl chamber. The effective potential contributed by a representation R has structure down to the overall scale determined by the size of the Weyl chamber, inversely proportional to the norm of the highest weight. Hence, very large representations induce potentials with short-distance scale on \mathcal{M} . The overall picture is that of an intricate pattern of rifts and valleys along the Weyl hyperplanes associated to different representations.

Fermionic contributions to the total effective potential look like “inverted” bosonic potentials. Hence, the singular locus of fermionic contributions is associated with local maxima rather than minima. Conversely, local minima of fermionic potentials are related to local maxima of bosonic potentials, and they could be smooth, just like the local maxima of the function (11.13). Such smooth local minima of the full potential will typically break the gauge symmetry in a complicated pattern.

An interesting question is the fate of vacua with “unbroken” gauge symmetry, corresponding to the zeros of the pure Yang–Mills effective potential. If the matter potential happens to be sufficiently smooth at those minima, its main effect is simply to lift the unbroken vacuum to a non-vanishing vacuum energy. The surprising fact is that these lifted vacua typically scan in a broad band of energies.

We now focus on $SU(N)$ gauge theories, which give rise to a very large group of central conjugations, i.e. $(\mathbf{Z}_N)^n$ with cardinal N^n . In this case, we have a large number of unbroken symmetry vacua on \mathcal{M} and we can enquire how are they lifted by the matter potentials. The zeros of the potential are at (11.17)

$$\vec{\phi}_0 = 4\pi \sum_i \vec{n}_i \nu^i, \quad \vec{n}_i \in \mathbf{Z}^n. \quad (\text{C.9})$$

In the pure Yang–Mills theory, all these vacua with unbroken gauge symmetry are strict copies of the zero-Higgs vacuum $\vec{\phi} = 0$. In fact, their occurrence is related to the action of the $(\mathbf{Z}_N)^n$ group of central conjugations, associated to large gauge transformations. Perturbatively, these vacua remain disconnected, since the tunneling amplitude across the potential barrier in V_{eff} is nonperturbative in the gauge coupling.

In the presence of additional matter degrees of freedom, these vacua get lifted according to the value of

$$\sum_R (-1)^{F_R} \mathcal{N}_R \sum_{\mu \in R} V_{M_R} \left(\mu \cdot \vec{\phi}_0 \right). \quad (\text{C.10})$$

Thus, for a given representation, we must evaluate

$$V_M \left(4\pi \sum_i \vec{n}_i \mu \cdot \nu^i \right) \quad (\text{C.11})$$

for all weights μ . In general, any weight can be found in the weight lattice generated by the ν^i . Therefore, the argument of the scalar function $V_M(\vec{\xi})$ will be determined by integer linear combinations of the scalar products

$$4\pi \nu^i \cdot \nu^j = 2\pi \delta^{ij} - \frac{2\pi}{N}. \quad (\text{C.12})$$

The term proportional to the Kronecker delta has no effect by the periodicity properties of (11.13), and we are left with a sum of terms of the form $V_M(2\pi\vec{K}/N)$, where \vec{K} is a \mathbf{Z}^n -valued vector defined modulo N . If \vec{K} is of $O(1)$ in the large N limit, then the full potential at this particular local vacuum is a sum of terms of $O(1/N^2)$, since the potential can be considered quadratic near the origin (for $d > 2$). On the other hand, if $\vec{K} = O(N)$, we have a sum of terms of $O(1)$. The final scaling of the potential depends in each case on the multiplicity from the sum over weights.

Our considerations refer only to the energy shift of the N^n “unbroken” vacua in a $(\mathbf{Z}_N)^n$ representation. In principle, the matter potential can alter the local properties of the vacua beyond a simple shift of vacuum energy. If the slope of V_R is large enough at $\vec{\phi}_0$, the local minimum can disappear. This is more likely to happen the larger is the representation contributing to V_{eff} , because the overall scale of the potential is proportional to the dimension of the representation. For this reason, stability of the unbroken vacua will require in general that the mass of matter representations be sufficiently large, so that the matter contributions are appropriately quenched by the $\exp(-ML)$ suppression factor. For $ML \gg 1$ and near the origin, we may approximate

$$V_M(\vec{\xi}) \approx \Delta \xi^2, \quad (\text{C.13})$$

with

$$\Delta \sim \frac{(ML)^{\frac{d+n-1}{2}}}{L^d} \exp(-ML). \quad (\text{C.14})$$

For $d = 2$ there is a correction by a logarithmic factor, $\log|\vec{\xi}|$, whereas for $d = 1$ the leading approximation is linear in $|\vec{\xi}|$. In the following we consider the case $d > 2$.

In general, the “unbroken” vacua are shifted by the matter contribution, so that the gauge symmetry at those vacua is actually broken. We can still refer to these vacua as

“unbroken” in order to make explicit their origin in the \mathbf{Z}_N -vacua of the pure Yang–Mills theory. In fact, if the matter is even slightly heavier than the compactification scale, $ML > 1$, we can have $\Delta \ll 1$ and the symmetry breaking effects (such as gauge boson masses) are suppressed by a factor of $O(\Delta)$.

C.2.1 Examples

To illustrate these points, we consider some examples. First, matter fields (fermionic or bosonic) in the fundamental representation of $SU(N)$. In this case, the weights are given directly by the ν^i , so that the potential is proportional to

$$\sum_i V_M \left(\frac{2\pi}{N} \sum_k \vec{n}_k \right) = N V_M \left(\frac{2\pi}{N} \sum_k \vec{n}_k \right). \quad (\text{C.15})$$

For small values of the argument, we approximate the potential as in (C.13). Then, as $\sum_k \vec{n}_k$ varies from $O(1)$ to $O(N)$, the lifted local minima scan a band ranging from $O(1/N)$ to $O(N)$, times the mass quenching factor Δ , with spacings of order Δ/N at the bottom, and only of order Δ at the top of the band.

A second example is given by matter fields in the antisymmetric representation of $SU(N)$. In this case, weights are of the form $\nu^i + \nu^j$, with $i < j$. The matter potential evaluated at the lattice of unbroken symmetry points is proportional to

$$\sum_{i < j} V_M \left(\frac{4\pi}{N} \sum_k \vec{n}_k \right) = \frac{1}{2} N(N-1) V_M \left(\frac{4\pi}{N} \sum_k \vec{n}_k \right). \quad (\text{C.16})$$

The same reasoning as before shows that the lattice of N^n points of unbroken $SU(N)$ symmetry is lifted to a band with typical (bottom) spacing of $O(1)\Delta$ and ranging up to $O(N^2)\Delta$ energies. If we consider the symmetric representation instead, we have to add the weights of the form $\mu = 2\nu^i$, introducing a finer structure of the type already described for the fundamental representation.

C.2.2 The general rules

In general, the condition for the unbroken vacua to be lifted into a broad band of energies is that the global $(\mathbf{Z}_N)^n$ symmetry be broken by the matter representations. At the same time, the local stability properties of the pure Yang–Mills potential at those vacua should

not be significantly upset, as is the case for matter potentials generated by relatively large masses on the compactification scale.

The misalignment responsible for the lifting of the vacua finds its origin in the slight non orthogonality of the basic weights ν^i . If the expression of a given weight μ in terms of the ν^i shows the same number of positive and negative signs modulo N , then the terms proportional to $2\pi/N$ cancel out in the argument of the scalar potential $V_M(\vec{x})$. The coefficient of this term only depends on the representation, and not on the particular weight within it, because all those differ by a integer linear combination of roots, and the scalar product of roots with the ν^i leaves no $O(1/N)$ residue.

If ν^i are the weights of the defining fundamental representation (the N), then $-\nu^i$ are weights of the conjugate representation (the \bar{N}). Any irreducible representation can be found in the decomposition of the tensor product of the N and the \bar{N} representations. Hence, the (mod N) number of ν^i minus the number of $-\nu^j$ in the expression for μ is the N -ality of the representation, i.e. the character under the \mathbf{Z}_N center of the group. At the end, the distribution of cosmological constants at the unbroken minima $\vec{\phi}_0 = 4\pi \sum_i \vec{n}_i \nu^i$ is given by (up to an additive cosmological constant that is not determined by the potential)

$$\Lambda(\vec{n}_i) = V_{\text{eff}}(\vec{\phi}_0) = \sum_R \mathcal{N}_R (-1)^{F_R} \dim(R) V_{M_R}(2\pi \vec{K}_R/N), \quad (\text{C.17})$$

with the integer vector \vec{K} ,

$$\vec{K}_R = \eta_R \sum_k \vec{n}_k, \quad (\text{C.18})$$

and η_R the N -ality of the representation R .

Provided ML is sufficiently large, each representation R lifts the N^n unbroken vacua into a band of width

$$\Delta\Lambda = \dim(R) \Delta \quad (\text{C.19})$$

and level spacings in the range of

$$\delta\Lambda = \dim(R) \left(\frac{\eta_R}{N}\right)^2 \Delta \quad (\text{C.20})$$

at the bottom of the band. The previous results for the fundamental representation are obtained by setting $\dim(R) = N$ and $\eta_R = 1$, whereas those for the symmetric and antisymmetric representations use $\dim(R) = \frac{1}{2}N(N \pm 1)$, $\eta_R = 2$. In general, it is found that a discretuum of vacuum energies is favored by group-theory effects in the case of matter in the fundamental representation. For higher-dimension matter representations, a

quasi-continuous band is still possible, but then it is entirely determined by the large mass hierarchy $ML \gg 1$.

The N -ality is defined modulo N , and any representation with vanishing η_R fails to lift the local unbroken vacua. This does not mean that these vacua remain unaltered, since local properties, such as masses of particles, depend on the relative contribution of matter and gauge terms (for example, fermion contributions tend to turn the minimum into a local maximum).

Appendix D

Mass of bifundamental fields in toron background

In this appendix we compute the square of the Euclidean Dirac operator acting over negative chirality bifundamental fields of orbifold field theories, in a background where there is a toron for each of the gauge groups.

The toron configurations are

$$A_\mu^i(x) = \frac{i\pi}{2gl_\mu l_\nu} \eta_{\mu\nu}^3 \omega (x - z^i)_\nu \quad (\text{D.1})$$

where z^i is the position of the toron and $i = 1, \dots, k$ label the group factors of the orbifold daughter and ω is a generator of a $U(1)$ subgroup of the gauge group. l_μ is the length along the μ direction of the torus. In our notation, fields will be anti-hermitian and canonically normalized. The election of the self-dual 't Hooft symbol η^3 is equivalent to the election of a discrete set of tori where the lengths are such that the toron is a solution of the equations of motion. Other elections will correspond to rotated tori.

It will be useful to write the next-neighbor configurations in terms of the difference

$$A_\mu^i = A_\mu^{i+1} - \Delta A_\mu^i \quad (\text{D.2})$$

where

$$\Delta A_\mu^i = \frac{i\pi}{2gl_\mu l_\nu} \eta_{\mu\nu}^3 \omega \Delta z^i = \frac{i\pi}{2gl_\mu l_\nu} \eta_{\mu\nu}^3 \omega (z^{i+1} - z^i)_\nu \quad (\text{D.3})$$

then, the covariant derivative of a bifundamental field is

$$D_\mu \lambda_{i,i+1} = (D_\mu^{i+1} \lambda_{i,i+1})_{\text{adj}} - g \Delta A_\mu^i \lambda_{i,i+1} \quad (\text{D.4})$$

where 'adj' means that the covariant derivative acts on the fermionic field as if it were in the adjoint representation. It is straightforward to see that (dropping the orbifold indices for clarity)

$$\delta_{\mu\nu} D_\mu D_\nu \lambda = D_{\text{adj}}^2 - g((D_\mu)_{\text{adj}} \Delta A_\mu) \lambda - 2g \Delta A_\mu ((D_\mu)_{\text{adj}} \lambda) + g^2 (\Delta A_\mu)^2 \quad (\text{D.5})$$

and

$$[D_\mu, D_\nu] \lambda = g(F_{\mu\nu}^+)_{\text{adj}} \lambda - 2g(D_{[\mu} \Delta A_{\nu]})_{\text{adj}} \lambda \quad (\text{D.6})$$

Since $D_\mu \Delta A_\nu = 0$, the square of the Dirac operator is

$$(i\sigma_\mu D_\mu)(i\bar{\sigma}_\nu D_\nu) = \left(-D^2 \mathbf{1}_2 - \frac{1}{2} g \sigma_{\mu\nu} F_{\mu\nu}^+ \right)_{\text{adj}} + 2g \Delta A_\mu (D_\mu)_{\text{adj}} \mathbf{1}_2 - g^2 (\Delta A_\mu)^2 \mathbf{1}_2 \quad (\text{D.7})$$

where we have used the Euclidean Pauli matrices $\sigma_\mu = (\mathbf{1}_2, i\vec{\sigma})$, $\bar{\sigma}_\mu = \sigma_\mu^\dagger$ and $\sigma_{\mu\nu} = \sigma_{[\mu} \bar{\sigma}_{\nu]}$.

The last term is an effective mass

$$M^2 = -g^2 (\Delta A_\mu)^2 = -g^2 \left(\frac{i\pi}{2g} \right)^2 \frac{\eta_{\mu\sigma}^3 \eta_{\mu\rho}^3}{l_\mu l_\sigma l_\mu l_\rho} \Delta z_\sigma \Delta z_\rho \omega^2. \quad (\text{D.8})$$

Using that

$$\eta_{ij}^3 = \epsilon_{3ij}, \quad \eta_{i0}^3 = -\eta_{0i}^3 = \delta_{3i}, \quad i = 1, 2, 3, \quad (\text{D.9})$$

the mass is

$$M^2 = \frac{\pi^2}{4} \left(\frac{(\Delta z_0)^2 + (\Delta z_3)^2}{l_0^2 l_3^2} + \frac{(\Delta z_1)^2 + (\Delta z_2)^2}{l_1^2 l_2^2} \right) \omega^2. \quad (\text{D.10})$$

Bibliography

Bibliography

- [1] O. Aharony, S. S. Gubser, J. M. Maldacena, H. Ooguri, and Y. Oz, Large N field theories, string theory and gravity, *Phys. Rept.* **323**, 183–386 (2000).
- [2] J. M. Maldacena, Lectures on AdS/CFT, (2003).
- [3] T. Gherghetta, Les Houches lectures on warped models and holography, (2006).
- [4] A. Zaffaroni, RTN lectures on the non AdS / non CFT correspondence, *PoS RTN2005*, 005 (2005).
- [5] M. R. Douglas and S. Randjbar-Daemi, Two lectures on AdS/CFT correspondence, (1999).
- [6] J. Gomis, Lectures on tachyon condensation: Towards time-dependent backgrounds and holography, *Class. Quant. Grav.* **22**, S107–S124 (2005).
- [7] K. Skenderis, Lecture notes on holographic renormalization, *Class. Quant. Grav.* **19**, 5849–5876 (2002).
- [8] J. de Boer, L. Maoz, and A. Naqvi, Some aspects of the AdS/CFT correspondence, (2004).
- [9] G. W. Semenoff, Perturbative SUSYM versus AdS/CFT: A brief review, Prepared for 23rd Annual MRST (Montreal-Rochester-Syracuse- Toronto) Conference on High-Energy Physics (MRST 2001), London, Ontario, Canada, 16-18 May 2001.
- [10] J. de Boer, Introduction to the AdS/CFT correspondence, Prepared for 10th International Conference on Supersymmetry and Unification of Fundamental Interactions (SUSY02), Hamburg, Germany, 17-23 Jun 2002.
- [11] I. R. Klebanov, TASI lectures: Introduction to the AdS/CFT correspondence, (2000).

- [12] I. R. Klebanov, Introduction to the AdS/CFT correspondence, Prepared for TMR Meeting on Quantum Aspects of Gauge Theories, Supersymmetry and Unification, Paris, France, 1-7 Sep 1999.
- [13] H. Ooguri, Gauge theory and string theory: An introduction to the AdS/CFT correspondence, Nucl. Phys. Proc. Suppl. **83**, 77–81 (2000).
- [14] E. T. Akhmedov, Introduction to the AdS/CFT correspondence, (1999).
- [15] P. Di Vecchia, An introduction to AdS/CFT correspondence, Fortsch. Phys. **48**, 87–92 (2000).
- [16] J. M. Maldacena, The large N limit of superconformal field theories and supergravity, Adv. Theor. Math. Phys. **2**, 231–252 (1998).
- [17] S. S. Gubser, I. R. Klebanov, and A. M. Polyakov, Gauge theory correlators from non-critical string theory, Phys. Lett. **B428**, 105–114 (1998).
- [18] E. Witten, Anti-de Sitter space and holography, Adv. Theor. Math. Phys. **2**, 253–291 (1998).
- [19] G. 't Hooft, A planar diagram theory for strong interactions, Nucl. Phys. **B72**, 461 (1974).
- [20] E. Witten, Baryons in the $1/N$ expansion, Nucl. Phys. **B160**, 57 (1979).
- [21] E. Witten, The $1 / N$ expansion in atomic and particle physics, HUTP-79/A078.
- [22] A. Jevicki and B. Sakita, The quantum collective field method and its application to the planar limit, Nucl. Phys. **B165**, 511 (1980).
- [23] L. G. Yaffe, Large N limits as classical mechanics, Rev. Mod. Phys. **54**, 407 (1982).
- [24] S. R. Das, Some aspects of large N theories, Rev. Mod. Phys. **59**, 235 (1987).
- [25] J. M. Maldacena and A. Strominger, AdS(3) black holes and a stringy exclusion principle, JHEP **12**, 005 (1998).
- [26] O. Aharony, M. Berkooz, and E. Silverstein, Non-local string theories on AdS(3) x S**3 and stable non- supersymmetric backgrounds, Phys. Rev. **D65**, 106007 (2002).

- [27] S. S. Gubser and I. Mitra, Double-trace operators and one-loop vacuum energy in AdS/CFT, *Phys. Rev.* **D67**, 064018 (2003).
- [28] S. S. Gubser and I. R. Klebanov, A universal result on central charges in the presence of double-trace deformations, *Nucl. Phys.* **B656**, 23–36 (2003).
- [29] D. Nolland, AdS/CFT boundary conditions, multi-trace perturbations, and the c-theorem, *Phys. Lett.* **B584**, 192–199 (2004).
- [30] T. Hartman and L. Rastelli, Double-trace deformations, mixed boundary conditions and functional determinants in AdS/CFT, (2006).
- [31] S. Kuperstein and J. Sonnenschein, Non-critical supergravity ($d \geq 1$) and holography, *JHEP* **07**, 049 (2004).
- [32] A. Dymarsky, I. R. Klebanov, and R. Roiban, Perturbative search for fixed lines in large N gauge theories, *JHEP* **08**, 011 (2005).
- [33] J. Troost, A note on causality in the bulk and stability on the boundary, *Phys. Lett.* **B578**, 210–214 (2004).
- [34] P. Minces, On the role of boundary terms in the AdS/CFT correspondence, *Nucl. Phys. Proc. Suppl.* **127**, 174–178 (2004).
- [35] P. Minces, Bound states in the AdS/CFT correspondence, *Phys. Rev.* **D70**, 025011 (2004).
- [36] T. Hertog and S. Hollands, Stability in designer gravity, *Class. Quant. Grav.* **22**, 5323–5342 (2005).
- [37] S. Elitzur, A. Giveon, M. Porrati, and E. Rabinovici, Multitrace deformations of vector and adjoint theories and their holographic duals, *JHEP* **02**, 006 (2006).
- [38] T. Hertog and G. T. Horowitz, Towards a big crunch dual, *JHEP* **07**, 073 (2004).
- [39] T. Hertog and G. T. Horowitz, Holographic description of AdS cosmologies, *JHEP* **04**, 005 (2005).
- [40] E. Witten, Multi-trace operators, boundary conditions, and AdS/CFT correspondence, (2001).

- [41] M. Berkooz, A. Sever, and A. Shomer, Double-trace deformations, boundary conditions and spacetime singularities, *JHEP* **05**, 034 (2002).
- [42] E. Witten, Anti-de Sitter space, thermal phase transition, and confinement in gauge theories, *Adv. Theor. Math. Phys.* **2**, 505–532 (1998).
- [43] N. Itzhaki, J. M. Maldacena, J. Sonnenschein, and S. Yankielowicz, Supergravity and the large N limit of theories with sixteen supercharges, *Phys. Rev.* **D58**, 046004 (1998).
- [44] J. L. F. Barbon, I. I. Kogan, and E. Rabinovici, On stringy thresholds in SYM/AdS thermodynamics, *Nucl. Phys.* **B544**, 104–144 (1999).
- [45] G. T. Horowitz and J. Polchinski, A correspondence principle for black holes and strings, *Phys. Rev.* **D55**, 6189–6197 (1997).
- [46] S. W. Hawking and D. N. Page, Thermodynamics of black holes in Anti-de Sitter space, *Commun. Math. Phys.* **87**, 577 (1983).
- [47] R. Gregory and R. Laflamme, Black strings and p-branes are unstable, *Phys. Rev. Lett.* **70**, 2837–2840 (1993).
- [48] S. S. Gubser and I. Mitra, The evolution of unstable black holes in anti-de Sitter space, *JHEP* **08**, 018 (2001).
- [49] O. Aharony, The non-AdS/non-CFT correspondence, or three different paths to QCD, (2002).
- [50] J. D. Edelstein and R. Portugues, Gauge / string duality in confining theories, (2006).
- [51] C. Csaki, H. Ooguri, Y. Oz, and J. Terning, Glueball mass spectrum from supergravity, *JHEP* **01**, 017 (1999).
- [52] R. de Mello Koch, A. Jevicki, M. Mihailescu, and J. P. Nunes, Evaluation of glueball masses from supergravity, *Phys. Rev.* **D58**, 105009 (1998).
- [53] T. Sakai and J. Sonnenschein, Probing flavored mesons of confining gauge theories by supergravity, *JHEP* **09**, 047 (2003).

- [54] J. Babington, J. Erdmenger, N. J. Evans, Z. Guralnik, and I. Kirsch, Chiral symmetry breaking and pions in non-supersymmetric gauge / gravity duals, *Phys. Rev.* **D69**, 066007 (2004).
- [55] M. Kruczenski, D. Mateos, R. C. Myers, and D. J. Winters, Meson spectroscopy in AdS/CFT with flavour, *JHEP* **07**, 049 (2003).
- [56] M. Kruczenski, D. Mateos, R. C. Myers, and D. J. Winters, Towards a holographic dual of large- $N(c)$ QCD, *JHEP* **05**, 041 (2004).
- [57] C. Nunez, A. Paredes, and A. V. Ramallo, Flavoring the gravity dual of $N = 1$ Yang-Mills with probes, *JHEP* **12**, 024 (2003).
- [58] N. J. Evans and J. P. Shock, Chiral dynamics from AdS space, *Phys. Rev.* **D70**, 046002 (2004).
- [59] T. Sakai and S. Sugimoto, Low energy hadron physics in holographic QCD, *Prog. Theor. Phys.* **113**, 843–882 (2005).
- [60] D. T. Son and A. O. Starinets, Minkowski-space correlators in AdS/CFT correspondence: Recipe and applications, *JHEP* **09**, 042 (2002).
- [61] A. Buchel, J. T. Liu, and A. O. Starinets, Coupling constant dependence of the shear viscosity in $N = 4$ supersymmetric Yang-Mills theory, *Nucl. Phys.* **B707**, 56–68 (2005).
- [62] A. Buchel, On universality of stress-energy tensor correlation functions in supergravity, *Phys. Lett.* **B609**, 392–401 (2005).
- [63] P. K. Kovtun and A. O. Starinets, Quasinormal modes and holography, *Phys. Rev.* **D72**, 086009 (2005).
- [64] P. Benincasa, A. Buchel, and A. O. Starinets, Sound waves in strongly coupled non-conformal gauge theory plasma, *Nucl. Phys.* **B733**, 160–187 (2006).
- [65] J. Mas, Shear viscosity from R-charged AdS black holes, (2006).
- [66] D. T. Son and A. O. Starinets, Hydrodynamics of R-charged black holes, (2006).
- [67] K. Maeda, M. Natsuume, and T. Okamura, Viscosity of gauge theory plasma with a chemical potential from AdS/CFT, (2006).

- [68] P. Kovtun and A. Starinets, Thermal spectral functions of strongly coupled $N = 4$ supersymmetric Yang-Mills theory, (2006).
- [69] E. Witten, Current algebra theorems for the $U(1)$ 'Goldstone boson', Nucl. Phys. **B156**, 269 (1979).
- [70] G. Veneziano, $U(1)$ without instantons, Nucl. Phys. **B159**, 213–224 (1979).
- [71] E. Witten, Large N chiral dynamics, Ann. Phys. **128**, 363 (1980).
- [72] P. Di Vecchia and G. Veneziano, Chiral dynamics in the large N limit, Nucl. Phys. **B171**, 253 (1980).
- [73] I. R. Klebanov and J. M. Maldacena, Superconformal gauge theories and non-critical superstrings, Int. J. Mod. Phys. **A19**, 5003–5016 (2004).
- [74] S. Kuperstein and J. Sonnenschein, Non-critical supergravity ($d \geq 1$) and holography, JHEP **07**, 049 (2004).
- [75] S. Kuperstein and J. Sonnenschein, Non-critical, near extremal $AdS(6)$ background as a holographic laboratory of four dimensional YM theory, JHEP **11**, 026 (2004).
- [76] M. Alishahiha, A. Ghodsi, and A. E. Mosaffa, On isolated conformal fixed points and noncritical string theory, JHEP **01**, 017 (2005).
- [77] A. Fotopoulos, V. Niarchos, and N. Prezas, D-branes and SQCD in non-critical superstring theory, JHEP **10**, 081 (2005).
- [78] S. K. Ashok, S. Murthy, and J. Troost, D-branes in non-critical superstrings and minimal super Yang-Mills in various dimensions, (2005).
- [79] R. Casero, A. Paredes, and J. Sonnenschein, Fundamental matter, meson spectroscopy and non-critical string / gauge duality, JHEP **01**, 127 (2006).
- [80] S. Charzynski, G. Rudolph, and M. Schmidt, On the topology of the reduced classical configuration space of lattice QCD, (2005).
- [81] F. Bigazzi, R. Casero, A. L. Cotrone, E. Kiritsis, and A. Paredes, Non-critical holography and four-dimensional CFT's with fundamentals, JHEP **10**, 012 (2005).
- [82] A. Karch and E. Katz, Adding flavor to AdS/CFT , JHEP **06**, 043 (2002).

- [83] J. Erlich, E. Katz, D. T. Son, and M. A. Stephanov, QCD and a holographic model of hadrons, *Phys. Rev. Lett.* **95**, 261602 (2005).
- [84] G. Veneziano, Some aspects of a unified approach to gauge, dual and Gribov theories, *Nucl. Phys.* **B117**, 519–545 (1976).
- [85] J. F. Donoghue, E. Golowich, and B. R. Holstein, Dynamics of the standard model, *Camb. Monogr. Part. Phys. Nucl. Phys. Cosmol.* **2**, 1–540 (1992).
- [86] C. Vafa and E. Witten, Restrictions on symmetry breaking in vector-like gauge theories, *Nucl. Phys.* **B234**, 173 (1984).
- [87] M. Gell-Mann, R. J. Oakes, and B. Renner, Behavior of current divergences under $SU(3) \times SU(3)$, *Phys. Rev.* **175**, 2195–2199 (1968).
- [88] S. Weinberg, The $U(1)$ problem, *Phys. Rev.* **D11**, 3583–3593 (1975).
- [89] G. 't Hooft, How instantons solve the $U(1)$ problem, *Phys. Rept.* **142**, 357–387 (1986).
- [90] G. 't Hooft, Symmetry breaking through Bell-Jackiw anomalies, *Phys. Rev. Lett.* **37**, 8–11 (1976).
- [91] G. 't Hooft, Computation of the quantum effects due to a four-dimensional pseudoparticle, *Phys. Rev.* **D14**, 3432–3450 (1976).
- [92] T. Banks and S. Yankielowicz, Dynamical explanation for the positivity of topological charge fluctuations in QCD, *Phys. Lett.* **B104**, 301 (1981).
- [93] E. Witten, Instantons, the quark model and the $1/N$ expansion, *Nucl. Phys.* **B149**, 285 (1979).
- [94] E. Seiler, Some more remarks on the Witten-Veneziano formula for the eta' mass, *Phys. Lett.* **B525**, 355–359 (2002).
- [95] P. H. Ginsparg and K. G. Wilson, A remnant of chiral symmetry on the lattice, *Phys. Rev.* **D25**, 2649 (1982).
- [96] L. Giusti, G. C. Rossi, M. Testa, and G. Veneziano, The $U(1)_A$ problem on the lattice with Ginsparg-Wilson fermions, *Nucl. Phys.* **B628**, 234–252 (2002).
- [97] L. Giusti, G. C. Rossi, M. Testa, and G. Veneziano, The $U(1)_A$ problem on the lattice, *Nucl. Phys. Proc. Suppl.* **106**, 1001–1003 (2002).

- [98] E. Witten, Dyons of charge $e\theta/2\pi$, *Phys. Lett.* **B86**, 283–287 (1979).
- [99] N. R. Constable and R. C. Myers, Exotic scalar states in the AdS/CFT correspondence, *JHEP* **11**, 020 (1999).
- [100] E. Witten, Theta dependence in the large N limit of four-dimensional gauge theories, *Phys. Rev. Lett.* **81**, 2862–2865 (1998).
- [101] A. Hashimoto and Y. Oz, Aspects of QCD dynamics from string theory, *Nucl. Phys.* **B548**, 167–179 (1999).
- [102] J. L. F. Barbon, C. Hoyos, D. Mateos, and R. C. Myers, The holographic life of the eta', *JHEP* **10**, 029 (2004).
- [103] A. Armoni, Witten-Veneziano from Green-Schwarz, *JHEP* **06**, 019 (2004).
- [104] A. De Rujula, H. Georgi, and S. L. Glashow, Vector model of the weak interactions, *Phys. Rev.* **D12**, 3589 (1975).
- [105] N. Isgur, Mass formula for nonets, *Phys. Rev.* **D13**, 122–124 (1976).
- [106] S. Kachru and E. Silverstein, 4d conformal theories and strings on orbifolds, *Phys. Rev. Lett.* **80**, 4855–4858 (1998).
- [107] A. E. Lawrence, N. Nekrasov, and C. Vafa, On conformal field theories in four dimensions, *Nucl. Phys.* **B533**, 199–209 (1998).
- [108] M. Bershadsky, Z. Kakushadze, and C. Vafa, String expansion as large N expansion of gauge theories, *Nucl. Phys.* **B523**, 59–72 (1998).
- [109] M. Bershadsky and A. Johansen, Large N limit of orbifold field theories, *Nucl. Phys.* **B536**, 141–148 (1998).
- [110] A. Hanany, M. J. Strassler, and A. M. Uranga, Finite theories and marginal operators on the brane, *JHEP* **06**, 011 (1998).
- [111] J. D. Lykken, E. Poppitz, and S. P. Trivedi, Chiral gauge theories from D-branes, *Phys. Lett.* **B416**, 286–294 (1998).
- [112] J. D. Lykken, E. Poppitz, and S. P. Trivedi, M(ore) on chiral gauge theories from D-branes, *Nucl. Phys.* **B520**, 51–74 (1998).

- [113] J. Erlich, A. Naqvi, and L. Randall, The Coulomb branch of $N = 2$ supersymmetric product group theories from branes, *Phys. Rev.* **D58**, 046002 (1998).
- [114] J. Erlich and A. Naqvi, Nonperturbative tests of the parent/orbifold correspondence in supersymmetric gauge theories, *JHEP* **12**, 047 (2002).
- [115] M. Schmaltz, Duality of non-supersymmetric large N gauge theories, *Phys. Rev.* **D59**, 105018 (1999).
- [116] M. J. Strassler, On methods for extracting exact non-perturbative results in non-supersymmetric gauge theories, (2001).
- [117] P. Kovtun, M. Unsal, and L. G. Yaffe, Non-perturbative equivalences among large $N(c)$ gauge theories with adjoint and bifundamental matter fields, *JHEP* **12**, 034 (2003).
- [118] P. Kovtun, M. Unsal, and L. G. Yaffe, Necessary and sufficient conditions for non-perturbative equivalences of large $N(c)$ orbifold gauge theories, *JHEP* **07**, 008 (2005).
- [119] P. Kovtun, M. Unsal, and L. G. Yaffe, Can large $N(c)$ equivalence between supersymmetric Yang-Mills theory and its orbifold projections be valid?, *Phys. Rev.* **D72**, 105006 (2005).
- [120] D. B. Kaplan, E. Katz, and M. Unsal, Supersymmetry on a spatial lattice, *JHEP* **05**, 037 (2003).
- [121] A. Gorsky and M. Shifman, Testing nonperturbative orbifold conjecture, *Phys. Rev.* **D67**, 022003 (2003).
- [122] A. Armoni, A. Gorsky, and M. Shifman, Spontaneous $Z(2)$ symmetry breaking in the orbifold daughter of $N = 1$ super-Yang-Mills theory, fractional domain walls and vacuum structure, *Phys. Rev.* **D72**, 105001 (2005).
- [123] M. Shifman, Non-perturbative Yang-Mills from supersymmetry and strings, or, in the jungles of strong coupling, *Acta Phys. Polon.* **B36**, 3783 (2005).
- [124] A. Adams and E. Silverstein, Closed string tachyons, AdS/CFT, and large N QCD, *Phys. Rev.* **D64**, 086001 (2001).
- [125] A. Adams, J. Polchinski, and E. Silverstein, Don't panic! Closed string tachyons in ALE space-times, *JHEP* **10**, 029 (2001).

- [126] D. Tong, Comments on condensates in non-supersymmetric orbifold field theories, *JHEP* **03**, 022 (2003).
- [127] J. L. F. Barbon and C. Hoyos, Small volume expansion of almost supersymmetric large N theories, *JHEP* **01**, 114 (2006).
- [128] A. Armoni, M. Shifman, and G. Veneziano, Exact results in non-supersymmetric large N orientifold field theories, *Nucl. Phys.* **B667**, 170–182 (2003).
- [129] A. Armoni, M. Shifman, and G. Veneziano, Refining the proof of planar equivalence, *Phys. Rev.* **D71**, 045015 (2005).
- [130] Z. Kakushadze, Gauge theories from orientifolds and large N limit, *Nucl. Phys.* **B529**, 157–179 (1998).
- [131] Z. Kakushadze, On large N gauge theories from orientifolds, *Phys. Rev.* **D58**, 106003 (1998).
- [132] C. Angelantonj and A. Armoni, Non-tachyonic type 0B orientifolds, non-supersymmetric gauge theories and cosmological RG flow, *Nucl. Phys.* **B578**, 239–258 (2000).
- [133] A. M. Polyakov, The wall of the cave, *Int. J. Mod. Phys.* **A14**, 645–658 (1999).
- [134] I. R. Klebanov and A. A. Tseytlin, D-branes and dual gauge theories in type 0 strings, *Nucl. Phys.* **B546**, 155–181 (1999).
- [135] I. R. Klebanov and A. A. Tseytlin, A non-supersymmetric large N CFT from type 0 string theory, *JHEP* **03**, 015 (1999).
- [136] I. R. Klebanov, Tachyon stabilization in the AdS/CFT correspondence, *Phys. Lett.* **B466**, 166–170 (1999).
- [137] R. Blumenhagen, A. Font, and D. Lust, Non-supersymmetric gauge theories from D-branes in type 0 string theory, *Nucl. Phys.* **B560**, 66–92 (1999).
- [138] A. Armoni, M. Shifman, and G. Veneziano, SUSY relics in one-flavor QCD from a new $1/N$ expansion, *Phys. Rev. Lett.* **91**, 191601 (2003).
- [139] A. Armoni, M. Shifman, and G. Veneziano, QCD quark condensate from SUSY and the orientifold large-N expansion, *Phys. Lett.* **B579**, 384–390 (2004).

- [140] F. Sannino and M. Shifman, Effective Lagrangians for orientifold theories, *Phys. Rev.* **D69**, 125004 (2004).
- [141] A. Armoni, M. Shifman, and G. Veneziano, From super-Yang-Mills theory to QCD: Planar equivalence and its implications, (2004).
- [142] A. Armoni, A. Gorsky, and M. Shifman, An exact relation for $N = 1$ orientifold field theories with arbitrary superpotential, *Nucl. Phys.* **B702**, 37–48 (2004).
- [143] P. van Baal, Gauge theory in a finite volume, *Acta Phys. Polon.* **B20**, 295–312 (1989).
- [144] P. van Baal, QCD in a finite volume, (2000).
- [145] A. Gonzalez-Arroyo, Yang-Mills fields on the 4-dimensional torus. (Classical theory), (1997).
- [146] G. 't Hooft, A property of electric and magnetic flux in nonabelian gauge theories, *Nucl. Phys.* **B153**, 141 (1979).
- [147] E. Witten, Constraints on supersymmetry breaking, *Nucl. Phys.* **B202**, 253 (1982).
- [148] E. Witten, Supersymmetric index in four-dimensional gauge theories, *Adv. Theor. Math. Phys.* **5**, 841–907 (2002).
- [149] D. J. Gross, R. D. Pisarski, and L. G. Yaffe, QCD and instantons at finite temperature, *Rev. Mod. Phys.* **53**, 43 (1981).
- [150] N. Weiss, The Wilson line in finite temperature gauge theories, *Phys. Rev.* **D25**, 2667 (1982).
- [151] N. Weiss, The effective potential for the order parameter of gauge theories at finite temperature, *Phys. Rev.* **D24**, 475 (1981).
- [152] Y. Hosotani, Dynamical mass generation by compact extra dimensions, *Phys. Lett.* **B126**, 309 (1983).
- [153] Y. Hosotani, Dynamical gauge symmetry breaking as the Casimir effect, *Phys. Lett.* **B129**, 193 (1983).
- [154] E. Alvarez and A. Nieto, Wilson loops at finite temperature, *Phys. Rev.* **D41**, 3857 (1990).

- [155] M. Luscher, Some analytic results concerning the mass spectrum of Yang-Mills theories on a torus, Nucl. Phys. **B219**, 233–261 (1983).
- [156] P. van Baal and J. Koller, QCD on a torus and electric flux energies from tunneling, Ann. Phys. **174**, 299 (1987).
- [157] J. L. F. Barbon and C. Hoyos, Dynamical Higgs potentials with a landscape, (2006).
- [158] O. Aharony et al., The phase structure of low dimensional large N gauge theories on tori, JHEP **01**, 140 (2006).
- [159] K. R. Dienes, Modular invariance, finiteness, and misaligned supersymmetry: New constraints on the numbers of physical string states, Nucl. Phys. **B429**, 533–588 (1994).
- [160] M. Luscher and G. Munster, Weak coupling expansion of the low lying energy values in the SU(2) gauge theory on a torus, Nucl. Phys. **B232**, 445 (1984).
- [161] J. Koller and P. van Baal, A rigorous nonperturbative result for the glueball mass and electric flux energy in a finite volume, Nucl. Phys. **B273**, 387 (1986).
- [162] P. van Baal and J. Koller, Finite size results for SU(3) gauge theory, Phys. Rev. Lett. **57**, 2783 (1986).
- [163] P. van Baal, The small volume expansion of gauge theories coupled to massless fermions, Nucl. Phys. **B307**, 274 (1988).
- [164] E. Cohen and C. Gomez, Chiral symmetry breaking in supersymmetric Yang-Mills, Phys. Rev. Lett. **52**, 237 (1984).
- [165] E. Cohen and C. Gomez, A computation of $\text{Tr}(-1)^{**}F$ in supersymmetric gauge theories with matter, Nucl. Phys. **B223**, 183 (1983).
- [166] S. Okubo and J. Patera, General indices of representations and Casimir invariants, J. Math. Phys. **25**, 219 (1984).
- [167] T. van Ritbergen, A. N. Schellekens, and J. A. M. Vermaseren, Group theory factors for Feynman diagrams, Int. J. Mod. Phys. **A14**, 41–96 (1999).
- [168] G. 't Hooft, Some twisted selfdual solutions for the Yang-Mills equations on a hypertorus, Commun. Math. Phys. **81**, 267–275 (1981).

- [169] D. R. Lebedev, M. I. Polikarpov, and A. A. Rosly, Summation over topological classes of gauge fields in lattice gauge theories, *Sov. J. Nucl. Phys.* **49**, 1113–1117 (1989).
- [170] A. R. Zhitnitsky, Torons, chiral symmetry breaking and the U(1) problem in the sigma model and in gauge theories, *Nucl. Phys.* **B340**, 56–112 (1990).
- [171] M. F. Atiyah, N. J. Hitchin, V. G. Drinfeld, and Y. I. Manin, Construction of instantons, *Phys. Lett.* **A65**, 185–187 (1978).
- [172] W. Nahm, A simple formalism for the BPS monopole, *Phys. Lett.* **B90**, 413 (1980).
- [173] P. J. Braam and P. van Baal, Nahm’s transformation for instantons, *Commun. Math. Phys.* **122**, 267 (1989).
- [174] E. Witten, Sigma models and the ADHM construction of instantons, *J. Geom. Phys.* **15**, 215–226 (1995).
- [175] E. Witten, Small Instantons in String Theory, *Nucl. Phys.* **B460**, 541–559 (1996).
- [176] D.-E. Diaconescu, D-branes, monopoles and Nahm equations, *Nucl. Phys.* **B503**, 220–238 (1997).
- [177] A. Astashkevich, N. Nekrasov, and A. S. Schwarz, On noncommutative Nahm transform, *Commun. Math. Phys.* **211**, 167–182 (2000).
- [178] M. Hamanaka and H. Kajiura, Gauge fields on tori and T-duality, *Phys. Lett.* **B551**, 360–368 (2003).
- [179] H. Schenk, On a generalized Fourier transform of instantons over flat tori, *Commun. Math. Phys.* **116**, 177 (1988).
- [180] A. Gonzalez-Arroyo and C. Pena, Nahm transformation on the lattice, *JHEP* **09**, 013 (1998).
- [181] P. van Baal, Nahm gauge fields for the torus, *Phys. Lett.* **B448**, 26–32 (1999).
- [182] M. Garcia Perez, A. Gonzalez-Arroyo, C. Pena, and P. van Baal, Nahm dualities on the torus: A synthesis, *Nucl. Phys.* **B564**, 159–181 (2000).
- [183] A. Gonzalez-Arroyo, On Nahm’s transformation with twisted boundary conditions, *Nucl. Phys.* **B548**, 626–636 (1999).

- [184] G. 't Hooft, Computation of the quantum effects due to a four- dimensional pseudoparticle, *Phys. Rev.* **D14**, 3432–3450 (1976).
- [185] S. Coleman, *Aspects of symmetry: selected Erice Lectures.*, Cambridge University Press (1985).
- [186] P. van Baal, Twisted boundary conditions: a nonperturbative probe for pure non-abelian gauge theories, INIS-mf-9631.
- [187] Z. Guralnik and S. Ramgoolam, Torons and D-brane bound states, *Nucl. Phys.* **B499**, 241–252 (1997).
- [188] Z. Guralnik and S. Ramgoolam, From 0-branes to torons, *Nucl. Phys.* **B521**, 129–138 (1998).
- [189] L. Susskind, The anthropic landscape of string theory, (2003).
- [190] R. Bousso and J. Polchinski, Quantization of four-form fluxes and dynamical neutralization of the cosmological constant, *JHEP* **06**, 006 (2000).
- [191] R. Bousso and J. Polchinski, The string theory landscape, *Sci. Am.* **291**, 60–69 (2004).
- [192] S. B. Giddings, S. Kachru, and J. Polchinski, Hierarchies from fluxes in string compactifications, *Phys. Rev.* **D66**, 106006 (2002).
- [193] S. Kachru, R. Kallosh, A. Linde, and S. P. Trivedi, De Sitter vacua in string theory, *Phys. Rev.* **D68**, 046005 (2003).
- [194] C. Escoda, M. Gomez-Reino, and F. Quevedo, Saltatory de Sitter string vacua, *JHEP* **11**, 065 (2003).
- [195] M. R. Douglas, The statistics of string / M theory vacua, *JHEP* **05**, 046 (2003).
- [196] S. Ashok and M. R. Douglas, Counting flux vacua, *JHEP* **01**, 060 (2004).
- [197] F. Denef and M. R. Douglas, Distributions of flux vacua, *JHEP* **05**, 072 (2004).
- [198] K. R. Dienes, Statistics on the heterotic landscape: Gauge groups and cosmological constants of four-dimensional heterotic strings, (2006).

- [199] B. Freivogel and L. Susskind, A framework for the landscape, *Phys. Rev.* **D70**, 126007 (2004).
- [200] A. D. Linde, Chaotic inflation, *Phys. Lett.* **B129**, 177–181 (1983).
- [201] A. H. Guth, Inflation and eternal inflation, *Phys. Rept.* **333**, 555–574 (2000).
- [202] S. Kachru et al., Towards inflation in string theory, *JCAP* **0310**, 013 (2003).
- [203] T. Banks, M. Dine, and E. Gorbatov, Is there a string theory landscape?, *JHEP* **08**, 058 (2004).
- [204] J. Gomis, F. Marchesano, and D. Mateos, An open string landscape, *JHEP* **11**, 021 (2005).
- [205] N. Arkani-Hamed, S. Dimopoulos, and S. Kachru, Predictive landscapes and new physics at a TeV, (2005).
- [206] K. R. Dienes, E. Dudas, and T. Gherghetta, A calculable toy model of the landscape, *Phys. Rev.* **D72**, 026005 (2005).
- [207] E. Witten, Toroidal compactification without vector structure, *JHEP* **02**, 006 (1998).
- [208] E. Alvarez and A. F. Faedo, Renormalized Kaluza-Klein theories. II: QED(4) on a two- torus, (2006).
- [209] E. Alvarez and A. F. Faedo, Renormalized Kaluza-Klein theories, (2006).